國 立 交 通 大 學

電 信 工 程 研 究 所

博 士 論 文

高速無線網路下短距離通訊協定之設計與分析

Design and Analysis of Short-Range Communication Protocols for High-Speed Wireless Networks

研究生：林佳仕

指導教授：方凱田 博士

中 華 民 國 一 〇 一 年 六 月

高速無線網路下短距離通訊協定之設計與分析

Design and Analysis of Short-Range Communication Protocols for High-Speed Wireless Networks

研究生：林佳仕　　Student: Jia-Shi Lin

指導教授：方凱田　　Advisor: Kai-Ten Feng

國立交通大學

電信工程研究所

博士論文

A Dissertation

Submitted to Institute of Communications Engineering

College of Electrical and Computer Engineering

National Chiao Tung University

in Partial Fulfillment of the Requirements

for the *Degree of Doctor of Philosophy*

in

Communications Engineering

June 2012

Hsinchu, Taiwan, Republic of China

中華民國一〇一年六月

高速無線網路下短距離通訊協定之設計與分析

研究生：林佳仕　　指導教授：方凱田

國立交通大學電信工程研究所

摘　要

在過去十年裡，如何設計無線短距離通訊協定以達到高資料傳輸速率一直備受關注。在眾多不同的標準裡，由於設計和佈建上的成功，IEEE 802.11 和毫微微蜂巢式基地台 (femtocell) 被視為是兩個最適合採用的技術。跟傳統蜂巢式基地台相比，IEEE 802.11 和 femtocell 系統因為連線品質較好的關係，可以提供更高的傳輸速度給使用者。然而在這些技術中仍然存在一些問題導致系統效能無法進一步提升。

分散式協調功能 (distributed coordination function, DCF) 是 IEEE 802.11 媒體存取控制 (media access control, MAC) 層中的基本機制。在無線區域網路 (wireless local area networks, WLANs) 裡，它被用來管理無線站台 (wireless stations, WSs) 之間隨機且複雜的通道存取。更進一步，為了支援服務品質 (quality-of-service, QoS)，IEEE 802.11e 提出了增強分散式通道存取 (enhanced distributed channel access, EDCA) 機制以提供不同的通道存取優先權給不同的資料傳輸型態。在資料封包傳輸前，隨機後退 (random backoff) 機制和 request-to-send (RTS)/clear-to-send (CTS) 交握需要分別被執行來減少封包碰撞機會和可能的終端機隱匿問題。然而眾多的開支 (overhead) 會導致系統的效能明顯降低。因此，本論文首先提出一個動態保留 -解決碰撞 (adaptive reservation-assisted collision resolution, ARCR) 的協定。藉著在競爭式 (contention-based) 通道存取網路中採用動態的保留區間 (adaptive reservation period)，ARCR 機制可以明顯改善封包碰撞和減少後退延遲 (backoff delay)。更進一步，本論文再提出一個增強式的動態保留 -解決碰撞 (enhanced-ARCR, E-ARCR) 協定，提供多種不一樣優先權的流量來支援服務品質。

接著，IEEE 802.11n 從媒體存取控制層的觀點提出了封包聚合 (frame aggregation) 技術來改善系統效能。為了達到可靠的資料傳輸和較高的系統吞吐量 (system throughput)，兩個自動重傳請求 (automatic repeat reQuest, ARQ) 機制在本論文被提出。聚合選擇性重送 -自動重傳請求 (aggregated selective repeat ARQ, ASR-ARQ) 機制考慮了封包選擇性

重送的自動重傳請求。另一方面，對於較差的通道狀況，藉由採用里德所羅門碼 (Reed-Solomon code, RS code) 充當前向錯誤更正 (forward error correction, FEC) 機制，聚合混合式自動重傳請求 (aggregated hybrid ARQ, AH-ARQ) 可以改善系統效能。

更進一步，對於 femtocell 的應用，如何選取適當的存取策略一直是個重要的議題。femtocell 考慮了兩個主要的策略：開放式存取模式 (open access mode) 與封閉式存取模式 (closed access mode)。當 femtocell 處於開放式存取模式時，所有的使用者都可以使用 femtocell。另一方面，當封閉式存取被採用時，femtocell 只允許註冊者 (*subscribers*) 連線，其他的非註冊者 (*nonsubscribers*) 只能和傳統基地台連線。明顯地，封閉式存取可以提供較多的資源給註冊者，但不利於整體網路。反之，開放式存取能可以提升整體網路的效能，但不利於註冊者。為了使存取策略有更高的彈性，本論文提出了混合式存取模式 (hybrid access mode)，讓非註冊者可以有限度地存取 femtocell。為了描述使用者的自私行為，我們建立了兩個基地台選擇的賽局 (cell selection games)，並在一些合理的假設下證明這些賽局有純策略納許均衡 (pure strategy Nash Equilibrium) 存在。藉由觀察在納許均衡下的結果，我們建議採用混合式存取模式，以達到在註冊者、整體網路和營運商 (operator) 之間較好的效能權衡。

此外，本論文也建立效能分析模型，以此來驗證所提出演算法的效率。由分析跟模擬的結果可發現藉著採用本論文所提出演算法，IEEE 802.11 和 femtocell 的網路效能可以進一步被提升。

Design and Analysis of Short-Range Communication Protocols for High-Speed Wireless Networks

Student: Jia-Shi Lin Advisor: Kai-Ten Feng

Institute of Communications Engineering
National Chiao Tung University

Abstract

Wireless short-range communication protocols for high data rate have attracted a lot of attentions over the past decade. Among different standards, IEEE 802.11 and femtocell techniques are considered the most two well-adopted suites due to their remarkable success in both design and deployment. Compared to conventional cellular network, higher data rate can be achieved for users in the IEEE 802.11 and femtocell systems due to better link qualities. However, some crucial issues still exist in these techniques such that system performance cannot be further enhanced.

Served as basic access mechanism in the IEEE 802.11 media access control (MAC) layer, distributed coordination function (DCF) is employed to regulate the random and complex medium accessing behaviors among the wireless stations (WSs) within the same wireless local area networks (WLANs). Moreover, in order to support quality-of-service (QoS) requirements, the enhanced distributed channel access (EDCA) mechanism is proposed in the IEEE 802.11e standard to provide prioritized channel accesses for different types of traffics. Before the data transmission, random backoff and request-to-send (RTS)/clear-to-send (CTS) handshaking are respectively executed in order to resolve packet collision and potential hidden terminal problems. Nevertheless, the system performance will be significantly decreased owing to heavy overhead in the DCF/EDCA. Therefore, an adaptive reservation-assisted collision resolution (ARCR) protocol modified from conventional DCF is proposed in this dissertation. By adoption of adaptive reservation periods within the contention-based channel access networks, proposed ARCR algorithm can significantly improve packet collision and reduce the backoff delays compared to other existing

works. Furthermore, in order to support QoS requirements for multiple prioritized traffics, the enhanced-ARCR (E-ARCR) protocol is further proposed as the enhanced version of the ARCR scheme.

Next, frame aggregation techniques are proposed in the IEEE 802.11n standard to improve the system performance of WLANs from the MAC perspective. In order to achieve both reliable data transmission and high system throughput, two MAC-defined automatic repeat reQuest (ARQ) mechanisms are proposed to consider the effect from frame aggregation. An aggregated selective repeat ARQ (ASR-ARQ) scheme is proposed which incorporates the selective repeat ARQ scheme with the consideration of frame aggregation. On the other hand, for worse channel quality, the aggregated hybrid ARQ (AH-ARQ) mechanism is proposed to further improve the throughput performance by adopting the Reed-Solomon block code as forward error correction scheme.

Moreover, how to choose a feasible access strategy for femtocell is considered an important issue. Two major access policies are considered in femtocell network, including the open access mode and closed access mode. All users are allowed to connect to the fBS by adopting the open access mode; while the closed access mode only permits authorized *subscribers* to utilize the femtocell BSs (fBS). Closed access will intuitively be advantageous to the femtocell *subscribers*, on the other hand, system performance of the entire system network can be enhanced if open access mode is adopted. In order to relax the inflexible access strategies, hybrid access policy is considered in this dissertation which allows *nonsubscribers* to possess limited connections to the fBS. Two cell selection games for distinct scenarios are theoretically modeled to formulate the behaviors of *nonsubscribers*, and the existences of pure strategy Nash equilibria (NEs) are also proven under feasible utility functions. By the observation at NEs, it is suggested to adopt hybrid access mode to achieve better tradeoff for performance enhancement from the perspectives of subscribers, heterogeneous network, and operator.

Besides, in order to validate the effectiveness of proposed algorithms, analytical models are also constructed in this dissertation. Both analytical and simulation results show that performance of IEEE 802.11 and femtocell techniques can be further enhanced by adopting proposed algorithms in this dissertation.

誌 謝

能夠順利取得博士學位，首先我要感謝指導教授方凱田老師在學術上的各種指導與建議，尤其在英文寫作方面，總是細心地逐字逐句批改我錯誤的單字與文法，讓論文不至於錯誤百出。而老師所提供的舒適環境也讓大家願意常常待在實驗室一起作研究。也特別感謝撥空蒞臨指導的口試委員們，有你們的寶貴建議，才能讓我從各個不同的角度重新看待自己的研究。

接著，我要感謝所有 MINT Lab 的成員。在尋找論文題目時，博士班學長仲賢、文俊、柏軒、建華不時地提供我一些適當意見，除了讓我順利完成論文外，也帶給我不同的啟發。碩士班學長裕彬、瑜智、信龍、伯泰、林志、文炫除了在研究上的幫忙外，也帶給實驗室許多的歡樂。同屆的同學俊傑、佳偉、瑞廷，在修課跟研究時的互相幫助外，一起外出運動打球也讓我碩士班生活多采多姿。感謝實驗室的其他同學和學弟妹們其懋、承澤、萬邦、俊宇、惟能、昭華、劭凱、宥儒、瑞鴻、子皓、志明、修銘、景維、智偉、裕平、唯慶、治緯、可婷、君容，在博士班過程中因為有你們，才不至於讓研究生活太苦悶。感謝張添壽博士在我論文修改時，總是適時地提供一些意見，讓我能順利完成論文修改。

此外，感謝交通大學所提供的豐富資源，讓我得以順利完成博士論文。也特別感謝國科會的出國補助和電信所的碩博士生獎學金，讓我能在沒有經濟壓力的情況下出國參加研討會和專心作研究。最後我要感謝我的家人，有你們一路上的支持，我才能順利完成博士學位。

林佳仕謹誌　　于新竹國立交通大學

Contents

List of Tables

List of Figures

List of Abbreviations

3GPP	3rd generation partnership project, page 1
ABS	almost blank subframe, page 98
AC	access category, page 3
ACK	acknowledge, page 12
AH-ARQ	aggregated hybrid ARQ, page 5
AIFS	arbitration interframe space, page 3
A-MPDU	aggregated MPDU, page 61
AP	access point, page 1
ARCR	adaptive reservation-assisted collision resolution, page 5
ARQ	automatic repeat reQuest, page 3
ASR-ARQ	aggregated selective repeat ARQ, page 5
AWGN	additive white Gaussian noise, page 77
BA	block acknowledgement, page 3
BE	best effort, page 47
BER	bit error rate, page 22
BK	background, page 48
CDF	cumulative distribution function, page 5
CFP	contention-free period, page 9
CP	contention period, page 9
CRC	cyclic redundancy check, page 62
CR	cognitive radio, page 91
CSMA/CA	carrier sensing multiple access with collision avoidance, page 2
CTS	clear-to-send, page 2

CW	contention window, page 3
DCF	distributed coordination function, page 1
DIFS	DCF interframe space, page 2
E-ARCR	enhanced-ARCR, page 5
EBA	early backoff announcement, page 8
EDCA	enhanced distributed channel access, page 2
FA	frame aggregation, page 3
fBS	femtocell base station, page 1
FCS	frame check sequence, page 64
FEC	forward error correction, page 59
GDCF	gentle DCF, page 8
H-ARQ	hybrid ARQ, page 59
HCA	handshake-based channel aware, page 8
HCF	hybrid coordination function, page 51
HetNet	heterogeneous network, page 4
i.i.d.	independent and identically distributed, page 101
IEEE	Institute of Electrical and Electronics Engineers, page 1
IESDS	iterated elimination of strictly dominated strategies, page 105
IR	incremental redundancy, page 59
LTE-A	long-term evolution-advanced, page 1
MAC	medium access control, page 1
mBS	macrocell base station, page 2
MCCA	multi-user polling controlled channel access, page 59
MCS	modulation and coding scheme, page 77
MIMO	multi-input multi-output, page 3
MPDU	multiple MAC protocol data unit, page 61
NAV	network allocation vector, page 10
NE	Nash equilibrium, page 6
NS-2	network simulator 2, page 27
NTO	next transmission order, page 13
PCF	point coordination function, page 1

PGF	probability generating function, page 70
PHY	physical, page 3
PIFS	PCF interframe space, page 10
PSDU	PHY service data unit, page 61
PUE	primary UE, page 93
QoS	quality-of-service, page 1
RCPC code	rate compatible punctured convolutional code, page 59
RCPT code	rate compatible punctured turbo code, page 59
RFD	request for data, page 14
RS code	Reed-Solomon code, page 60
RSRP	reference signal receiving power, page 94
RTS	request-to-send, page 2
SIFS	short interframe space, page 10
SINR	signal-to-interference-plus-noise-ratio, page 91
SNR	signal-to-noise ratio, page 22
SUE	secondary UE, page 93
SW-ARQ	stop-and-wait ARQ, page 60
TAR	table-adding request, page 12
TGn	task group N, page 3
TXOP	transmission opportunity, page 61
UE	user equipment, page 2
UP	unique pattern, page 62
VI	video, page 47
VO	voice, page 47
WLAN	wireless local area network, page 1
WP	worst player, page 95
WS	wireless station, page 1

Chapter 1

Dissertation Overview

1.1 Introduction

In recent years, requirement of wireless data rate has continuously been increased due to vigorous development of new applications, e.g., multimedia transmission. However, it is difficult to provide users high data rate for these new applications in conventional cellular networks owing to longer transmission distance. In order to support higher throughput, more and more research focuses on short-range communications over the past decade. Among different standards, IEEE 802.11 and femtocell techniques are considered the two most well-adopted suites due to their popularization in the deployment. Various amendments are contained in the IEEE 802.11 suite, mainly including IEEE 802.11a/b/g [1–3] and IEEE 802.11e [4] for quality-of-service (QoS) support. Moreover, with increasing demands to support multimedia applications, the new amendment IEEE 802.11n [5, 6] has been proposed for achieving much higher throughput performance. The medium access control (MAC) protocol within the IEEE 802.11 standard supports the distributed coordination function (DCF) to regulate the random and complex medium accessing behaviors among the wireless stations (WSs) within the same wireless local area networks (WLANs). Furthermore, the point coordination function (PCF) initiated by the access point (AP) provides centralized polling-based schemes to support time-constrained traffic for the WSs.

On the other hand, according to the statistical data in [7], it is expected that there will be nearly 90% of data services and 60% of phone calls taken place in indoor environments. Hence, for long-term evolution-advanced (LTE-A), 3rd generation partnership project (3GPP) suggests that femtocell base stations (fBSs) with the properties of short-range, low-power, low-cost, and plug-and-play can be designed to connect into the end

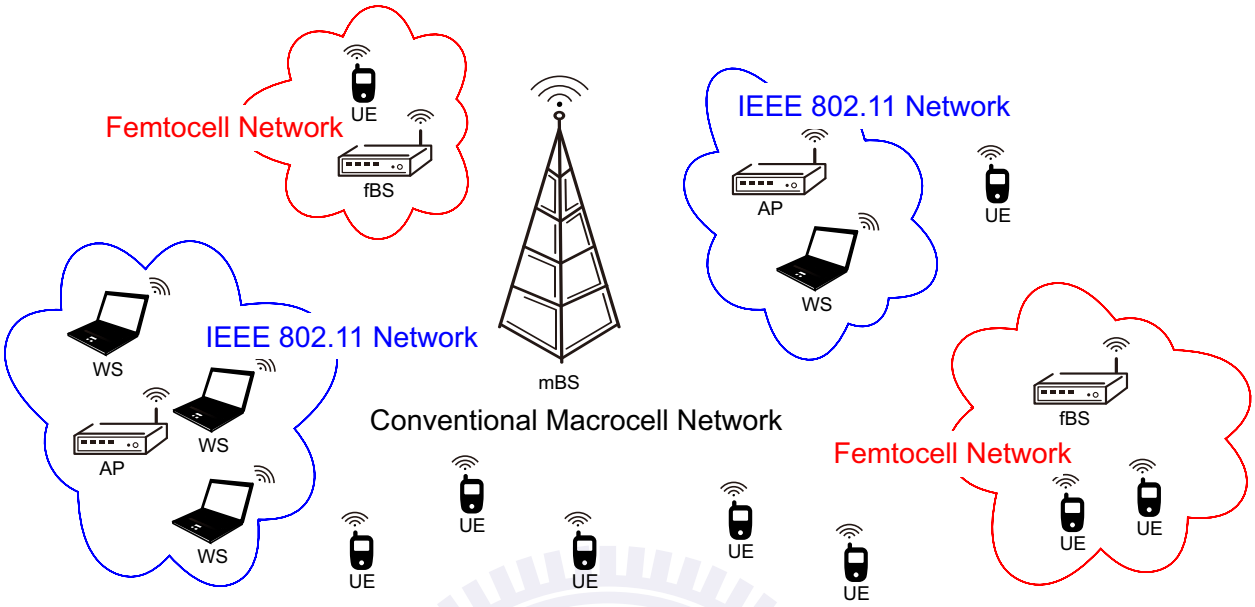

Figure 1.1: Wireless environment that contains macrocell, femtocell and IEEE 802.11 networks

user's broadband line in order to provide high throughput and QoS for the user equipments (UEs). Moreover, installation of fBSs can share the traffic load of its coexisting macrocell BSs (mBSs) [8]. Note that in order to distinguish IEEE 802.11 and LTE-A systems, "WS" and "AP" are employed in the IEEE 802.11 networks; while "UE" and "BS" are applied in the LTE-A system. Fig. 1.1 shows a wireless environment that contains macrocell, femtocell and IEEE 802.11 networks. It can be observed that WSs/UEs can benefit from better link qualities in IEEE 802.11 and femtocell networks than in conventional macrocell network due to shorter distance transmission.

The DCF is utilized as the basic access mechanism in the IEEE 802.11 MAC protocol. Based on the carrier sensing multiple access with collision avoidance (CSMA/CA) scheme, a WS will first perform carrier sensing to verify if the channel is available before data transmission. As the channel is idle for the time interval of DCF interframe space (DIFS), the random backoff process will be started for the purpose of decreasing the probability of data collision. Moreover, both the request-to-send (RTS) and clear-to-send (CTS) packets exchanged before the data transmission is exploited to resolve the potential hidden terminal problem. Moreover, in order to support QoS requirements, the enhanced distributed channel access (EDCA) mechanism is proposed in the IEEE 802.11e standard [4]. The EDCA protocol inherits conventional DCF's CSMA/CA scheme with the en-

hanced RTS/CTS handshaking process. Furthermore, four prioritized access categories (ACs) are defined in EDCA in order to support different types of network traffic. The QoS requirements for each AC is defined by selecting feasible values of the contention window (CW) size and arbitration interframe space (AIFS) length. It is intuitive to observe that higher priority AC should possess smaller values of CW and AIFS sizes. Each AC will wait for its AIFS length and independently select its own backoff number. Until the backoff number for a specific AC has been decremented to zero, the corresponding AC can initiate an RTS frame for channel contention. Each AC within a WS is considered as a standalone entity to contend with the ACs both in the same WS and the other WSs for channel access in the network. Distributed DCF/EDCA algorithms can be well-adapted for the irregular WLANs, nevertheless the performance cannot be further improved due to their low efficiency. Both RTS packet collisions and backoff delays will significantly reduce the network throughput.

Furthermore, the IEEE 802.11 task group N (TGn) [5] enhances the physical (PHY) layer data rate up to 600 Mbps by adopting advanced communication techniques, such as multi-input multi-output (MIMO) technology [9]. The MIMO technique utilizes spatial diversity to improve both the range and spatial multiplexing for achieving higher data rate. However, it has been investigated in [10] that simply improves the PHY data rate will not be sufficient for enhancing the system throughput from the MAC perspective. Accordingly, the IEEE 802.11 TGn further exploits frame aggregation (FA) and block acknowledgement (BA) techniques [6, 11] to moderate the drawbacks that are originated from the MAC/PHY overheads. Owing to adoptions of FA and BA, high-efficiency automatic repeat reQuest (ARQ) mechanisms are necessary to further improve system performance for IEEE 802.11n.

With the properties of easy implementation and low cost, DCF/EDCA schemes are popularly employed for the short-range wireless communication. However, it is difficult to execute seamless handover from IEEE 802.11 system to conventional macrocell due to definitely different core designs. On the other hand, since being proposed by telecommunication operator, femtocell techniques are much compatible with conventional macrocell. The seamless handover from femtocell to macrocell can therefore be achieved. Moreover, with adoption of centralized scheduling scheme, the efficiency of MAC layer in the femtocell is higher than that in the IEEE 802.11 network. That is why femtocell plays more and more important role in the current wireless networks. Nevertheless, there still exist several critical issues in the femtocell techniques, especially for the interference coordina-

tion between the macrocell/femtocell coexisting heterogeneous networks (HetNets). In order to enhance the spectrum efficiency, femtocell can be operated in the same band as the macrocell to serve its UEs. However, co-channel interference to the macrocell UEs may therefore be produced. The level of interference mainly depends on the access strategies of fBSs. Two major access policies are considered in femtocell network, including the closed access mode and open access mode. The closed access mode only permits authorized *subscribers* to utilize the fBS; while all users are allowed to connect to the fBS by adopting the open access mode. Closed access will intuitively be advantageous to the femtocell *subscribers*, however interference from the fBS to mBS's UEs can become severe in the closed access mode than in open access mode. On the other hand, system performance of the entire HetNet can be improved if fBS is operated in the open access mode. Nevertheless, open access mode is an obvious barrier to promote the popularization of femtocells since *subscribers* will not be interested in installing fBSs but accessed by other users [12].

1.2 Problem Statement

With the property of short-range transmission, both IEEE 802.11 series protocol and femtocell techniques can provide higher data rate for users. However, as mentioned in previous section 1.1, several crucial challenges restrain system performance from being further improved.

Problem 1 (Overhead). *How to reduce RTS collision probability and backoff delay for IEEE 802.11 WLANs?*

Problem 2 (Efficient ARQ Schemes). *For IEEE 802.11n WLANs, how to design efficient ARQ schemes to achieve both reliable data transmission and high system throughput?*

Problem 3 (Femtocell Access Strategies). *For macrocell/femtocell coexisting HetNets, which femtocell access strategy is recommended considering performance from the perspectives of* subscribers, *entire HetNet, and operator?*

The main goal in this dissertation is to proposed novel mechanisms for resolving these problems. In addition, analytical models will also be established to validate the performance of proposed algorithms.

1.3 Dissertation Organization

In order to solve **Problem 1**, an adaptive reservation-assisted collision resolution (ARCR) protocol modified from conventional DCF is proposed in Chapter 2 to both mitigate packet collision and reduce the backoff delays from the random access scheme for the WLANs. With its adaptable reservation period, the contention-based channel access can be adaptively transformed into a reservation-based system if there are pending packets required to be transmitted between the WSs and the AP. Furthermore, in order to support QoS requirements for multiple prioritized traffic, the enhanced-ARCR (E-ARCR) protocol is further proposed in Chapter 3 as the enhanced version of the ARCR scheme. Analytical models are derived for both proposed schemes to evaluate their throughput performance. It can be observed from both analytical and simulation results that the proposed ARCR and E-ARCR protocols outperform existing schemes with enhanced channel utilization and network throughput.

Furthermore, for the IEEE 802.11n standard, frame aggregation is considered one of the major factors to improve the system performance of WLANs from the MAC perspective. In order to achieve both reliable data transmission and high system throughput (**Problem 2**), two MAC-defined ARQ protocols are proposed in Chapter 4 to consider the effect from frame aggregation for the enhancement of network performance. An aggregated selective repeat ARQ (ASR-ARQ) scheme is proposed which incorporates the selective repeat ARQ scheme with the consideration of frame aggregation. On the other hand, for worse channel quality, the aggregated hybrid ARQ (AH-ARQ) mechanism is proposed to further enhance the throughput performance by adopting the Reed-Solomon (RS) block code as forward error correction scheme. Novel analytical models for both the ASR-ARQ and AH-ARQ protocols are established to evaluate the cumulative distribution function (CDF) of packet service time. Simulations are conducted to validate and compare the proposed ARQ mechanisms based on the service time and system throughput. Numerical evaluations show that the proposed AH-ARQ protocol can outperform the other schemes under worse channel condition; while the ASR-ARQ scheme is superior to the other mechanisms under better channel condition.

On the other hand, how to choose a feasible femtocell access strategy is considered an important issue for LTE-A HetNet system. It is concluded in [13] that open access mode can alleviate the interference and improve throughput for the entire HetNet compared to closed access mode. Moreover, from the economic viewpoint, open access is suggested

by telecommunication operators if the operators can charge from the users that connect to the femtocell. However, according to [12], *subscribers* or customers prefer femtocells with closed access than with open access since it is undesirable that their femtocells are accessed by the other users. In order to acquire better tradeoff between closed and open access modes, it is necessary to propose a new design, hybrid access mode, to allow some *nonsubscribers* to possess limited connections to the fBS. In order to evaluate the performance of closed, open, and hybrid access modes for **Problem 3**, *subscribers'* throughput, system throughput and operator's revenue will be compared in Chapter 5. The cell selection schemes for *nonsubscribers* to access the fBS are formulated based on theoretical gaming models to describe selfish behavior of individual UE. The existences of pure strategy Nash Equilibria (NEs) will be illustrated and proven for the defined cell selection games. By the observation at NEs, it is suggested to adopt hybrid access mode in order to provide higher flexibility for the performance enhancement of all *subscribers*, entire HetNet system and operator. Finally, conclusions are drawn in the Chapter 6 for this dissertation.

Chapter 2

Reservation-Assisted Protocol for IEEE 802.11 WLANs

- Adaptive reservation-assisted collision resolution (ARCR) protocol is proposed in this chapter to solve ***Problem 1*** *for IEEE 802.11 wireless local area networks. By adoption of adaptive reservation periods within the contention-based channel access networks, proposed ARCR algorithm can significantly improve packet collision and reduce the backoff delay compared to the other existing works.* [1]

2.1 Introduction

In recent years, the techniques for wireless local area networks (WLANs) have been prevailing exploited for both indoor and mobile communications. The applications for WLANs include wireless home gateways, hotspots for commercial usages, and ad-hoc networking for inter-vehicular communications. Among different techniques, IEEE 802.11 standard is considered the well-adopted suite due to its remarkable success in both design and deployment. Various amendments are contained in the IEEE 802.11 standard suite, mainly including IEEE 802.11a/b/g [1–3] and IEEE 802.11e [4] for quality-of-service (QoS)

[1] The chapter is based on

- Jia-Shi Lin and Kai-Ten Feng, "QoS-based Adaptive Contention/Reservation Medium Access Control Protocols for Wireless Local Area Networks," *IEEE Trans. Mobile Computing*, vol. 10, no. 12, pp. 1785-1803, Dec. 2011.
- Jia-Shi Lin and Kai-Ten Feng, "Design and Performance Analysis on Adaptive Reservation-Assisted Collision Resolution Protocol for WLANs," *ACM/Springer Journal on Wireless Networks (WINET)*, vol. 17, no. 4, pp. 973-986, May 2011.

support. The medium access control (MAC) protocol within the IEEE 802.11 standard supports the distributed coordination function (DCF) to regulate the random and complex medium accessing behaviors among the wireless stations (WSs) within the same WLAN. How to alleviate the probability of packet collision has been considered a crucial issue for the enhancement of network throughput.

Different types of schemes have been proposed in order to resolve the packet collision problem within the WLAN. The adjustment of contention window (CW) size has been considered an effective scheme in most of the existing research work [1, 14–21]. The binary exponential backoff scheme [1] as described in the IEEE 802.11 MAC protocol controls the waiting time duration for channel contention. The CW size will be increased or decremented with failed or successful transmission respectively. In general, the probability of packet collision can be decreased with augmented value of CW size, especially with a larger number of WSs in the network. However, excessive idle time resulted from the enlarged CW size will consequently degrade the channel utilization. In order to enhance the throughput performance for the conventional IEEE 802.11 protocol, the algorithm proposed in [14] increases the transition rate between the backoff stages associated with decreased value of minimum CW and incremented value of maximum CW size. The hybrid algorithm proposed in [15] combines both the exponential and the linear backoff for the purpose of decreasing packet collision; while the slow CW decrease (SD) scheme in [16] either doubles or halves the CW size according to the successfulness of packet transmission. The early backoff announcement (EBA) protocol [17] proposed a WS to record its next backoff number into the MAC head while transmitting data packets. All the other WSs will select their corresponding backoff numbers excluding this value in order to avoid potential packet collisions. Similar design concept was also presented in [18]; while [19] proposed a MAC protocol with multiple-step distributed in-band channel reservation. The gentle DCF (GDCF) protocol as proposed in [20, 21] maintains a larger value of the CW size compared to the conventional backoff scheme in order to decrease the probability of packet collision. The work in [22] proposed a handshake-based channel aware (HCA) MAC protocol which selects the WSs to access the channel according to its corresponding channel condition. Nevertheless, all the existing contention-based protocols suffer from the tradeoff between packet collision and transmission delay. Moreover, the throughput performance by adopting these algorithms is greatly influenced by the total number of WSs within the WLAN.

Compared to the DCF-based random access schemes, there are also polling-based al-

gorithms proposed for WLAN in order to provide feasible performance to fulfill time-constrained requirements. Various centralized polling protocols and scheduling algorithms (e.g., [23]) have been proposed to increase the channel utilization for the IEEE 802.11 point coordination function (PCF) [1]. The operation time period for each WS is divided into cycles of contention period (CP) and contention-free period (CFP), where CFP is utilized by either the PCF for real-time packet delivery. A reservation-based MAC protocol was employed in [24] to provide support for real-time traffic. The work in [25, 26] proposed piggyback schemes by adjusting the transmission rate of WS for throughput enhancement. However, the requirement to specifically assign the designated CFP for the implementation of polling-based algorithms will lead to excessive overhead if the WSs have no packet to be delivered to the access point (AP). Moreover, these AP-initiated polling protocols can not completely fulfill the throughput requirement while the WSs are intending to conduct uplink data transmissions. Moreover, the channel reservation MAC protocol was presented in [27] to provide automatic scheduling of channel usage between the WSs. However, this scheme requires both a busy tone channel and multple antennas in order to resolve the hidden terminal problem.

It is noted that there are tradeoffs between the centralized-based and contention-based schemes under different network environments. It will be beneficial to provide a channel access mechanism that can adaptively switch between these two types of schemes. Therefore, an adaptive reservation-assisted collision resolution (ARCR) protocol is proposed in this chapter in order to alleviate packet collisions within the random access scheme. The main feature of proposed ARCR scheme is that the original contention-based channel access will be adaptively transformed into a reservation-based system in the case that there are pending requests for packet transmission from the WSs. With the adaptable reservation period by exploiting the ARCR algorithm, packet collision resulting from channel contention can be effectively reduced which consequently leads to enhanced network throughput. Analytical model for throughput analysis is developed in this chapter to provide feasible observations on the behaviors of proposed ARCR protocol. Numerical results are conducted via simulations both to provide validation on the analytical models and to evaluate the effectiveness of proposed scheme. It can be observed that network throughput can be enhanced by adopting the ARCR algorithm compared with other existing protocols.

The remainder of this chapter is organized as follows. Section 2.2 briefly summarizes the IEEE 802.11, the GDCF, and the EBA protocols. The proposed ARCR scheme is de-

scribed in Section 2.3 associated with its throughput analysis presented in Section 2.4. Section 2.5 illustrates the performance validation and evaluation for the proposed ARCR protocol; while conclusions are drawn in Section 2.6.

2.2 Preliminaries

2.2.1 IEEE 802.11 MAC Protocol

The DCF is based on the carrier sensing multiple access with collision avoidance (CSMA/CA) scheme to ensure that each WS can acquire a fair chance to access the wireless medium. A WS that intends to transmit data will first sense the channel to verify if it is at the idle state. As the channel is idle for the time interval of DCF interframe space (DIFS), the random backoff process will be started which is executed in each WS for the purpose of decreasing the probability of data collision. The random number k_{dcf} at the backoff stage i is chosen within the range of a uniform distribution $U[a, b]$, i.e., $k_{dcf} = U[0, 2^i W - 1]$ where W denotes the minimum backoff window size. It is noted that the backoff stage i corresponds to the number of transmission retries. Moreover, both the request-to-send (RTS) and clear-to-send (CTS) packets exchanged before the data transmission is exploited to resolve the potential hidden terminal problem. In order to avoid packet collision during data transmission, the virtual carrier sensing mechanism carried out by the network allocation vector (NAV) is utilized to record the duration of on-going data transmission. It is noted that the NAV information adopted within each WS will be delivered to its neighbor nodes. A nonzero NAV value recorded in a WS will consequently prohibit the surrounding neighbor nodes to initiate a new data transmission.

Unlike the contention-based DCF scheme, the PCF supported by IEEE 802.11 standard is designed to be a centralized polling protocol. Periodic occurrences of CP and CFP are designed for each WS, where CP is operated by DCF and CFP is executed by polling mechanism. The AP will broadcast a beacon message to inform all the WSs regarding the start of CFP. Based on a polling list of WSs recorded within the AP, the AP will sequentially transmit the CF-Poll control frame to the WS within the list by adopting the round-robin scheduling algorithm. If a WS that receives the CF-Poll frame has data to be delivered, the WS will transmit data packets to the AP after waiting for a short interframe space (SIFS). The AP correctly receiving data packets will send a CF-ACK frame in response to the WS after waiting for the SIFS time interval. On the other hand, in the case that the AP did not receive any data packet within the time interval of PCF interframe space (PIFS), it will

continue to poll the next WS in its corresponding polling list. After all the WSs in the list have been consecutively polled, the AP will broadcast the CF-End frame as the indication for the end of CFP. Afterwards, all the WSs in the network will enter into the CP mode with the adoption of contention-based DCF scheme.

2.2.2 Gentle DCF (GDCF) Protocol

The GDCF algorithm in [20, 21] modifies the conventional backoff scheme within the IEEE 802.11 protocol for the enhancement of network throughput. The major parameter in GDCF scheme is the design of a successful counter for recording the number of consecutive successful transmissions. The counter will be reset to zero every time a failed transmission occurs. Similar to the conventional DCF scheme, the CW size will be doubled if the packet for the WS is failed in transmission. On the other hand, in the case of successful packet transmission, the CW size by adopting the GDCF protocol will not be reset back to the minimal CW size as the DCF scheme. The CW size will be maintained until there exist c successful transmissions of data packets, and the size will be halved only after the c consecutive transmissions have been achieved. Consequently, the packet collision owing to the channel contention can be alleviated with the adoption of GDCF scheme. However, the network throughput can only be enhanced with the reduction of RTS packet collisions while there exists a large number of WSs within the network. In the case that there is a comparably smaller number of WSs in the considered network, the design of an enlarged CW size will degrade the network throughput, which consequently results in elongated transmission delay.

2.2.3 Early Backoff Announcement (EBA) Protocol

The main concept of EBA protocol [17] is to select the next backoff counter earlier and also inform the other WSs in the current transmission. An extra field, called EBA field, is piggybacked after the MAC header in order to record the value for the WS to select in its next contention. The other WSs will hear the value of backoff counter chosen by this WS, and avoid picking the same slot for channel contention. Each WS will maintain a reservation window to record the slots occupied by other WSs according to the EBA field received from others. If a WS selects a backoff number but hears that this number will be utilized by another WS, it will choose another empty slot to avoid collision with that WS. Moreover, the authors proposed two different methods for CW selection, i.e., the EBA-1 and EBA-2 schemes. Similar to the conventional DCF protocol, the EBA-1 scheme

randomly chooses a value based on the current CW. The difference is that the WS will be kept away from the occupied slot by adopting the EBA-1 scheme. On the other hand, in the EBA-2 method, the WS will calculate the number of occupied slot a to estimate the number of WSs existed in the network. The CW size will be set as $2a$ and the backoff counter will be randomly selected in this range excluding the occupied slot. Moreover, the minimum CW size (W) is assumed to be 8 in the EBA-2 method except that $W = 0$ is chosen if the WS enters the network for the first time. Intuitively, the EBA-2 scheme can adapt to the environment change faster than the EBA-1 method.

2.3 Proposed ARCR Protocol

The design concept of proposed ARCR algorithm is to adaptively provide reservation periods for specific WSs within the contention-based channel access networks. In order to promote the network throughput without incurring excessive control overhead, the piggyback mechanism [28] is utilized to append the control messages after either the data or the acknowledge (ACK) packets. The piggybacked fields introduced by the ARCR protocol are applied in order to alleviate the RTS/CTS/ACK overheads, to regulate the backoff processes, and to schedule the transmission orders, which ultimately can achieve higher network throughput. With the enhanced channel utilization by adopting the proposed ARCR scheme, it will be illustrated in the numerical evaluation that the overheads from the piggybacked control fields are observed to be insignificant. The functional description of proposed ARCR scheme is described in Subsection 2.3.1. The examples of both ideal and realistic network scenarios for the proposed scheme are addressed in Subsections 2.3.2 and 2.3.3.

2.3.1 Functional Description

As a WS intends to transmit data packets within an IEEE 802.11 AP-based network, an RTS/CTS exchange process will be initiated before the transmission of data packets. In the case that there are additional data packets to be delivered, a control field called table-adding request (TAR) will be appended after the data packet for piggyback purpose, i.e., denoted as DATA+TAR. On the other hand, the conventional DCF scheme will be adopted if there is no further data packet to be dispatched. The TAR control field is defined as follows.

Definition 2.1 (TAR). *TAR (Table-Adding Request) is defined as a control field used to inform the AP that a WS is intending to join the AP's reservation table.*

After receiving the DATA+TAR packet from the WS, the AP will record the MAC address of the corresponding WS within its reservation table $\mathbf{T} = \{T_r(S), \forall r, S\}$ that consists a list of prioritized numbering for each WS, e.g., $T_0(A)$ indicates that WS A is recorded in the first entry (i.e., $r = 0$) of the reservation table $\mathbf{T}$. Consequently, the AP will respond with an ACK packet associated with a piggybacked field called next transmission order NTO(r), which is defined as follows.

Definition 2.2 (NTO(r)). *NTO(r) (Next Transmission Order) is defined as a control field adopted by the AP to inform a WS that its order for the next transmission is r.*

For example, $r = 0$ indicates that the WS is recorded at the top of the reservation list $\mathbf{T}$, which will be the next WS to conduct packet transmission. Therefore, each WS that are recorded in the reservation table will be informed by the AP with the ACK+NTO(r) packet. By adopting the ARCR scheme, the random backoff number k_{arcr} for the WS will be selected based on the corresponding index r as

$$k_{arcr} = \begin{cases} U[0, 2^0 W - 1], & r = 0, \\ U[2^{r-1} W, 2^r W - 1], & 1 \leq r \leq M, \\ U[\ell \cdot 2^{M-1} W, u \cdot 2^{M-1} W - 1], & r > M, \end{cases} \tag{2.1}$$

where $\ell = r - M + 1$, $u = r - M + 2$, and the parameter M denotes the maximum number of backoff stage. According to the transmission order r, it can be observed from (2.1) that each specific WS S within the table entry $T_r(S)$ will possess a distinct range of values for its corresponding random backoff number k_{arcr}. This design will assure that small value of r will result in smaller random backoff number k_{arcr}. Consequently, based on the reservation system of the ARCR scheme, the WS with the smallest value of r (i.e., at the top of the reservation table) will be ensured to acquire the channel access comparing with the other WSs within the table $\mathbf{T}$. It is also noticed that the backoff scheme is transformed from exponential to linear increase for the purpose of limiting the range of random number k_{arcr} after $r > M$.

Definition 2.3 (RTS-R). *The RTS-R packet signifies the initiation of the reservation period, which is delivered by the WS after acquiring the ACK+NTO(r) packet from the AP.*

After the WS is informed by the AP that it will be the next station to conduct packet transmission, the WS is ready to transmit its RTS-R packet in order to initiate the reservation period. The transmission of RTS-R packet will be delivered from the WS after it has succeeded in contending the channel access by adopting its random backoff number k_{arcr} as in (2.1). After the RTS-R/CTS handshake has been completed, either the DATA +TAR packet or the DATA packet will be transmitted from the WS to the AP. Once the data transmission has been accomplished, the table entry $T_r(S)$ will remain in or be removed from the reservation table if the DATA+TAR packet or the DATA packet is transmitted respectively. Furthermore, in the case that there are remaining table entries within $\mathbf{T}$, the AP will transmit its ACK packet appended with a request for data (RFD) field towards the WS that is recorded within the next table entry. The RFD field is defined as follows.

Definition 2.4 (RFD(r)). *RFD(r) (Request for DATA) is defined as a control field utilized by the AP to inform the r-th WS in the reservation table that it can conduct packet transmission after waiting for a short interframe space (SIFS) duration.*

The ACK+RFD(r) packet is employed to serve as the indication message from the AP to the WS for requesting the next data transmission, which is delivered within the reservation period. Without conducting the backoff process, the corresponding WS can immediately transmit its DATA+TAR (or DATA) packet to the AP after a SIFS interval. The procedures for transmitting the ACK+RFD(r) packet will be continuously conducted until all the table entries within the reservation table $\mathbf{T}$ have been processed. The ARCR algorithm will be switched from the reservation-based system back to the contention-based DCF scheme. It is especially noticed that there is only one RTS-R packet required for channel contention within the entire reservation period. With the exploration of adaptive reservation period, the proposed ARCR scheme can reduce packet collision from the RTS packets, which effectively increases the channel utilization.

Furthermore, the fairness for packet transmission between the WSs is also considered within the reservation period of proposed ARCR scheme. All WSs within the reservation table will be scheduled by the AP based on the round-robin fashion in order to maintain the fairness for packet transmission. Considering that all the WSs continuously have data packets to be delivered, i.e., the DATA+TAR packets are always transmitted by the WSs, the WS that is informed by the AP with the order r (i.e., NTO(r)) will be assigned with the order of $r-1$ for its next transmission with NTO$(r-1)$. It is noted that the WS with the order of $r=0$ will therefore be assigned with the maximum value of r for its next transmission order.

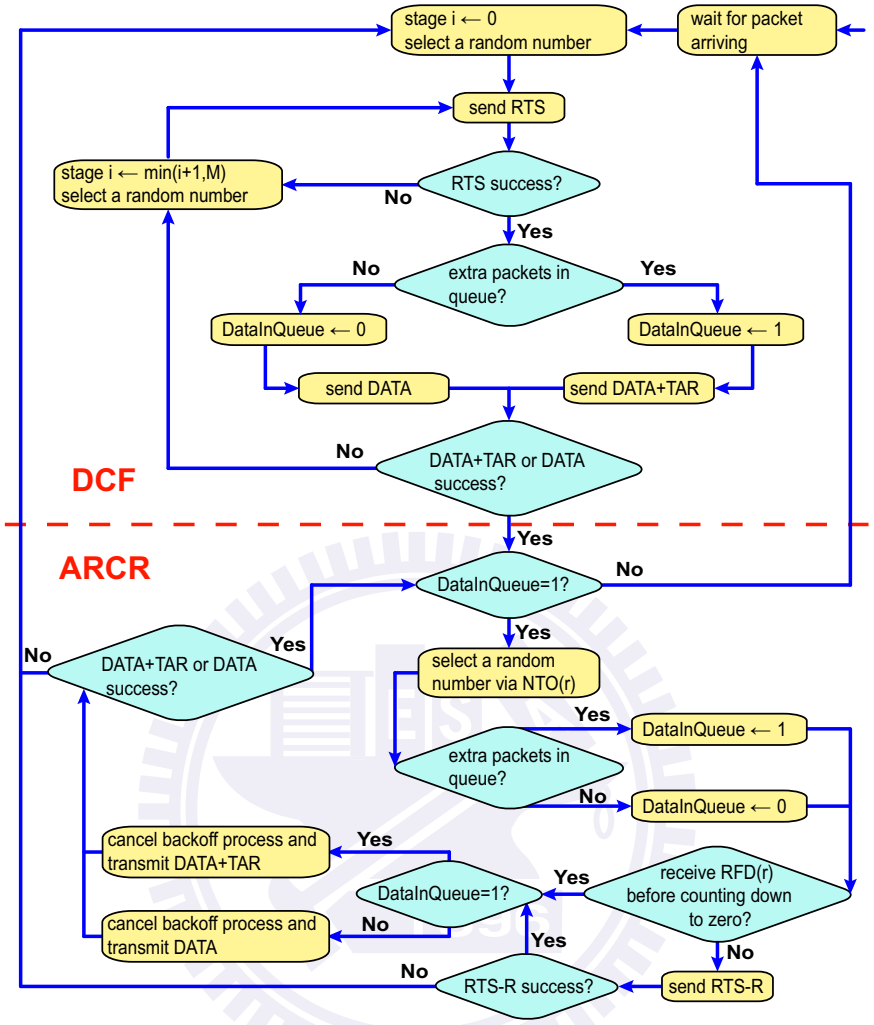

Figure 2.1: The flow chart for the behavior of WS by adopting the proposed ARCR protocol.

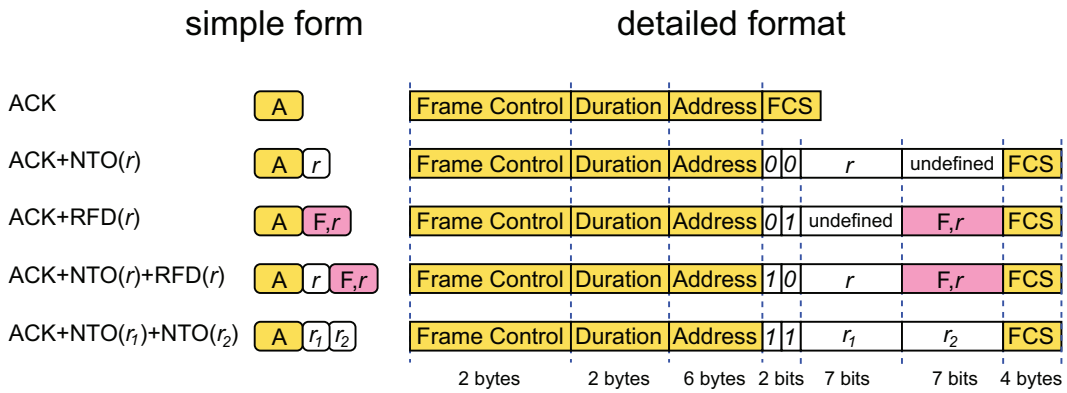

Figure 2.2: The formats of ACK packets with different piggybacked control fields.

Fig. 2.1 shows the flow chart for each WS by adopting the proposed ARCR protocol. As a WS enters the network at the first time, it will stay in the DCF mode and wait for packet arrival. In the case that the WS possesses data packets to be delivered, the WS will send out an RTS packet to contend for channel access. Assuming that the WS wins the channel contention, it will verify there exists additional packet in its queue to be delivered. If there are extra packets, the flag *DataInQueue* will be set to 1, and the DATA+TAR packet will be transmitted. Otherwise, the flag *DataInQueue* will be 0 and a pure DATA packet will be delivered. After successful transmission of the packet, if *DataInQueue* $= 1$, the WS will select a random number in the range based on the NTO(r) value given by the AP. Afterwards, if the WS receives the RFD(r) field before the backoff counter goes down to 0, the WS will cancel its backoff process and transmit either the DATA+TAR or DATA packet after waiting for a SIFS interval. Otherwise, the WS will send out an RTS-R packet for channel contention. The transitions between the conventional DCF scheme and the ARCR algorithm are also illustrated. Either the WS failed in packet transmission or it has no further data to be delivered, the ARCR scheme will be switched back to the DCF protocol with the implementation of random backoff scheme for packet retransmission. It is noted that the AP is in charge of all the WS within the reservation table; while those WSs that are out of the reservation table will conduct the RTS/CTS handshakes with the AP. Therefore, the hidden terminal problem can be resolved in the proposed ARCR algorithm since the AP will set the NAV vector to all the WSs in the network. Moreover, several types of control fields can be piggybacked after the ACK packet, e.g., NTO(r) or RFD(r). Fig. 2.2 shows the formats of ACK packet with different piggybacked control fields. Therefore, while receiving the ACK packet, the WS can recognize the type of ACK packet according to the value within the two-bit flag as illustrated in Fig. 2.2. Different types of transmission scenarios will be exemplified in the following two subsections.

2.3.2 Ideal Network Scenarios

Fig. 2.3(a) shows an example for an ideal network scenario by exploiting the proposed ARCR algorithm. In this case, it is assumed that the channel is error-free without any packet collision occurred. Three WSs A, B, and C within the network are intending to continuously transmit data packets to the AP. At the beginning time instant t_1, no entry is recorded within the AP's reservation table $\mathbf{T}$; while the three WSs are contending for channel access by adopting the IEEE 802.11 DCF mechanism. It is assumed that WS A acquires the channel access after the contention, the conventional RTS/CTS exchange will

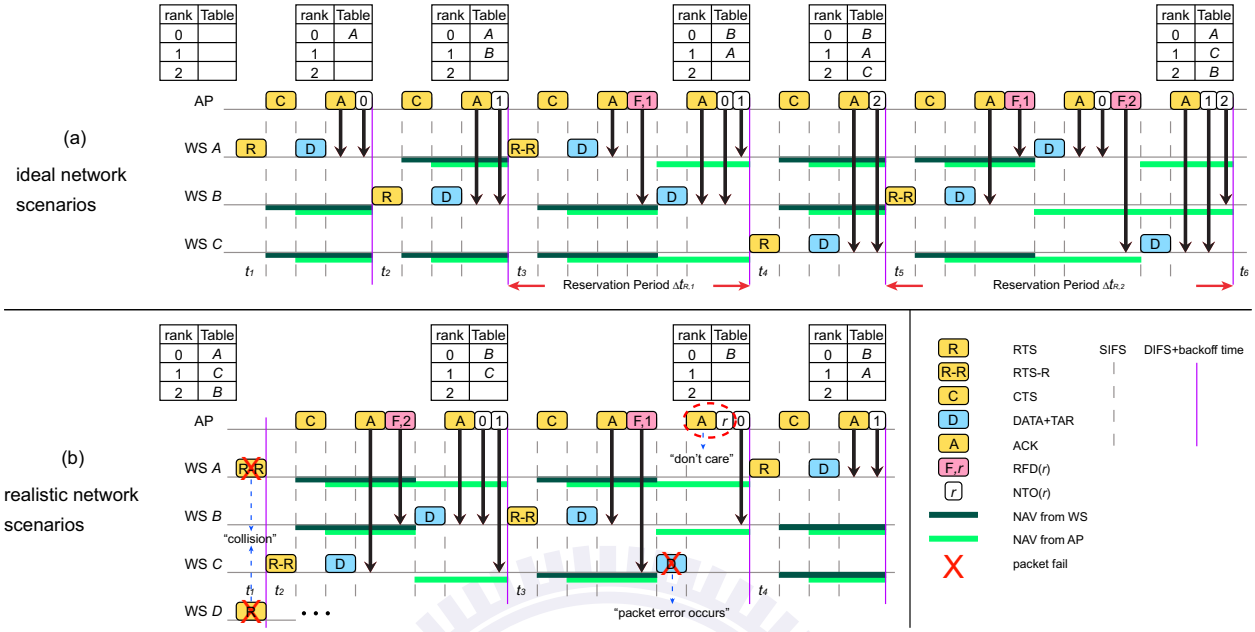

Figure 2.3: The timing diagram for the proposed ARCR protocol under ideal network scenarios.

be conducted between WS A and the AP. The DATA+TAR packet will be delivered from WS A to the AP, where the TAR field indicates the request from node A that it still possesses remaining data packet to be transmitted. After the table entry $T_0(A)$ has been added to the reservation table $\mathbf{T}$, the AP will transmit the ACK+NTO(0) packet to WS A indicating that it will be the first WS to conduct packet transmission in the next reservation period. It is noted that the NAV vector is utilized to suspend potential channel sensing and packet transmissions from both WSs B and C during the interaction time interval between WS A and the AP.

After WS A completes its first transmission with the AP, the three WSs will continue to compete for the channel access at time t_2. Since WS A has received the NTO(0) packet from the AP, it will employ the random backoff scheme in (2.1) by adopting the ARCR scheme; while the conventional backoff scheme from the DCF mechanism will be applied to both WSs B and C. Considering that WS B has obtained the channel access, similar procedures between WS B and the AP will be taken place, i.e., the transmission of RTS, CTS, DATA +TAR, and ACK+NTO(1) packets between WS B and the AP. The table entry $T_1(B)$ will also be included in the AP's reservation table $\mathbf{T}$. Due to the reason that both WSs A and B have received the NTO(r) packets, the random backoff scheme from (2.1) is exploited for both nodes at time instant t_3; while the conventional DCF backoff mechanism will be

adopted by WS C. Owing to the special design of the random backoff algorithm as in (2.1), the WS with the smallest r value (i.e., WS A in this case) will be ensured to have the highest opportunity to acquire the channel access among the WSs recorded in the table. Therefore, there will only be either WS A or C that will finally win the channel access after the time instant t_3.

Assuming that WS A acquires the channel access after t_3, the RTS-R packet will be initiated by WS A to start the reservation period for both WSs A and B, i.e., $\Delta t_{R,1}$ as shown in Fig. 2.3. After the reception of the DATA+TAR packet from WS A, the AP will respond with the ACK+RFD(1) packet where the ACK packet is intended for WS A and the RFD(1) field is targeting for WS B. Note that as WS A receives this type of ACK packet, i.e., ACK +RFD(r), WS A will know that it is the first successfully transmitted WS in this reservation period. Based on the received RFD(1) field from the AP, WS B will terminate its backoff process and conduct the transmission of DATA+TAR packet to the AP after a SIFS time interval. It is noted that the cancelation of the backoff process for WS B can reduce the channel idle time, and consequently promotes the network throughput. After the completion of the DATA+TAR packet from WS B, the AP will respond with an ACK+NTO(0) +NTO(1) packet where the ACK+NTO(0) packet is delivered to WS B and NTO(1) packet is intended for WS A. It is noticed that the transmission order within the reservation system has been swapped for the consideration of fairness, i.e., $\mathbf{T} = \{T_0(B), T_1(A)\}$.

Considering that WS C finally acquires the channel access at t_4, the table-adding procedures will be conducted for WS C after the completion of its data transmission, i.e., $\mathbf{T} = \{T_0(B), T_1(A), T_2(C)\}$. Consequently, at t_5, the reservation period $\Delta t_{R,2}$ will be utilized to conduct packet transmission for all the three WSs that are recorded within the reservation table $\mathbf{T}$. First of all, the AP does not have the information regarding the total number of WSs that will continue to stay in the reservation table before the end of reservation period. Therefore, the AP will not give out the NTO(r) field after WS B finished its data transmission, i.e., only the ACK+RFD(1) packet is delivered where the ACK packet is intended for WS B and the RFD(1) field is targeting for WS A. WS B will understand that it is the first successfully transmitted WS in the reservation period after receiving the ACK+RFD(1) packet where the ACK packet is targeting for itself. Next, as WS A finishes its data transmission, the AP will deliver the ACK+NTO(0)+RFD(2) packet where the ACK+NTO(0) part is for WS A to inform WS A to be the first WS in the next round's reservation table. Note that the RFD(2) part is to inform WS C that it will be the next WS for data transmission. After WS C transmits its data packet, it will receive an ACK

+NTO(1)+NTO(2) packet and recognize that NTO(1) is targeting for itself since the ACK packet is specified for WS C. WS C recognizes that it will be the second item recorded in the reservation table for the next round. On the other hand, as WS B receives the same ACK+NTO(1)+NTO(2) packet, it will understand that the second NTO, i.e., NTO(2), is designated for itself since this type of ACK packet specifies the end of this reservation period. WS B will be assigned with a lower priority on the next reservation period based on the round-robin fashion. Afterwards, the transmission order will be rotated for the purpose to ensure the transmission fairness i.e., $\mathbf{T} = \{T_0(A), T_1(C), T_2(B)\}$. Therefore, with the recognition of the different types of ACK packets, it is not required for the WSs to include their station identifier in the NTO field. In the case that there exists a new WS (e.g., WS D) that joins the network at the time instant t_6, channel contention will occur between WSs A and D. Otherwise, a new reservation period $\Delta t_{R,3}$ will be initiated to continuously transmit the packets from WSs A, B, and C.

2.3.3 Realistic Network Scenarios

The examples for the proposed ARCR scheme to alleviate the packet collision problems under an realistic network scenario is shown in Fig. 2.3(b). First of all, the adaptive adjustment of ARCR scheme owing to the RTS-R packet collision is considered. Assuming that the AP's reservation table is recorded as $\mathbf{T} = \{T_0(A), T_1(C), T_2(B)\}$ before the time instant t_1. Since WS A is situated at the top of table $\mathbf{T}$, it will possess the smallest backoff number k_{arcr} according to (2.1) which results in the acquisition of channel access.

WS A will initiate the RTS-R packet to the AP, and it is assumed to be unsuccessfully transmitted due to packet collision. Without receiving the CTS packet from the AP, WS A will change its channel access mechanism from the ARCR algorithm back to the conventional DCF scheme. As shown in the flow chart from Fig. 2.1, the random number k_{dcf} will be selected via the original DCF scheme with backoff stage $i = 0$, i.e., within the range of $U[0, 2^0W - 1]$. On the other hand, since WS C did not obtain the RFD(1) field from the AP, it will continue its random backoff process. Therefore, both WSs A and C will be involved in contending the channel access at time t_2. Considering that WS C is successful in acquiring the channel, it will start the reservation period by sending the RTS-R packet to the AP. With the reception of the RTS-R packet, the AP will notice that its first table entry $T_0(A)$ is not available for data transmission. Consequently, the entry $T_0(A)$ is removed such that the reservation table will become $\mathbf{T} = \{T_0(B), T_1(C)\}$. It can be observed that all the WSs within the reservation table are assigned with the random number k_{dcf} based on

the ARCR scheme. If the RTS-R packet of the WS with NTO(0) fails, the WS with NTO(1) can continue to conduct the corresponding reservation process.

The transmission priorities that are recorded within the reservation table will be changed after the packet transmissions for both WSs B and C, i.e., $\mathbf{T} = \{T_0(B), T_1(C)\}$. For the next reservation period starting from t_3, after WS B accomplishes its packet transmission with the AP, WS C will receive the RFD(1) message from the AP and start to dispatch its DATA +TAR packet. Considering that the DATA+TAR packet failed in transmission due to channel error, the AP will wait for a period required for successful packet transmission, i.e., the AP timout period, to recognize this situation and consequently remove WS C from its reservation table as $\mathbf{T} = \{T_0(B)\}$. Moreover, if there are still other table entries recorded behind the removed table entry, the AP will continue to initiate the RFD message to the remaining WSs for packet transmissions. On the other hand, without any further acknowledgement from the AP, WS C will change its channel access mechanism from the ARCR algorithm back to the DCF scheme. At time t_4, all the three WSs will be in the process to contend for channel access, and similar procedures are implemented to conduct packet transmission.

Similar processes can be examined as above in the case that either the ACK+NTO or the ACK+RFD packet failed in its transmission from the AP to the corresponding WS. The AP will remove the table entry for the WS after waiting for the AP timeout period; while the WS will be adaptively switched back to its original DCF mode for channel contention.

2.4 Throughput Analysis of Proposed ARCR Protocol

Analytical study is performed in order to explore the benefits of proposed ARCR protocol. The backoff process of DCF scheme is first modeled by the Markov chain model in Subsection 2.4.1. The probability for a WS to join the reservation table is derived in Subsection 2.4.2. As a consequence, the analytical model of throughput performance for proposed ARCR protocol will be obtained in Subsection 2.4.3.

2.4.1 Backoff Process of DCF Scheme

There are existing research [29–34] establishing the analytical models for the backoff process of DCF scheme under certain assumptions. Bianchi [29] proposed a Morkov Chain model to evaluate the throughput performance of DCF scheme under staturation. The research work in [34] improved the Bianchi's model by considering the retry limit specified

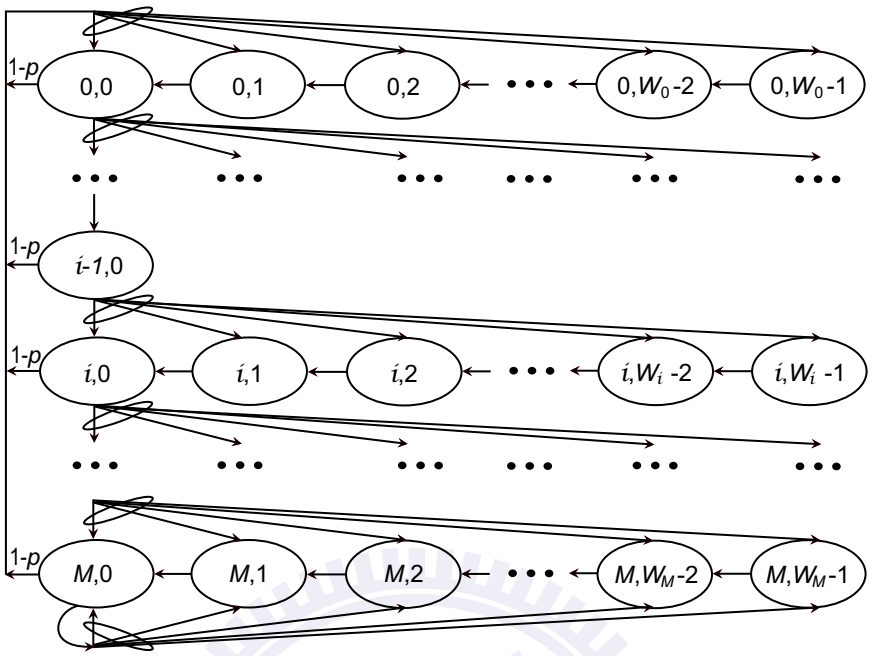

Figure 2.4: The two-dimensional Markov chain model for the backoff process of the DCF scheme.

in the IEEE 802.11 MAC protocol; while backoff suspension is considered in [33]. The work proposed in [30] ponders both retry limit and fading channel in the proposed model, and [32] considers both retry limit and backoff suspension. Moreover, the retry limit, backoff suspension, and fading channel are considered in the model for throughput and delay analysis as proposed in [31]. The two-dimensional Markov chain model utilized in [30] is adopted as the baseline model to analyze the random backoff process in the proposed ARCR protocol.

As shown in Fig. 2.4, the parameter p represents the probability of failed transmission due to packet collisions or channel noise. $W_i = 2^i W$ is defined as the backoff window size at the stage i for $0 \leq i \leq M$, where W denotes the minimum backoff window size. Let $s(t)$ and $b(t)$ be two stochastic processes represent the backoff stage and the backoff time counter of a WS at time t, respectively. It is noted that discrete and integral time scale for the decrements of backoff time counter is adopted in the analysis. The backoff time counter will decrease by one in a slot time σ as the channel is sensed idle.

Let $b_{i,k}$ denotes the stationary distribution of the two-dimensional stochastic process $\{s(t), b(t)\}$ as a WS lies at the ith backoff stage with its counter equal to k. As shown in Fig. 2.4, a WS in backoff stage i will randomly select a number within $[0, W_i - 1]$ and start to countdown if the channel is sensed to be idle. The WS will successfully transmit with

probability $1-p$ after the counter k decreases to zero. It will consequently be reset to the minimum window size, i.e., $i=0$, for the next channel contention. On the other hand, the WS will be at the $(i+1)$th backoff stage if collision happens for packet transmission. In the case that the current backoff stage is M and the transmission fails, the next backoff stage will still remain at the stage M. The relationship between each state is derived as follows:

$$\begin{cases} P(b_{i,k}|b_{i,k+1}) = 1, & 0 \le k \le W_i - 2, 0 \le i \le M, \\ P(b_{0,k}|b_{i,0}) = (1-p)/W_0, & 0 \le k \le W_0 - 1, 0 \le i \le M, \\ P(b_{i,k}|b_{i-1,0}) = p/W_i, & 0 \le k \le W_i - 1, 1 \le i \le M, \\ P(b_{M,k}|b_{M,0}) = p/W_M, & 0 \le k \le W_M - 1. \end{cases} \tag{2.2}$$

It is noticed that each steady state probability $b_{i,k}$ can be expressed as a function of $b_{0,0}$ after transformation based on the equations in (2.2). Since the sum of all the states will be equal to 1, namely $\sum_{i=0}^{M}\sum_{k=0}^{W_i-1} b_{i,k} = 1$, $b_{0,0}$ can be obtained as

$$b_{0,0} = \frac{2(1-p)(1-2p)}{(1-2p)(W+1) + pW\left[1-(2p)^M\right]}. \tag{2.3}$$

let τ be defined as the probability that a WS transmits a RTS packet in a randomly selected time slot. Based on the model in Fig. 2.4, a WS can transmits its RTS packets only if the backoff counter k reaches zero. Therefore, the parameter τ can be acquired as

$$\tau = \sum_{i=0}^{M} b_{i,0} = \frac{b_{0,0}}{1-p} = \frac{2(1-2p)}{(1-2p)(W+1) + pW\left[1-(2p)^M\right]}. \tag{2.4}$$

In order to solve τ and p in (2.4), another relationship between these two parameters should be obtained. Let P_f be denoted as the packet error rate due to the existence of channel noises and P_c be the probability that the packet issued by one WS collides with those from other WSs. Noted that the packet error rate P_f can be computed from the bit error rate (BER) which is derived from signal-to-noise ratio (SNR) of the channel states. Assuming that there are N WSs in the wireless network, P_c can be interpreted as the event that at least one WS transmits packets among the remaining $N-1$ WSs, i.e., $P_c = 1-(1-\tau)^{N-1}$. Therefore, the probability of failed transmission p can be obtained as

$$p = P_c + P_f - P_c P_f = 1-(1-\tau)^{N-1} + P_f(1-\tau)^{N-1}. \tag{2.5}$$

By iteratively solving the nonlinear functions (2.4) and (2.5), the two parameters τ and p

can therefore be obtained. In the next subsection, the behavior that whether a WS will become an entry in the reservation table will be depicted.

2.4.2 Derivation of Reservation Probability

The major task in this subsection is to derive the parameter P_t which refers as the transition probability that a WS either is in or will join the reservation table, named as *reservation probability*. As described in Subsection 2.3.3, the WSs will be added into or removed from the AP's reservation table $\mathbf{T}$ according to the proposed ARCR scheme. Therefore the total number of effective WSs will vary with the transmission events that happen in the network. In the proposed ARCR protocol, the effective WSs are defined as the set which consists of (a) the WSs that adopt the DCF scheme for channel contention and (b) the WS in the first entry of the reservation table $\mathbf{T}$. Consider that the AP has recorded several WSs in its reservation table $\mathbf{T}$. If a WS successfully completes its transmission by applying the DCF scheme, it will be added as the last entry in $\mathbf{T}$ and the number of effective WSs will be decreased by one. On the other hand, the number of the effective WSs will be increased by one if any of the WSs recorded in $\mathbf{T}$ is forced to be removed from the table under certain network scenarios. Let $n_{e,r}$ be referred as the number of the effective WSs in the network on the condition that there are r WSs in the reservation table $\mathbf{T}$. The relationship between the number of WSs r in the reservation table $\mathbf{T}$ and the number of effective WSs $n_{e,r}$ in the network is represented as

$$n_{e,r} = \begin{cases} N, & r = 0, \\ N - r + 1, & 1 \leq r \leq N. \end{cases} \tag{2.6}$$

According to (2.6), if the reservation table $\mathbf{T}$ is empty (i.e., $r = 0$), $n_{e,0}$ will be equal to N and all the effective WSs will compete the channel by using the DCF scheme. In the case that there is one WS in $\mathbf{T}$, the parameter $n_{e,1}$ will still be equal to N since the WS in $\mathbf{T}$ will need to contend for channel access with the other $N - 1$ WSs that are not in the table. Considering that there are $n_{e,r}$ effective WSs in the network, the numbers of WSs reside inside and outside the reservation table $\mathbf{T}$ will be $N - n_{e,r} + 1$ and $n_{e,r} - 1$ respectively.

A WS which joins in or departs from the reservation table $\mathbf{T}$ will affect the degree of channel contention in the wireless network. If a WS joins in the reservation table $\mathbf{T}$, the number of effective WSs will decrease and the occurrence of packet collisions will be reduced. On the other hand, the transmitted packets will potentially suffer from more collisions when the number of effective WSs is increased owing to the departure of WSs

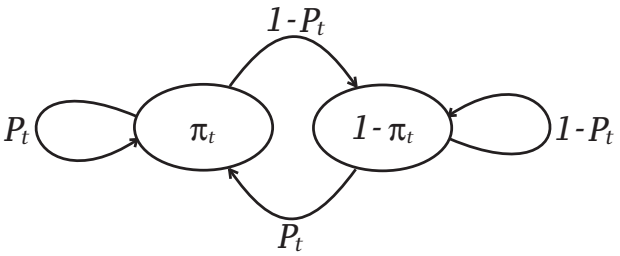

Figure 2.5: The Markov model of reservation probability P_t for the proposed ARCR protocol.

from the reservation table $\mathbf{T}$. To simplify the interactions among the WSs, it is assumed that whether a WS will join in or depart from the reservation table is independent to the strategies adopted by the other WSs. Fig. 2.5 shows the transitions between the steady states according to whether a WS will be recorded in the reservation table $\mathbf{T}$. The parameter π_t is defined as the steady state probability that a WS will reside in the reservation table $\mathbf{T}$, which can be obtained as

$$\pi_t = \pi_t \cdot P_t + (1 - \pi_t) \cdot P_t = P_t. \tag{2.7}$$

In order to solve the reservation probability P_t, another relationship between π_t and P_t will be required. Given that there are r WSs in the reservation table which corresponds to $n_{e,r}$ effective WSs in the network, the parameters $P_{c,r}$ and τ_r are respectively denoted as the probabilities of collisions and the events that a WS transmits its RTS packet in a random slot time. Based on the iterative computation between (2.4) and (2.5), the set of parameters $P_{c,r}$ and τ_r can be solved from $r = 0$ to $r = N$. In other words, $P_{c,r}$ and τ_r can be calculated by replacing N with $n_{e,r}$. Moreover, the probability for a WS to be in the reservation table can be contributed to either one of the following two factors: (a) a WS is added into the reservation table $\mathbf{T}$ after successfully transmitting packets via channel contention or (b) a WS that exists in table $\mathbf{T}$ has conducted successful packet transmission. Therefore, the parameter P_t can also be regarded as the probability of successful transmission considering the situations that a WS is either inside or outside of the reservation table. Based on the value of $P_{c,r}$ as described above, the probability P_t in the steady state can consequently be derived as

$$P_t = \sum_{r=0}^{N} C_r^N \pi_t^r (1 - \pi_t)^{N-r} \left[\frac{n_{e,r}}{N} (1 - P_f)(1 - P_{c,r}) + \frac{N - n_{e,r}}{N} (1 - P_f) \right]. \tag{2.8}$$

where P_f denotes the packet error rate due to the existence of channel noises. It is noted that $\frac{n_{e,r}}{N}$ in (2.8) is denoted as the probability that a WS is required to contend with the other WSs in the network. On the other hand, $\frac{N-n_{e,r}}{N}$ represents the probability that the WS resides within the reservation table to be scheduled for packet transmission. Therefore, only the packet error rate P_f is required to be addressed without the consideration of collision probability $P_{c,r}$. By substituting (2.7) into the (2.8), the parameters π_t and P_t can consequently be obtained by solving the corresponding nonlinear function.

2.4.3 Throughput Performance of Proposed ARCR Protocol

Compared to conventional analytical models for DCF scheme, the analysis for throughput performance of proposed ARCR protocol is to further investigate the effect from the reservation table to the channel contention. Let $P_{tr,r}$ be the probability that there is at least one WS transmitting in a slot time while r WSs are recorded in the reservation table $\mathbf{T}$, i.e.,

$$P_{tr,r} = 1 - (1 - \tau_r)^{n_{e,r}}. \tag{2.9}$$

Moreover, the probability $P_{s,r}$ is denoted as the event that exactly one WS occupies the channel without any transmission from the other WSs given that there are r WSs in the reservation table. The probability $P_{s,r}$ can be derived as

$$P_{s,r} = \frac{n_{e,r}\tau_r(1-\tau_r)^{n_{e,r}-1}}{P_{tr,r}}. \tag{2.10}$$

To obtain the system throughput with r WSs recorded in $\mathbf{T}$, the average payload delivered in successful transmissions will be considered. The parameter $E[P_r]$ represents the average payload size for one transmission given that there are r $(r \neq 0)$ WSs in the reservation table $\mathbf{T}$, which can be obtained as

$$E[P_r] = \frac{n_{e,r}-1}{n_{e,r}}E[P] + \frac{1}{n_{e,r}}(N - n_{e,r} + 1)E[P] = \frac{N}{n_{e,r}}E[P], \tag{2.11}$$

where $E[P]$ denotes the average intended transmitted payload size for each WS. It is noted that $\frac{n_{e,r}-1}{n_{e,r}}$ represents the probability that the transmitters do not reside in the reservation table $\mathbf{T}$, and each of them has payload $E[P]$ to be delivered. On the other hand, the fraction $\frac{1}{n_{e,r}}$ stands for the transmission probability of the WS that possesses the first transmission priority among all the WSs in the reservation table $\mathbf{T}$. The total payload issued at this case by the entire r WSs in $\mathbf{T}$ becomes $(N - n_{e,r} + 1)E[P]$. In the case that $r = 0$, all the WSs

will adopt the conventional DCF scheme which results in $E[P_{r=0}] = E[P]$ that can also be verified by substituting $r = 0$ in (2.11).

In order to evaluate the total required time $T_{av,r}$ for packet transmission given that there are r WSs in the reservation table, the time durations owing to packet collisions T_c, successful transmissions $T_{s,r}$, and noise corruptions $T_{f,r}$ will be taken into account. Note that the required time owning to noise corruption $T_{f,r}$ is assumed to be equal to that for successful transmissions $T_{s,r}$. With the consideration of the three events mentioned before, the average required time $T_{av,r}$ can be derived as

$$T_{av,r} = (1 - P_{tr,r})\sigma + P_{tr,r}(1 - P_{s,r})T_c + P_{tr,r}P_{s,r}(1 - P_f)T_{s,r} + P_{tr,r}P_{s,r}P_f T_{f,r}, \tag{2.12}$$

where σ represents the slot time. The probabilities $P_{tr,r}$ and $P_{s,r}$ can be obtained from (2.9) and (2.10) respectively. The parameter T_c denotes the time for a WS to sense the occurrence of packet collisions which can be expressed as

$$T_c = T_{RTS-R} + \delta + T_{CTS} + \delta + T_{SIFS} + T_{DIFS}, \tag{2.13}$$

where δ is the propagation delay, and the remaining parameters in (2.13) are indicated by their corresponding subscripts. Noted that T_{RTS-R} represents the required time for either the RTS or the RTS-R packet since no additional control field is required by adopting the designed RTS-R packet. On other other hand, the required time for successful transmissions can be acquired as

$$\begin{aligned} T_{s,r} =& \frac{n_{e,r} - 1}{n_{e,r}} \Big[T_{RTS-R} + T_{CTS} + T_{PHY} + T_{MAC} + T_{E[P]} + T_{ACK+NTO} + 3T_{SIFS} + 4\delta + T_{DIFS} \Big] \\ &+ \frac{1}{n_{e,r}} \Big[T_{RTS} + T_{CTS} + T_{SIFS} + 2\delta + T_{DIFS} + (N - n_{e,r} + 1)(T_{PHY} + T_{MAC} + T_{E[P]} \\ &+ T_{ACK} + 2T_{SIFS} + 2\delta) \Big], \end{aligned} \tag{2.14}$$

where $T_{E[P]}$, $T_{ACK+NTO}$, T_{PHY}, and T_{MAC} are defined as the required time intervals for transmitting payload, ACK+NTO frame, PHY header, and MAC header. Noted that the time interval for transmitting the designed RFD field is considered within the MAC header. Similar to the concept in (2.11), the first term in (2.14) that associated with probability $\frac{n_{e,r}-1}{n_{e,r}}$ denotes the successful transmission conducted by a WS that adopts the DCF scheme. The second term associated with probability $\frac{1}{n_{e,r}}$ indicates the required time for a successful transmission while the WS resides in the reservation table, which exploits the ARCR pro-

tocol to compete the channel access. Furthermore, a transmitter will need to perceive whether its transmission has completed or not according to the reception of ACK packet. Therefore, the required time owing to noise corruption will be equal to that for successful transmissions, i.e., $T_{f,r} = T_{s,r}$. Based on (2.11) and (2.12), the average system throughput S can consequently be derived as

$$S = \frac{\sum_{r=0}^{N} C_r^N \pi_t^r (1-\pi_t)^{N-r} P_{tr,r} P_{s,r} (1-P_f) E[P_r]}{\sum_{r=0}^{N} C_r^N \pi_t^r (1-\pi_t)^{N-r} T_{av,r}}, \tag{2.15}$$

where π_t can be obtained by solving (2.7) and (2.8). It is noted the term $P_{tr,r}P_{s,r}(1-P_f)E[P_r]$ in (2.15) denotes the expected payload to be transmitted with r WSs in the reservation table. The term $(1-P_f)$ shown in (2.15) indicates that only partial payload can be successfully transmitted with the consideration of packet error rate P_f. The validation of throughput performance S in (2.15) for the proposed ARCR protocol will be conducted in Subsection 2.5.1.

2.5 Performance Evaluation

In this section, the performance of proposed ARCR protocol will be validated and compared with existing schemes via well-known network simulator (NS-2) [35]. All the simulation runs will be conducted for 100 seconds. Performance validation of the ARCR scheme is conducted in Subsection 2.5.1, and performance comparison with other schemes will be shown in Subsection 2.5.2. The system parameters and MAC configurations based on IEEE 802.11b standard are listed in Table 2.1.

2.5.1 Performance Validation

In order to validate the analytical model for proposed ARCR scheme, the system throughput S as derived in (2.15) is compared with simulation results as shown in Figs. 2.6 and 2.7. Noted that the legends "ana" and "sim" in both figures represent the results from analytical model and simulations respectively. In addition, saturation traffic is assumed for each WS to deliver its data packets. Fig. 2.6 shows the performance validation for throughput performance versus the number of WSs (N) under BER $= 0, 10^{-5}$, and 10^{-4}.

Parameter	Value
Minimum window (W)	32
Maximum backoff (M)	5
Data rate	11 Mbps
Basic rate	1 Mbps
Slot time (σ)	20 μs
T_{SIFS}	10 μs
T_{DIFS}	50 μs
PHY header	24 Bytes
MAC header + TAR	28 Bytes
Propagation delay (δ)	1 μs
Payload size ($E[P]$)	1023 Bytes
RTS/RTS-R	20 Bytes
CTS	14 Bytes
ACK + RFD/NTO	14 + 2 Bytes

Table 2.1: System parameters and MAC configurations for proposed ARCR algorithm

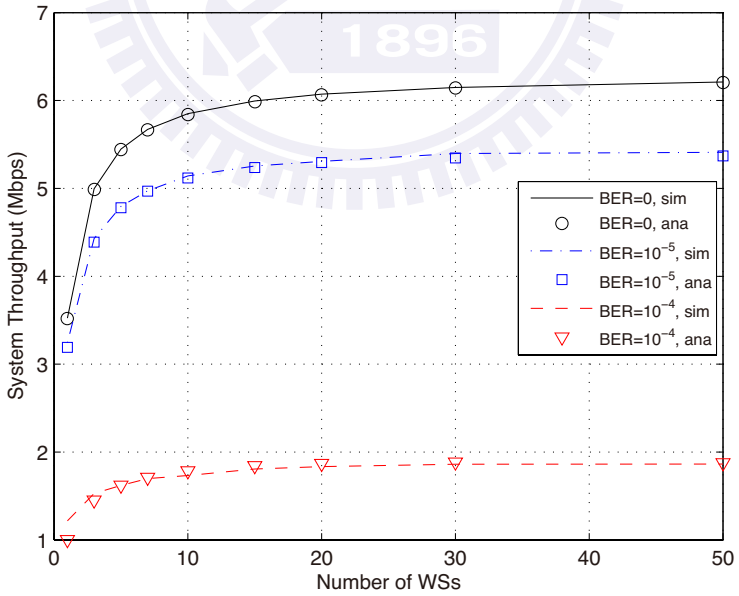

Figure 2.6: Performance validation for ARCR protocol: system throughput versus number of WSs.

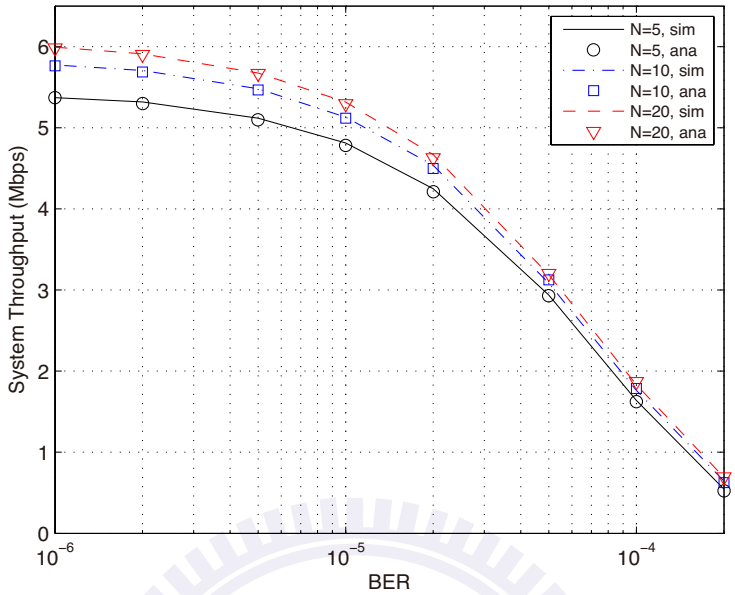

Figure 2.7: Performance validation for ARCR protocol: system throughput versus BER.

It can be intuitively observed that the system throughput increases as the total number of WSs in the network is augmented. Moreover, Fig. 2.7 illustrates the throughput versus BER under $N = 5, 10,$ and 20. The throughput performance decreases as the BER values are increased. It can be seen from both figures that the proposed analytical model can match with the simulation results under different numbers of WSs and BER values.

2.5.2 Performance Comparison

As shown in Figs. 2.8 to 2.11, the proposed ARCR protocol is compared to the DCF, GDCF [20, 21], PCF, and EBA-2 [17] schemes through a series of simulations in terms of both the number of WSs and the BER values. The system parameters in Table 1 are utilized in performance comparison with saturation traffic considered for each WS. It is also assumed that the successful counter c of GDCF is set equal to 2. Fig. 2.8 shows the performance comparison of system throughput w.r.t. different numbers of WSs under BER $= 0$ and 10^{-5}. It can be observed that the proposed ARCR scheme possesses higher throughput performance than the other three protocols under different numbers of WSs. The only exception is at the case of $N = 1$ that the EBA-2 scheme provides better performance than the ARCR protocol mainly due to the reason that the parameter W is selected to be 8 and 32 for EBA-2 and ARCR schemes, respectively. It is intuitively that smaller W will en-

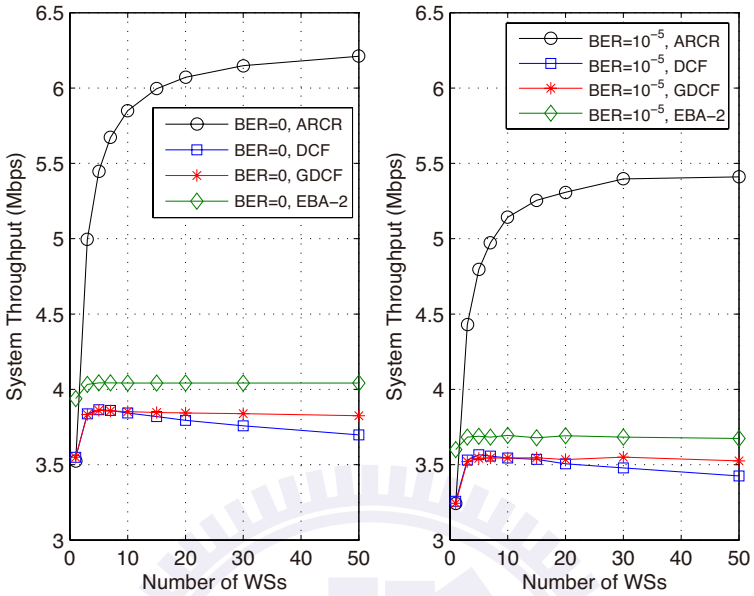

Figure 2.8: Performance Comparison for ARCR protocol: system throughput versus number of WSs.

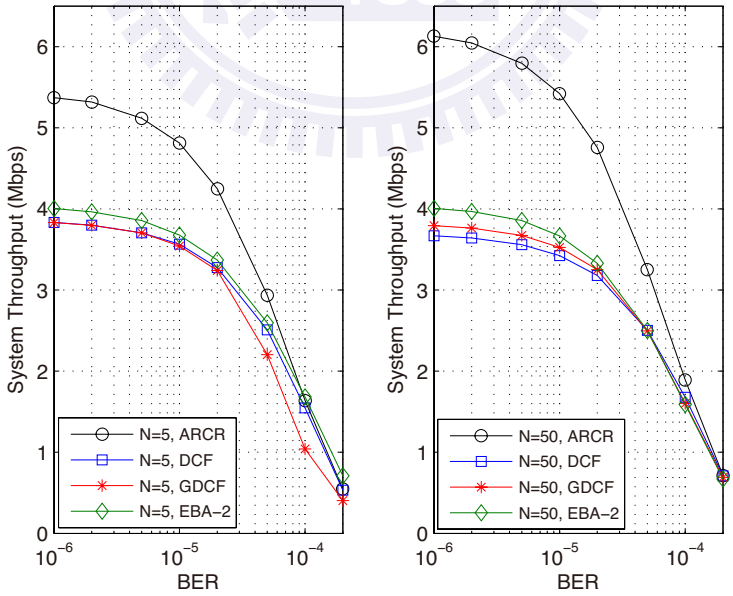

Figure 2.9: Performance Comparison for ARCR protocol: system throughput versus BER.

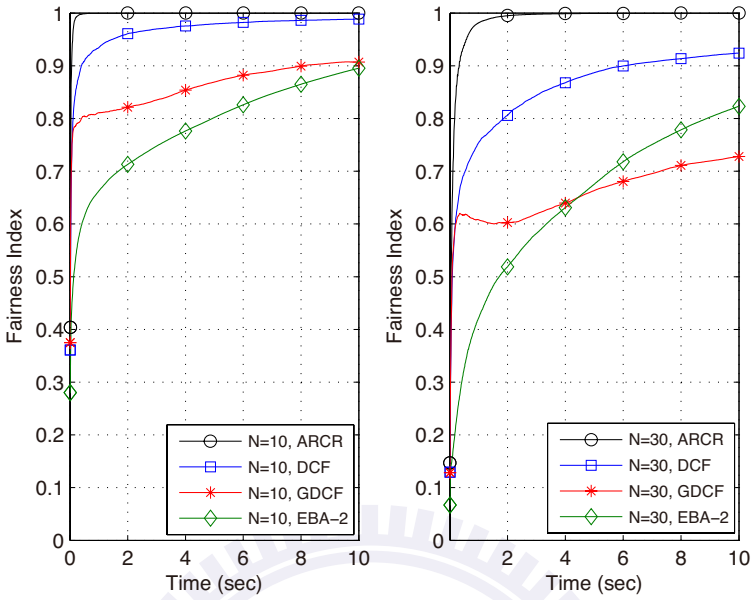

Figure 2.10: Fairness comparison for ARCR protocol: fairness index versus time.

hance the throughput performance if there exists only one WS in the network. The EBA-2 protocol has better performance than the GDCF and DCF schemes since most of the WSs are not allowed to choose the same slot to transmit their RTS packets. Collision overhead and backoff delay can therefore be reduced. Moreover, the GDCF method is slightly superior to the DCF scheme with larger number of WSs in the network. The reason is that the GDCF scheme has higher probability of staying at the stages with larger backoff window sizes compared to the DCF protocol. Less packet collisions will be incurred by adopting the GDCF scheme especially under larger number of WSs, which results in higher system throughput.

Fig. 2.9 illustrates the comparison of throughput performance versus different BER values under $N = 5$ and 50. The proposed ARCR protocol still outperforms the other three schemes under various BER values. It can also be observed that the system throughput of four schemes decrease and converge with the augmentation of BER values. At higher BER values, the proposed ARCR protocol behaves similar to the DCF scheme since almost all the WSs in the network will be removed from the reservation table due to occurrence of packet error . On the other hand, with higher BER values, the GDCF method is also comparable to the DCF scheme owing to the reason that its backoff stage will eventually remain at the maximum value. Furthermore, the fairness index F [36] is introduced to

estimate the fairness of each protocol, which is formulated as

$$F = \frac{\left(\sum_{i=1}^{N} S_i\right)^2}{N \cdot \sum_{i=1}^{N} S_i^2} \tag{2.16}$$

where S_i represents the throughput of WS i. The maximum value of F is equal to 1 which indicates the fairest situation; while minimal value $F = 1/N$ denotes the most unbalanced case. Intuitively, the value of F will be approximated to 1 for the steady state response of each protocol since every WS has equal opportunity to contend the channel. Therefore, the rates of achieving steady state for all the schemes are compared in order to determine the fairness levels. Fig. 2.10 shows the fairness comparison F versus time under different numbers of WSs. It can be observed that the proposed ARCR protocol can quickly achieve the steady state value of the fair index, i.e., $F = 1$, compared to the other schemes. On the other hand, both the GDCF and EBA-2 schemes result in worse performance compared to that of the DCF protocol due to their inherent designs. The WS with RTS packet collision will suffer from larger backoff delay for the GDCF scheme than that for the DCF protocol since the WS will slowly return back to the minimum CW size in the GDCF scheme, which makes the GDCF scheme become more unfair between the WSs. Furthermore, the WSs that receive the EBA field from the other WS should reselect another backoff counter, which is advantageous for the WS to easily win the channel contention. Therefore, the EBA-2 scheme possesses inferior fairness compared to the DCF protocol. Note that it takes more time for the fairness index to achieve steady state with the $N = 30$ scenario compared to the $N = 10$ case.

Moreover, the proposed ARCR protocol is compared with the distributed DCF scheme and the centralized PCF protocol given the condition of non-saturated queue in each WS with M/G/1 queuing system. In order to illustrate the pure reservation-based system, the PCF scheme is implemented only with the CFP while the CP is not considered in performance comparisons. It is assumed that there are two types of WSs in the network, including the WSs with high packet-arrival rate (λ_1 bits/sec (bps)) and with low packet-arrival rate (λ_2 bps). Let n_{λ_1} and n_{λ_2} be respectively defined as the numbers of WSs with λ_1 and λ_2 as the packet-arrival rates, the corresponding average throughput for each WS with λ_1 and λ_2 is respectively denoted as μ_{λ_1} and μ_{λ_2} with the unit of bps. It is considered that there are total of 10 WSs in the network for performance comparison, i.e., $n_{\lambda_1} + n_{\lambda_2} = 10$.

The performance comparisons of average throughput for each WS (i.e., either μ_{λ_1} or μ_{λ_2}) versus the number of WSs with the packets arrive rate equal to λ_1 are shown in Fig.

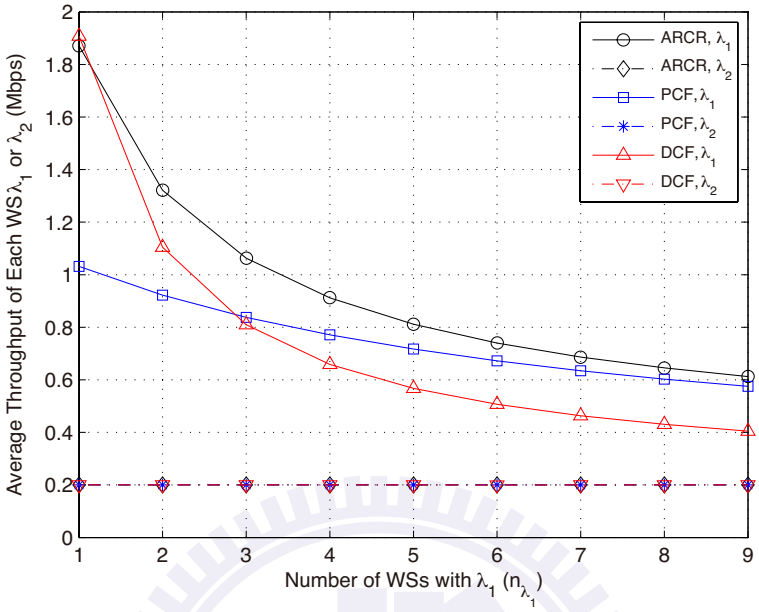

Figure 2.11: Performance Comparison for ARCR protocol: average throughput of each WS versus number of WSs with λ_1 (n_{λ_1}) ($n_{\lambda_2} = 10 - n_{\lambda_1}$, $\lambda_1 = 2$Mbps, $\lambda_2 = 0.2$Mbps).

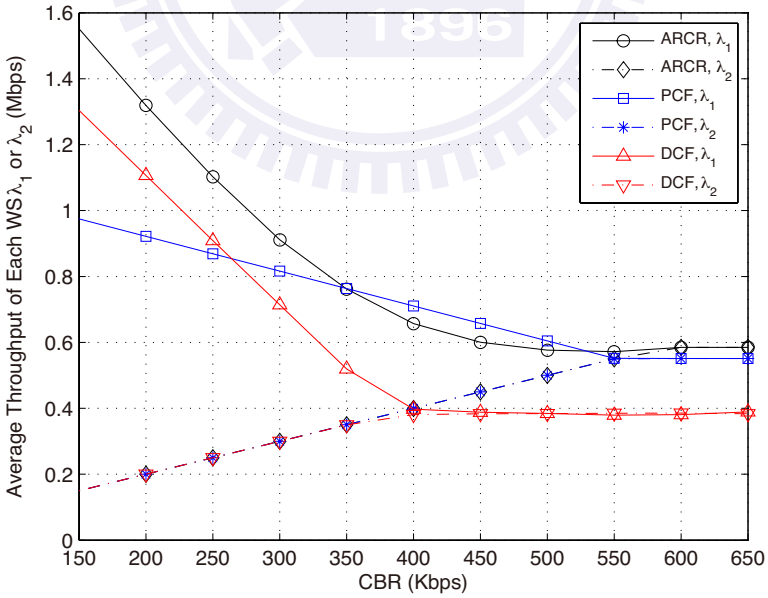

Figure 2.12: Performance Comparison for ARCR protocol: average throughput of each WS versus packet arrival rate λ_2 ($n_{\lambda_1} = 2$, $n_{\lambda_2} = 8$, $\lambda_1 = 2$Mbps).

2.11. Noted that the packet arrival rates $\lambda_1 = 2$ Mbps and $\lambda_2 = 200$ Kbps, and the number of WSs with packets arrive rate λ_2 becomes $n_{\lambda_2} = 10 - n_{\lambda_1}$. It can be observed from Fig. 2.11 that the average throughput for the WSs with λ_2 is approximately the same for all these three protocols, i.e., $\mu_{\lambda_2} \simeq 0.2$ Mbps. The results indicate that all three schemes can provide satisfactory services for the WSs with packet arrival rate $\lambda_2 = 0.2$ Mbps since μ_{λ_2} is around the same as the theoretically maximal throughput for each WS with λ_2. On the other hand, the effectiveness of proposed ARCR scheme can be revealed by observing the average throughput μ_{λ_1} for the WSs with λ_1. As n_{λ_1} is small, the polling-based PCF scheme becomes inefficient comparing with the ARCR and the DCF protocols since the network bandwidth is wasted as the AP is scheduled to periodically poll the larger numbers of WS with λ_2. The proposed ARCR protocol and the DCF scheme can provide higher throughput for WSs with λ_1 since there is more opportunity for these WSs to frequently transmit their data packets. Furthermore, with larger values of n_{λ_1}, the contention-based DCF scheme will spend significant amount of time to resolve for packet collisions, which results in reduced system throughput of μ_{λ_1}. The proposed ARCR protocol and the PCF scheme can provide higher throughput performance since there is greater chance for the larger amount of WSs with λ_1 to be scheduled for packet transmission. As a result, the ARCR protocol can provide better throughput performance under different arrival rates of the WSs in the network.

Fig. 2.12 illustrates the average throughput of each WSs (μ_{λ_1} or μ_{λ_2}) versus the packet arrival rate λ_2 on the conditions that $n_{\lambda_1} = 2$, $n_{\lambda_2} = 8$, and $\lambda_1 = 2$ Mbps. As can be expected, with the augmentation of λ_2, the throughput μ_{λ_2} will be increased, however, the throughput performance μ_{λ_1} for the WSs with λ_1 is reduced for all three schemes. A saturation point will be reached by the WSs with either λ_1 or λ_2 for all three protocols due to the availability of total network bandwidth. Owing to the severe packet collision, the DCF scheme will result in the lowest throughput among the three protocols with the earliest saturation point at $\lambda_2 \simeq 400$ Kbps. Furthermore, the ARCR scheme will provide higher throughput performance with around $\mu_{\lambda_1} \simeq \mu_{\lambda_2} \simeq 0.58$ Mbps. On the other hand, the proposed ARCR scheme and DCF can outperform the PCF protocol under smaller values of packet arrival rate λ_2 owing to the polling overheads resulting from the centralized-based PCF scheme.

Moreover, in each channel competition, based on our proposed ARCR protocol, the first WS in the reservation table possesses the same range of CW size compared to the newly joining WSs. In other words, unsaturated WSs that may not have constant packet

to be delivered will have the same level of opportunity for channel contention with the saturated WSs. As shown from Fig. 2.12 that the average throughput of WSs with λ_1 is around 1.32 Mbps and that with λ_2 is around 0.2 Mbps at packet arrival rate $\lambda_2 = 200$ Kbps. It can be seen that the throughput of the unsaturated WS with λ_2 will always be identical to its packet arrival rate before the saturation occurs at around 580 Kbps. That is to say, the WSs with λ_2 will not encounter large backoff timer due to packet collisions. As the packet arrival rate λ_2 is increased to 580 Kbps, it can be observed that all the WSs will achieve around the same throughput performance. Therefore, the merits of adopting the proposed ARCR scheme can be perceived.

2.6 Concluding Remarks

In this chapter, an adaptive reservation-assisted collision resolution (ARCR) protocol is proposed in order to enhance the network throughput for IEEE 802.11 wireless local area networks. According to the ARCR scheme, adaptive reservation periods will be imposed within the conventional contention-based system by adopting the proposed piggyback mechanisms. Based on the design of reservation table at the access point, excessive packet collision can effectively be alleviated in the network. The analytical model of system throughput for the proposed ARCR protocol is derived and validated via simulations. Numerical results show that the ARCR scheme outperforms other existing protocols with enhanced network throughput and better channel utilization.

Chapter 3

Enhanced Reservation-Assisted Protocol for IEEE 802.11e WLANs

- Served as enhanced version of adaptive reservation-assisted collision resolution (ARCR) scheme in Chapter 2, enhanced-ARCR (E-ARCR) protocol is proposed in this chapter to support quality-of-service requirements. Compared to conventional IEEE 802.11e mechanism, E-ARCR protocol can significantly improve throughput performance for all prioritized access traffics. [1]

3.1 Introduction

In order to provide reliable services for multimedia applications, IEEE 802.11e standard [4] has been proposed to fulfill quality-of-service (QoS) requirements. For achieving prioritized channel access, the enhanced distributed channel access (EDCA) mechanism defines four access categories (ACs) in a wireless station (WS) associated with their distinct arbitration inter-frame spaces (AIFSs) and contention window (CW) sizes. Each AC within a WS is considered as a standalone entity to contend with the ACs both in the same WS and the other WSs for channel access in the network. Intuitively, in order to have higher chance of data transmission, higher priority AC should possess smaller values of CW and AIFS sizes compared to low priority AC. Each AC will wait for its AIFS length and independently select its own backoff number. Until the backoff number for a specific AC

[1] The chapter is based on

- Jia-Shi Lin and Kai-Ten Feng, "QoS-based Adaptive Contention/Reservation Medium Access Control Protocols for Wireless Local Area Networks," *IEEE Trans. Mobile Computing*, vol. 10, no. 12, pp. 1785-1803, Dec. 2011.

has been decremented to zero, the corresponding AC can initiate request-to-send (RTS)/ clear-to-send (CTS) handshaking with access point (AP) before the data transmission.

In order to provide higher throughput performance comparing with conventional EDCA scheme, research work has been proposed in [37, 38] by providing adjustment on the four CW sizes for their corresponding ACs in a WS. Adaptation of AIFS has been studied in [39] for achieving stable capacity ratios between the ACs; while random AIFS algorithm was proposed in [40] to both decrease packet collisions and increase throughput performance. With the adjustment of CW size and randomized AIFS values, the work proposed in [41] improves channel utilization and fairness by preventing starvation on lower priority classes under higher traffic loads. Nevertheless, all the existing contention-based protocols suffer from the same problem (**Problem 1**: high overhead) as described in Chapter 2. Hence, with the consideration of four prioritized access categories (ACs) within a WS, the enhanced-ARCR (E-ARCR) protocol is further proposed in order to both improve the system performance and fulfill the QoS requirements. Moreover, analytical model for throughput analysis is developed in this chapter to provide feasible observations on the behaviors of proposed E-ARCR protocol. Numerical results are conducted via simulations both to provide validation on the analytical model and to evaluate the effectiveness of proposed scheme. Compared with conventional EDCA protocol, the network throughput can be enhanced by adopting the E-ARCR algorithm.

The remainder of this chapter is organized as follows. The proposed E-ARCR scheme is described in Section 3.2 associated with its throughput analysis presented in Section 3.3. Section 3.4 presents the performance validation and evaluation for the proposed E-ARCR protocol. Finally, conclusions are drawn in Section 3.5.

3.2 Proposed E-ARCR Protocol

As is not considered in the DCF mechanism, the IEEE 802.11e EDCA scheme [4] supports different traffic types and fulfills their corresponding QoS requirements. In order to achieve the advancement from the DCF method to the EDCA scheme, the E-ARCR protocol is proposed as the enhanced version of the ARCR scheme in order to fulfill the QoS requirements as specified in the EDCA scheme. The E-ARCR protocol will support four ACs in a WS in order to serve various traffic types which possess different priorities for the competition of channel access. As specified in the standard, the access categories are denoted as AC[Z] with $Z = 3, 2, 1,$ and 0, where AC[3] represents the highest priority and AC[0] has the lowest priority. The special control functions described in Subsection

3.2.1 are designed to facilitate the implementation of E-ARCR protocol. The operations of proposed E-ARCR scheme is explained with an arbitrary network scenario in Subsection 3.2.2.

3.2.1 Functional Description

In order to provide prioritized ACs for different traffic, four queues in the same WS are utilized as four virtual stations to contend for channel access. Therefore, instead of adopting a single reservation table as in the ARCR scheme, the proposed E-ARCR protocol exploits four reservation tables in order to record different types of traffic from all the WSs in the network. Each of the four reservation tables will be labeled as $\mathbf{T}_{AC[Z]}$ which matches with the AC[Z] traffic, where $Z = 3, 2, 1,$ and 0. The control fields similar to Definitions 2.1 to 2.4 are utilized in the E-ARCR protocol associated with different AC[Z]s, including TAR(Z), NTO(Z, r), RTS-R(Z), and RFD(Z, r). For example, TAR(Z) is defined as a control field to inform the AP that AC[Z] of a WS is intending to join the reservation table $\mathbf{T}_{AC[Z]}$.

Considering different priorities among the AC[Z]s, the initial window size $W_{AC[Z]}$ as well as the maximum backoff stage $M_{AC[Z]}$ will be different between the four AC[Z]s. Based on the information acquired from the control field NTO(Z, r), the random backoff number $k_{earcr,AC[Z]}$ for the specific AC[Z] within a WS will be selected as

$$k_{earcr,AC[Z]} = \begin{cases} U[0,\ 2^0 W_{AC[Z]} - 1], & r = 0, \\ U[2^{r-1} W_{AC[Z]},\ 2^r W_{AC[Z]} - 1], & 1 \le r \le M_{AC[Z]}, \\ U[\ell \cdot 2^{M_{AC[Z]}-1} W_{AC[Z]},\ u \cdot 2^{M_{AC[Z]}-1} W_{AC[Z]} - 1], & r > M_{AC[Z]}, \end{cases} \tag{3.1}$$

where $\ell = r - M_{AC[Z]} + 1$ and $u = r - M_{AC[Z]} + 2$. Moreover, the AIFS value in the EDCA scheme for each AC[Z] is denoted as $AIFS_{AC[Z]}$ in order to govern different waiting time intervals to start the backoff process. Therefore, the parameters $W_{AC[Z]}$, $M_{AC[Z]}$, and $AIFS_{AC[Z]}$ for each of the four AC[Z] can be manipulated to affect different priorities among the ACs.

3.2.2 Network Scenarios

The operations of proposed E-ARCR protocol without packet collisions and channel noise are depicted in Fig. 3.1. To clearly visualize the network behaviors of proposed E-ARCR scheme, each of the two WSs is associated with two ACs including AC[1] for high

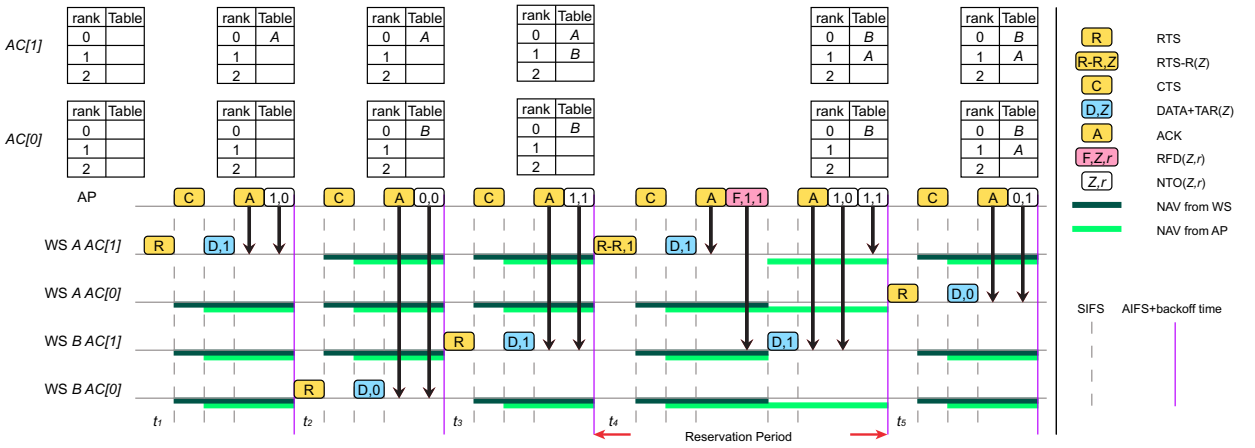

Figure 3.1: The timing diagram for the proposed E-ARCR protocol.

priority and AC[0] for low priority transmission. Therefore, there will be two reservation tables $\mathbf{T}_{AC[1]}$ and $\mathbf{T}_{AC[0]}$ exploited within the AP. At the beginning, all the four ACs contend for channel by adopting the EDCA scheme and there is no entry recorded in AP's reservation tables, i.e., $\mathbf{T}_{AC[1]} = \mathbf{T}_{AC[0]} = \{\}$. As AC[1] of node A successfully acquires the channel at time t_1, WS A will be added into the reservation table $\mathbf{T}_{AC[1]}$ as the first entry, i.e., $\mathbf{T}_{AC[1]} = \{T_0(A)\}$. After data packets have been successfully delivered from AC[1] of WS A to the AP, the AP will transmit the ACK+NTO$(1, 0)$ packet to WS A which indicates that AC[1] of WS A has the transmission order of 0. At the time instant t_2, all the four ACs will continue to contend for the channel access. As WS A has received the NTO$(1, 0)$ packet from the AP, WS A will adopt the E-ARCR scheme with random backoff mechanism as defined in (3.1); while the other three ACs will employ conventional backoff scheme from the EDCA algorithm. Considering that AC[0] of WS B wins the channel contention and hence it will be recorded as a new entry in the reservation table as $\mathbf{T}_{AC[0]} = \{T_0(B)\}$. Similarly, in the case that AC[1] of WS B acquires the channel access at time t_3, it will join in the reservation table $\mathbf{T}_{AC[1]}$ as the second entry, i.e., $\mathbf{T}_{AC[1]} = \{T_0(A), T_1(B)\}$, and finally receives the ACK+NTO$(1, 1)$ packet from the AP after packet transmission.

Assuming that AC[1] of WS A obtains the channel access at time t_4, the RTS-R(1) packet will be delivered by WS A to initiate the reservation period for AC[1] in both WSs A and B. After receiving the DATA+TAR(1) packet from WS A, the AP will respond with the ACK +RFD$(1, 1)$ packet where the ACK packet is targeting for AC[1] of WS A and the RFD$(1, 1)$ packet is for AC[1] of WS B. According to the received RFD$(1, 1)$ message from the AP, AC[1] of WS B can deliver DATA+TAR(1) packet without the requirement for channel contention. At the end of the reservation period, the AP will change the entry order within

the reservation table $\mathbf{T}_{AC[1]}$ in a round-robin manner, i.e., $\mathbf{T}_{AC[1]} = \{T_0(B), T_1(A)\}$. It is noted that similar reservation period will be implemented for AC[0] of both WSs A and B. Moreover, the proposed E-ARCR scheme can also be implemented in a more realistic network scenarios with the existence of packet collisions and channel noises, which can be extended from the descriptions as addressed in Subsection 2.3.3 for the ARCR protocol.

It is noticed that packet collision will not happen in the original ARCR scheme if all the WSs reside within the reservation table under error-free network environments. In the E-ARCR scheme, however, collisions may still exist even though all ACs in WSs are recorded within their corresponding reservation tables in the AP. The reason is contributed to the usage of more than one reservation table in the network. The first entries in those reservation tables will still contend with each other which results in the occurrence of packet collisions. This is considered the tradeoffs by adopting the E-ARCR protocol as the QoS requirement is specified to be fulfilled. The performance of the proposed E-ARCR scheme will be evaluated and compared in Section 3.4.

3.3 Throughput Analysis of Proposed E-ARCR Protocol

The throughput analysis of proposed E-ARCR protocol can be regarded as an extension of that for the ARCR scheme addressed in Section 2.4. It is noted that certain portion of the WSs will still adopt conventional EDCA scheme for channel contention; while others utilize the E-ARCR protocol. Therefore, the backoff process of EDCA scheme will first be described in Subsection 3.3.1. The reservation probability for E-ARCR scheme and the corresponding network throughput will be derived in Subsections 3.3.2 and 3.3.3, respectively.

3.3.1 Backoff Process of EDCA Scheme

Existing research work [42–47] has been conducted to analyze the backoff process of EDCA protocol. An analytical approach for throughput and delay performance of IEEE 802.11e EDCA scheme has been proposed in [42, 43] in order to observe the effect of different CWs and retry limits for each AC. Three-dimensional Markov Chain has been utilized in [44, 45] to model the EDCA mechanism. On the other hand, two-dimensional Markov Chain is adopted in [46, 47] by dividing the backoff interval into different time zones, which will be employed as the baseline model for analyzing the performance of proposed E-ARCR scheme with additional consideration of error-prone channel effects. As was

specified in previous work, without loss of generality, each of the N WSs is considered to possess two ACs in the analysis, including AC[1] and AC[0].

Apart from considering the WS as a whole in the DCF and ARCR schemes, each AC in a WS is viewed individually in the backoff process by adopting both the EDCA and E-ARCR protocols. The Markov chain model as shown in Fig. 2.4 can still be applied to the EDCA scheme except that individual AC is considered instated of the entire WS. Let $\tau_{AC[Z]}$ denote the probability that AC[Z] transmits the RTS packet in a randomly selected time slot, and $\overline{p}_{AC[Z]}$ is defined as the average probability that AC[Z] fails in transmission due to packet collision or frame errors. Similar to (2.4), the relationship between $\tau_{AC[Z]}$ and $\overline{p}_{AC[Z]}$ can be acquired as

$$\tau_{AC[Z]} = 2(1-2\overline{p}_{AC[Z]}) \cdot \left[(1-2\overline{p}_{AC[Z]})(W_{AC[Z]}+1) + \overline{p}_{AC[Z]} W_{AC[Z]}(1-(2\overline{p}_{AC[Z]})^{M_{AC[Z]}}\right]^{-1}. \tag{3.2}$$

It is noted that the averaged value $\overline{p}_{AC[Z]}$ is considered in (3.2) since the fail transmission probabilities are calculated in two different time zones for each AC[Z], which will be explained as follows. In order to distinguish different QoS requirements among distinct ACs, the ACs which belong to higher priorities will start their backoff processes after a shorter AIFS duration. A smaller number will be obtained by the ACs with higher priorities for backoff countdown, and therefore suffer from fewer channel contentions comparing with the ACs of lower priorities. As illustrated in Fig. 3.2, resulting from the various values of AIFSs, the backoff period can be divided into two different time regions including Zone A and Zone B. Let L_A and L_B be referred as the numbers of time slots in Zone A and Zone B respectively. The entire time duration $L_A + L_B$ can be obtained as the maximal backoff window size $M_{AC[1]}$ of the highest priority AC[1], i.e., $L_A + L_B = \min\{2^{M_{AC[Z]}} \cdot W_{AC[Z]} | Z = 1, 0\} = 2^{M_{AC[1]}} W_{AC[1]}$. Within the duration of Zone A, only the high priority AC[1]s can decrement their backoff numbers and have the chance to transmit their RTS packets. On other other hand, all ACs including both AC[1]s and AC[0]s will contend for channel access in Zone B if there does not exist AC[1] that intends to transmit in Zone A. As can be expected, the states of channel contention for Zones A and B respectively will be different.

To evaluate the stationary probability of each zone, it is assumed that every AC is independent to each other and the Morkov chain model for state transition between backoff slots is shown in Fig. 3.3. Suppose that there are $n_{AC[1]}$ AC[1]s and $n_{AC[0]}$ AC[0]s in the

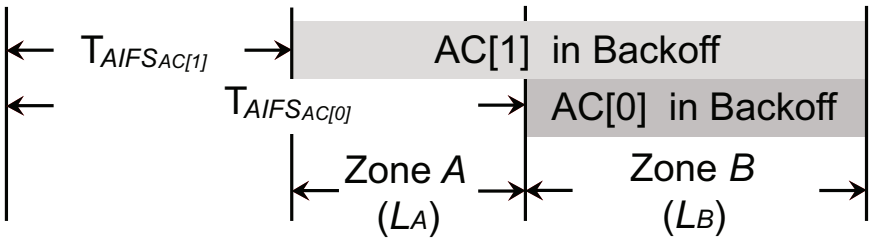

Figure 3.2: The EDCA backoff process after the occurrence of busy medium.

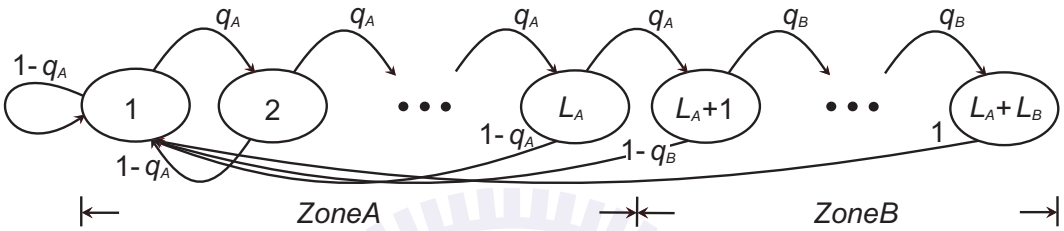

Figure 3.3: The Morkov chain model for state transition between backoff slots in two different zones.

network, and let q_X denote the probability that there does not exist any AC transmitting in Zone X. Therefore, q_A and q_B can be calculated as

$$\begin{cases} q_A = (1-\tau_{AC[1]})^{n_{AC[1]}}, \\ q_B = (1-\tau_{AC[1]})^{n_{AC[1]}}(1-\tau_{AC[0]})^{n_{AC[0]}}. \end{cases} \tag{3.3}$$

Let z_k be referred as the stationary probability that time slot k locates in the contention zones, which can consequently be acquired as

$$\begin{cases} z_k = z_1\left(\prod_{i=2}^{k} q_A\right), & 1 < k \le L_A+1, \\ z_k = z_1\left(\prod_{i=2}^{L_A+1} q_A\right)\left(\prod_{i=L_A+2}^{k} q_B\right), & L_A+1 < k \le L_A+L_B. \end{cases} \tag{3.4}$$

By associating (3.4) with the relationship $\sum_{k=1}^{L_A+L_B} z_k = 1$, the probability z_1 can be derived as

$$z_1 = \left[\frac{1-{q_A}^{L_A+1}}{1-q_A} + {q_A}^{L_A} q_B \frac{1-{q_B}^{L_B-1}}{1-q_B}\right]^{-1}. \tag{3.5}$$

Furthermore, let π_A and π_B be the stationary probabilities for a random time slot lies in Zone A and Zone B, respectively. Both parameters can be calculated by incorporating the

results from (3.4) and (3.5) as

$$\begin{cases} \pi_A = \sum_{k=1}^{L_A} z_k, \\ \pi_B = \sum_{k=1}^{L_B} z_{L_A+k}. \end{cases} \tag{3.6}$$

Since two different zones are considered in the analytical model of the EDCA scheme, additional derivations are required in order to depict the situations of packet collision. Let $P_{c,AC[Z],X}$ be defined as the collision probability of AC[Z] given that packet collisions occur within Zone X. The collision probabilities for the two types of ACs in contention zones A and B are respectively obtained as

$$\begin{cases} P_{c,AC[1],A} = 1-(1-\tau_{AC[1]})^{n_{AC[1]}-1}, \\ P_{c,AC[1],B} = 1-(1-\tau_{AC[1]})^{n_{AC[1]}-1}(1-\tau_{AC[0]})^{n_{AC[0]}-1}, \\ P_{c,AC[0],A} = 0, \\ P_{c,AC[0],B} = 1-(1-\tau_{AC[1]})^{n_{AC[1]}}(1-\tau_{AC[0]})^{n_{AC[0]}-1}. \end{cases} \tag{3.7}$$

Noted that the reason for $P_{c,AC[0],A} = 0$ in (3.7) is that AC[0] will only conduct packet transmission within Zone B. Moreover, let $\overline{P}_{c,AC[Z]}$ with $Z = 1$ and 0 be defined as the average collision probability of AC[Z] in these two contention zones. Since $\pi_A + \pi_B = 1$, the average collision probability $\overline{P}_{c,AC[1]}$ and $\overline{P}_{c,AC[0]}$ can be obtained by averaging (3.7) as

$$\begin{cases} \overline{P}_{c,AC[1]} &= \dfrac{P_{c,AC[1],A}\cdot\pi_A + P_{c,AC[1],B}\cdot\pi_B}{\pi_A+\pi_B} = P_{c,AC[1],A}\cdot\pi_A + P_{c,AC[1],B}\cdot\pi_B, \\ \overline{P}_{c,AC[0]} &= P_{c,AC[0],B}. \end{cases} \tag{3.8}$$

The average probability $\overline{p}_{AC[Z]}$ that AC[Z] fails in transmission due to packet collisions or channel noises can be acquired from (3.8) as

$$\overline{p}_{AC[Z]} = \overline{P}_{c,AC[Z]} + P_f - (\overline{P}_{c,AC[Z]}\cdot P_f) \tag{3.9}$$

for $Z = 1, 0$, and P_f denotes the packet error rate. From (3.3) to (3.9), it is observed that both $\overline{p}_{AC[1]}$ and $\overline{p}_{AC[0]}$ are functions of $\tau_{AC[1]}$ and $\tau_{AC[0]}$; while (3.2) provides another relationship between $\overline{p}_{AC[Z]}$ and $\tau_{AC[Z]}$ for $Z = 1$ and 0. Consequently, the unknown parameters $\overline{p}_{AC[1]}$, $\overline{p}_{AC[0]}$, $\tau_{AC[1]}$, and $\tau_{AC[0]}$ can be iteratively solved.

3.3.2 Derivation of Reservation Probability

The reservation probability $P_{t,AC[Z]}$ will be derived in this subsection. It is noted that $P_{t,AC[Z]}$ represents the transition probability that an AC[Z] of a WS either is in or will join in the reservation table $\mathbf{T}_{AC[Z]}$ for $Z = 1, 0$. As shown in Fig. 2.5, the derivation of reservation probability for the ARCR scheme can be extended to the E-ARCR protocol by considering the Markov model for each reservation table $\mathbf{T}_{AC[Z]}$ with $Z = 1, 0$. Let $\pi_{t,AC[Z]}$ be defined as the stationary probability that an AC[Z] of a WS stays in the reservation table $\mathbf{T}_{AC[Z]}$. Similar to (2.7), the relationship between $P_{t,AC[Z]}$ and $\pi_{t,AC[Z]}$ can be obtained as

$$\pi_{t,AC[Z]} = P_{t,AC[Z]} \tag{3.10}$$

for $Z = 1, 0$. Another relationship between $P_{t,AC[Z]}$ and $\pi_{t,AC[Z]}$ is required for solving the reservation probability $P_{t,AC[Z]}$. Given that there are i AC[1]s and j AC[0]s in the reservation tables $\mathbf{T}_{AC[1]}$ and $\mathbf{T}_{AC[0]}$ respectively, the effective numbers of AC[1]s and AC[0]s that actually contend for channel access become $n_{e,i}$ and $n_{e,j}$ which can be obtained from (2.6) by replacing r with i and j. The parameters $P_{c,AC[Z],X,i,j}$ and $\tau_{AC[Z],i,j}$ are respectively denoted as the collision probabilities and the events that an AC[Z] transmits its RTS packet in a random slot time. Noted that the subscript X in $P_{c,AC[Z],X,i,j}$ indicates that the probability is computed for either Zone A or B with $X = A$ or B. By iteratively computing the relationship from (3.2) to (3.9), the set of parameters $P_{c,AC[Z],X,i,j}$ and $\tau_{AC[Z],i,j}$ can be obtained for $i, j = 0$ to N. It is noticed that the parameters $n_{AC[1]}$ and $n_{AC[0]}$ in (3.2) to (3.9) are respectively replaced by $n_{e,i}$ and $n_{e,j}$ with the consideration of reservation tables. Moreover, the reservation probability $P_{t,AC[Z]}$ can also be regarded as the probability of successful transmission under the situations that an AC[Z] is either inside or outside of its corresponding reservation table $\mathbf{T}_{AC[Z]}$, i.e.,

$$P_{t,AC[Z]} = \sum_{i=0}^{N}\sum_{j=0}^{N} C_i^N \pi_{t,AC[1]}^i (1-\pi_{t,AC[1]})^{N-i} \cdot C_j^N \pi_{t,AC[0]}^j (1-\pi_{t,AC[0]})^{N-j} P_{t,AC[Z],i,j} \tag{3.11}$$

for $Z = 1, 0$. Note that $P_{t,AC[Z],i,j}$ in (3.11) means the probability that an AC[Z] of a WS joins in the reservation table $\mathbf{T}_{AC[Z]}$ (for $Z = 1, 0$) given that there are i AC[1]s and j AC[0]s in the reservation tables $\mathbf{T}_{AC[1]}$ and $\mathbf{T}_{AC[0]}$ respectively. Both parameters can be derived as

$$P_{t,AC[0],i,j} = (1-P_f)\left[\frac{n_{e,j}}{N}(1-P_{c,AC[0],B,i,j}) + \frac{N-n_{e,j}}{N}\right], \tag{3.12}$$

and

$$P_{t,AC[1],i,j} = \pi_{A,i,j}(1-P_f)\left[\frac{n_{e,i}}{N}(1-P_{c,AC[1],A,i,j})+\frac{N-n_{e,i}}{N}\right]+ \pi_{B,i,j}(1-P_f)\left[\frac{n_{e,i}}{N}(1-P_{c,AC[1],B,i,j})+\frac{N-n_{e,i}}{N}\right], \tag{3.13}$$

where $\pi_{A,i,j}$ and $\pi_{B,i,j}$ are extended from (3.6) by considering i AC[1]s and j AC[0]s in their corresponding reservation tables. As a result, the reservation probability $P_{t,AC[Z]}$ in (3.11) and $\pi_{t,AC[Z]}$ in (3.10) for $Z = 1, 0$ can be acquired by solving the corresponding nonlinear function, which will be utilized in the computation of throughput performance for the E-ARCR protocol.

3.3.3 Throughput Performance of Proposed E-ARCR Protocol

The analytical model for throughput performance of proposed E-ARCR protocol can be regarded as an extension of that derived for the ARCR scheme in Subsection 2.4.3 with additional consideration of different prioritized traffic. As there are i AC[1]s and j AC[0]s in the reservation tables $\mathbf{T}_{AC[1]}$ and $\mathbf{T}_{AC[0]}$ respectively, the parameter $P_{tr,AC[Z],i,j}$ is defined as the probability that there exists at least one AC[Z] to be transmitted in a slot time; while $P_{s,AC[Z],X,i,j}$ is referred as the probability that one AC[Z] successfully transmits its packet in Zone X for $X = A, B$ and $Z = 1, 0$. Therefore, the corresponding probabilities can be obtained as

$$\begin{cases} P_{tr,AC[1],i,j} = 1-\left(1-\tau_{AC[1],i,j}\right)^{n_{e,i}}, \\ P_{tr,AC[0],i,j} = 1-\left(1-\tau_{AC[0],i,j}\right)^{n_{e,j}}, \end{cases} \tag{3.14}$$

and

$$\begin{cases} P_{s,AC[1],A,i,j} = \dfrac{n_{e,i}\cdot\tau_{AC[1],i,j}\left(1-\tau_{AC[1],i,j}\right)^{n_{e,i}-1}}{P_{tr,AC[1],i,j}}, \\ P_{s,AC[1],B,i,j} = \dfrac{n_{e,i}\cdot\tau_{AC[1],i,j}\left(1-\tau_{AC[1],i,j}\right)^{n_{e,i}-1}\left(1-\tau_{AC[0],i,j}\right)^{n_{e,j}-1}}{P_{tr,AC[1],i,j}}, \\ P_{s,AC[0],B,i,j} = \dfrac{n_{e,j}\cdot\tau_{AC[0],i,j}\left(1-\tau_{AC[1],i,j}\right)^{n_{e,i}}\left(1-\tau_{AC[0],i,j}\right)^{n_{e,j}-1}}{P_{tr,AC[0],i,j}}, \end{cases} \tag{3.15}$$

where $\tau_{AC[Z],i,j}$ for $Z = 1, 0$ can be computed from previous subsection given that there exists $n_{e,i}$ AC[1]s and $n_{e,j}$ AC[0]s contending for the channel access. Furthermore, it is re-

quired to calculate the average payload size in each transmission for the E-ARCR protocol. Let $E[P_{AC[Z],i,j}]$ be the average payload size of AC[Z]s in a transmission while there are i AC[1]s and j AC[0]s in the reservation tables $\mathbf{T}_{AC[1]}$ and $\mathbf{T}_{AC[0]}$ respectively. The parameter $E[P_{AC[Z],i,j}]$ can be obtained as

$$\begin{cases} E[P_{AC[1],i,j}] = \left(\pi_{A,i,j} P_{tr,AC[1],i,j} P_{s,AC[1],A,i,j} + \pi_{B,i,j} P_{tr,AC[1],i,j} P_{s,AC[1],B,i,j}\right)(1-P_f)\frac{N}{n_{e,i}} E[P], \\ E[P_{AC[0],i,j}] = \pi_{B,i,j} P_{tr,AC[0],i,j} P_{s,AC[0],B,i,j} \cdot (1-P_f)\frac{N}{n_{e,j}} E[P] \end{cases} \tag{3.16}$$

for $Z = 1, 0$, and $E[P]$ denotes the average payload size for both AC[1] and AC[0]. Therefore, the average slot time $\mathcal{T}_{av,i,j}$ for a transmission can be written as

$$\mathcal{T}_{av,i,j} = \pi_{A,i,j} \cdot \rho_{A,i,j} + \pi_{B,i,j} \cdot \rho_{B,i,j}, \tag{3.17}$$

where $\rho_{X,i,j}$ is referred as the average slot time utilized for a transmission in Zone X as

$$\begin{cases} \rho_{A,i,j} &= P_{I,A,i,j} \cdot \sigma + P_{tr,AC[1],i,j} P_{s,AC[1],A,i,j} \cdot \mathcal{T}_{s,i} + \left(1 - P_{I,A,i,j} - P_{tr,AC[1],i,j} P_{s,AC[1],A,i,j}\right) \cdot \mathcal{T}_c, \\ \rho_{B,i,j} &= P_{I,B,i,j} \cdot \sigma + P_{tr,AC[1],i,j} P_{s,AC[1],B,i,j} \cdot \mathcal{T}_{s,i} + P_{tr,AC[0],i,j} P_{s,AC[0],B,i,j} \cdot \mathcal{T}_{s,j} + \\ & \left(1 - P_{I,B,i,j} - P_{tr,AC[1],i,j} P_{s,AC[1],B,i,j} - P_{tr,AC[0],i,j} P_{s,AC[0],B,i,j}\right) \cdot \mathcal{T}_c. \end{cases} \tag{3.18}$$

It is noted that $P_{I,X,i,j}$ in (3.18) denotes the probability that the channel is idle in Zone X, which can be acquired as

$$\begin{cases} P_{I,A,i,j} = \left(1 - \tau_{AC[1],i,j}\right)^{n_{e,i}}, \\ P_{I,B,i,j} = \left(1 - \tau_{AC[1],i,j}\right)^{n_{e,i}} \left(1 - \tau_{AC[0],i,j}\right)^{n_{e,j}}. \end{cases} \tag{3.19}$$

The time $\mathcal{T}_c$ for an AC of a WS to sense the collisions can be obtained similar to T_c in (2.13) with additional consideration of QoS requirement, i.e.,

$$\mathcal{T}_c = T_{RTS-R} + \delta + T_{CTS} + \delta + T_{SIFS} + T_{AIFS_{AC[1]}}. \tag{3.20}$$

On the other hand, similar to (2.14), both the required time $\mathcal{T}_{s,k}$ (for $k = i$ or j) for a successful transmission and the time duration of failed transmission $\mathcal{T}_{f,k}$ are considered equal with the same reason as described in Subsection 2.4.3. Since $\mathcal{T}_{f,k} = \mathcal{T}_{s,k}$, both values are combined and utilized in (3.18) as

Access Category (AC[Z])	$W_{AC[Z]}$	$M_{AC[Z]}$	$AIFSN_{AC[Z]}$
VO	8	1	2
VI	16	1	2
BE	32	5	3
BK	32	5	7

Table 3.1: Backoff parameters for different ACs

$$\begin{aligned}\mathcal{T}_{s,k} =& \frac{n_{e,k}-1}{n_{e,k}}\Big[T_{RTS-R}+T_{CTS}+T_{PHY}+T_{MAC}+T_{E[P]}+T_{ACK+NTO}+3T_{SIFS}+4\delta \\ &+T_{AIFS_{AC[1]}}\Big]+\frac{1}{n_{e,k}}\Big[T_{RTS-R}+T_{CTS}+T_{SIFS}+2\delta+T_{AIFS_{AC[1]}} \\ &+(N-n_{e,k}+1)(T_{PHY}+T_{MAC}+T_{E[P]}+T_{ACK+NTO}+2T_{SIFS}+2\delta)\Big]. \end{aligned} \tag{3.21}$$

By incorporating $\pi_{t,AC[Z]}$ in (3.10), $E[P_{AC[Z],i,j}]$ in (3.16), and $\mathcal{T}_{av,i,j}$ in (3.17), the average system throughput $S_{AC[Z]}$ conditioned on i AC[1]s and j AC[0]s within the reservation tables $\mathbf{T}_{AC[1]}$ and $\mathbf{T}_{AC[0]}$ can be derived as (3.22) for $Z=1,0$. The throughput performance $S_{AC[Z]}$ in (3.22) for the proposed E-ARCR scheme will be validated and evaluated in Subsection 3.4.1.

$$S_{AC[Z]}=\frac{\sum_{i=0}^{N}\sum_{j=0}^{N}C_i^N\pi_{t,AC[1]}^i(1-\pi_{t,AC[1]})^{N-i}C_j^N\pi_{t,AC[0]}^j(1-\pi_{t,AC[0]})^{N-j}\cdot E[P_{AC[Z],i,j}]}{\sum_{i=0}^{N}\sum_{j=0}^{N}C_i^N\pi_{t,AC[1]}^i(1-\pi_{t,AC[1]})^{N-i}C_j^N\pi_{t,AC[0]}^j(1-\pi_{t,AC[0]})^{N-j}\cdot \mathcal{T}_{av,i,j}}. \tag{3.22}$$

3.4 Performance Evaluation

In this section, the performance of proposed E-ARCR scheme will be validated and compared with conventional EDCA via the well-developed network simulator (NS-2) [35]. All the simulation runs will be conducted for 100 seconds. The backoff parameters for different ACs in the proposed E-ARCR protocol are referred from the EDCA scheme and are listed in Table 3.1. It is noted that the four ACs defined in the EDCA protocol has the priority from high to low as follows: voice (VO), video (VI), best effort (BE), and background

Parameter	Value
Data rate	11 Mbps
Basic rate	1 Mbps
Slot time (σ)	20 μs
T_{SIFS}	10 μs
PHY header	24 Bytes
Propagation delay (δ)	1 μs
Payload size ($E[P]$)	1023 Bytes
MAC header + TAR	30 Bytes
RTS/RTS-R	22 Bytes
CTS	14 Bytes
ACK + RFD/NTO	$16 + 2$ Bytes

Table 3.2: System parameters and MAC configurations for proposed E-ARCR algorithm

(BK). Saturation traffic is assumed for the queue of each AC. The corresponding $T_{AIFS_{AC[Z]}}$ value for each AC[Z] traffic can be obtained as $T_{AIFS_{AC[Z]}} = \sigma \cdot AIFSN_{AC[Z]} + T_{SIFS}$. Moreover, the system parameters and MAC configurations are listed in Table 3.2, and saturation traffic is assumed for each WS to deliver its data packets. Performance validation and comparison for the E-ARCR scheme are respectively conducted in Subsections 3.4.1 and 3.4.2.

3.4.1 Performance Validation

The analytical model for throughput performance $S_{AC[Z]}$ in (3.22) of the proposed E-ARCR scheme is validated via simulations with prioritized ACs in terms of different numbers of WSs (N) and bit error rate (BER) values. Figs. 3.4 and 3.5 show the performance validation for both the VI (i.e., AC[1]s) and BE (i.e., AC[0]s) traffic. It is assumed that each WS has both AC[1] and AC[0] to be transmitted, and the relationship between the system throughput and the number of WSs is represented in Fig. 3.4 under BER $= 0$ and 10^{-5}. It can be seen that the analytical model can match with the simulated results under different numbers of WSs. By observing the case of AC[0] with BER $= 10^{-5}$, the system throughput first increases and decreases afterwards as the number of WSs is augmented. This is mainly caused by its lower priority and higher BER conditions that make most of the AC[0]s depart from the reservation table $\mathbf{T}_{AC[0]}$ to compete for the channel access with the increased number of WSs. Severe packet collision will consequently be incurred which leads to the degradation of system throughput. Fig. 3.5 shows the system throughput

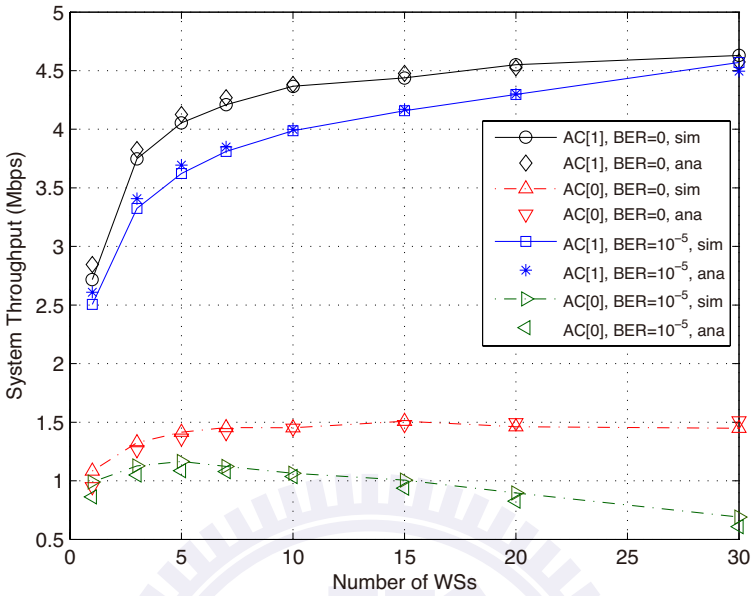

Figure 3.4: Performance validation for E-ARCR protocol: system throughput versus number of WSs for the VI (AC[1]s) and BE (AC[0]s) traffic.

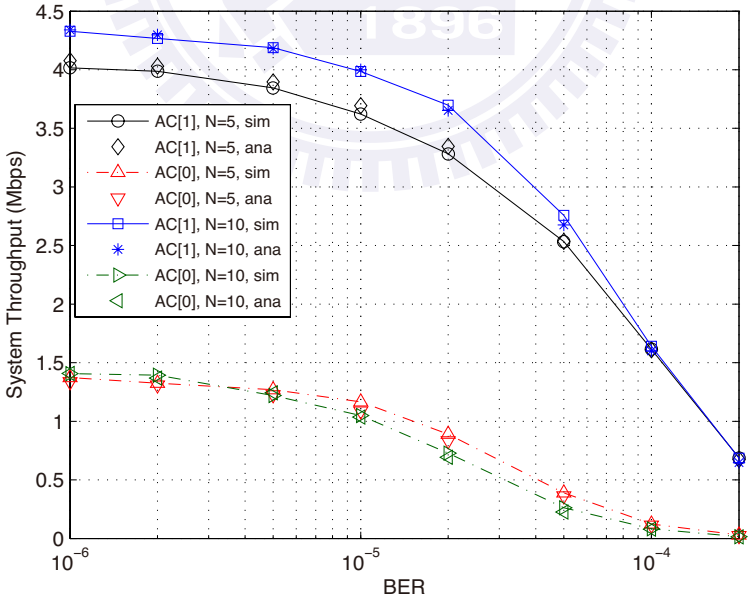

Figure 3.5: Performance validation for E-ARCR protocol: system throughput versus BER for the VI (AC[1]s) and BE (AC[0]s) traffic.

versus the BER values with $N = 5$ and 10, in which both the analytical and simulation results are coincide with each other. It is also observed that the two cases of AC[0]s (i.e., with $N = 5$ and 10) intersect with each other around BER $= 3.5 \times 10^{-6}$. With lower BER values, most of the AC[0]s are located in the reservation table $\mathbf{T}_{AC[0]}$ such that the throughput will be higher with larger number of WSs, i.e., $N = 10$. However, with increased BER values, it is difficult for the AC[0]s to be recorded in $\mathbf{T}_{AC[0]}$ which results in severe packet collisions and degraded system throughput as the number of WSs is larger.

In order to verify the analytical throughput with different AC pairs, the ACs with BE and BK types are chosen as AC[1]s and AC[0]s respectively in the following validations. As depicted in Table 2, the time slot difference between the BE and BK traffic is four, i.e., $AIFSN_{AC[0]} - AIFSN_{AC[1]} = 4$; while that for the previous case between the VI and BE traffic is one. Therefore, a larger size of Zone A will be acquired in this case as shown in Fig. 3.2 since larger difference between $T_{AIFS_{AC[0]}}$ and $T_{AIFS_{AC[1]}}$ is obtained. With larger size of Zone A, AC[1]s will have better chance to win the channel access, which consequently results in declined throughput performance for AC[0]s as the BER values are increased. This intuitive concepts can be validated by observing the difference between the two cases with AC[1] and AC[0] in both Figs. 3.4 and 3.6 as follows. By adopting the E-ARCR scheme under the case with BER $= 0$, almost all AC[1]s and AC[0]s should be recorded in their corresponding reservation tables, which results in the situations that only the first two entries in $\mathbf{T}_{AC[1]}$ and $\mathbf{T}_{AC[0]}$ are contending for the channel access. However, as the BER value becomes 10^{-5}, some of the ACs will be removed from their corresponding reservation tables, which incurs comparably severe channel contention. In the case that larger Zone A is acquired by implementing both BE and BK traffic, AC[1]s will have higher opportunity to obtain the channel access compared to AC[0]s.

As shown in Fig. 3.6, AC[1]s with BER $= 10^{-5}$ can even exceed that with BER $= 0$ under larger number of WSs since most of the AC[0]s are blocked from contending the channel under BER $= 10^{-5}$. Consequently, as the number of WSs is increased, AC[0] will suffer from the degraded system throughput as illustrated in Fig. 3.6. It is also noted that the total system throughput from AC[1]s and AC[0]s at BER $= 0$ is still higher than that at BER $= 10^{-5}$, e.g., around 6 Mbps at BER $= 0$ compared to 5.3 Mbps at BER $= 10^{-5}$ under $N = 30$ in Fig. 3.6. This prioritized blocking situations is not remarkable in Fig. 3.4 due to the smaller size of Zone A, which will not significantly promote the system throughput for AC[1]s. Fig. 3.7 shows the system throughput versus BER for both the BE and BK traffic under $N = 5$ and 20. Similar performance trends can be observed in comparison with Fig.

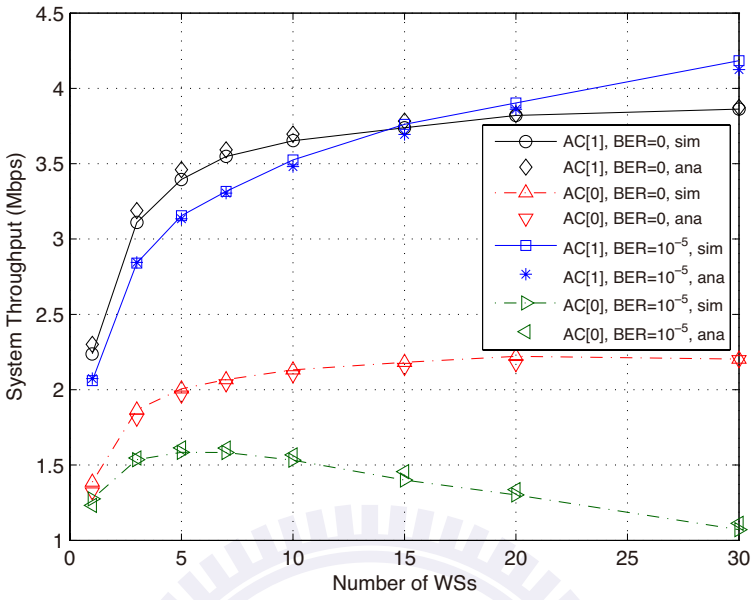

Figure 3.6: Performance validation for E-ARCR protocol: system throughput versus number of WSs for the BE (AC[1]s) and BK (AC[0]s) traffic.

3.5 where the system throughput in all cases decrease as the BER values are increased. Owing to the prioritized blocking situation as described in the previous paragraph, the throughput with AC[1]s and $N = 20$ will be slightly augmented as the BER values are increased until the BER value reaches around 5×10^{-6}.

3.4.2 Performance Comparison

To evaluate the throughput performance in the sense of QoS requirements, the proposed E-ARCR protocol is compared with the EDCA scheme under different prioritized ACs. It is also assumed that the queue of each AC is saturated. Noted that the centralized hybrid coordination function (HCF) controlled channel access (HCCA) protocol is not utilized for performance comparison due to its fair scheduling-based polling approach, which will not be suitable to be compared with the prioritized-based classifications within the E-ARCR scheme. In the HCCA protocol, the CFP supports high priority traffic and low priority packets are transmitted in the CP. There does not exist a convincing method to determine the ratio of CFP to CP, which makes the comparison between the proposed E-ARCR scheme and HCCA protocol difficult. The simulation parameters can be obtained from Tables 1 and 2.

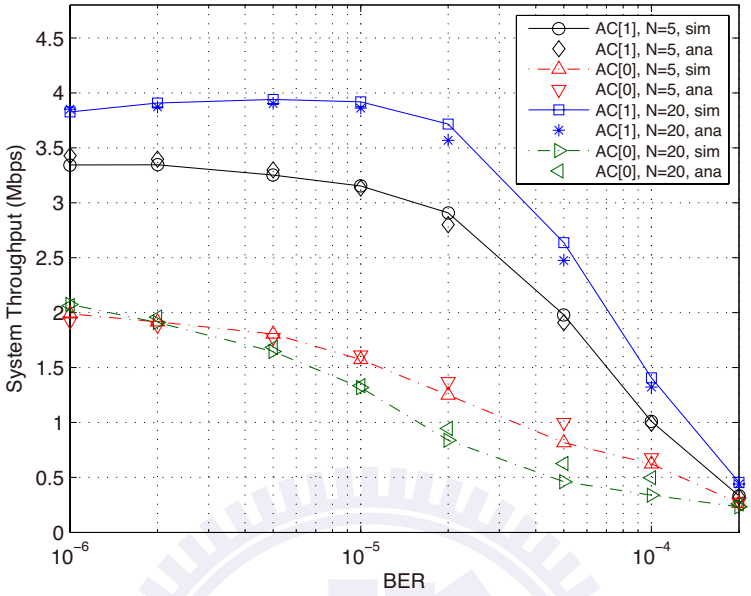

Figure 3.7: Performance validation for E-ARCR protocol: system throughput versus BER for the BE (AC[1]s) and BK (AC[0]s) traffic.

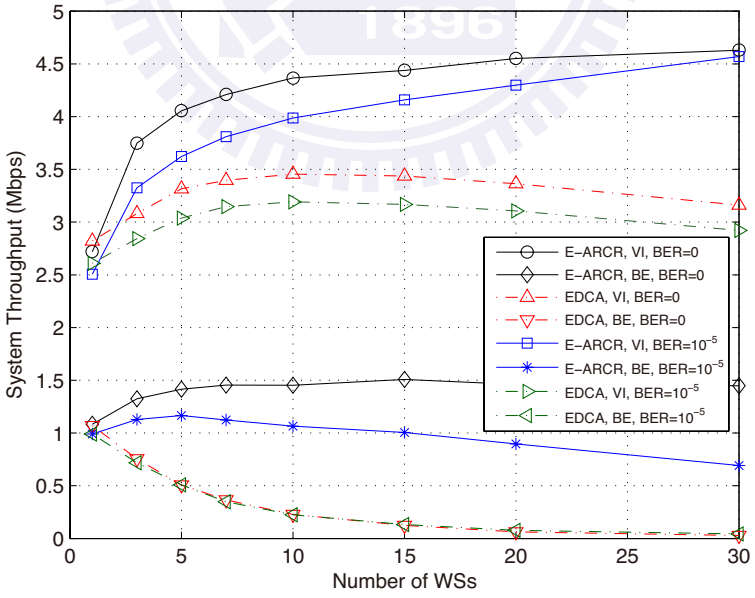

Figure 3.8: Performance comparison for E-ARCR protocol: system throughput versus number of WSs for the VI and BE traffic.

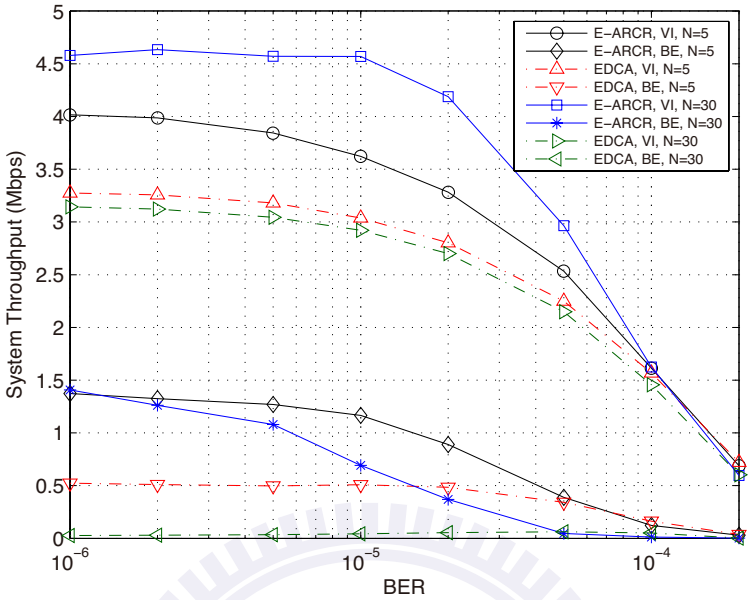

Figure 3.9: Performance comparison for E-ARCR protocol: system throughput versus BER for the VI and BE traffic.

Fig. 3.8 shows the system throughput of VI and BE traffic versus the number of WSs under BER $= 0$ and 10^{-5}. The E-ARCR protocol can provide higher throughput performance in both the VI and BE traffic compared to that from the EDCA scheme under different numbers of WSs, e.g., around 20% gain and 200% gain for VI and BE traffic at $N = 5$ under BER = 0 condition, respectively. As the number of WSs is augmented, the system throughput from EDCA method with VI traffic under both BER $= 0$ and 10^{-5} will increase and decrease afterwards owing to severe packet collisions with larger numbers of WSs. Moreover, the EDCA scheme also results in poor system throughput on the BE traffic primarily due to both the severe packet collisions and the BE's comparably lower priority. Fig. 3.9 illustrates the system throughput of both the VI and BE traffic versus BER under $N = 5$ and 30. It can be observed that the throughput of E-ARCR scheme with VI cases is higher as $N = 30$ compared to that equals to 5 until BER exceeds 10^{-4}. On the other hand, due to severe packet collisions, the throughput performance for the VI traffic with larger number of WSs ($N = 30$) will be less than that with smaller number of WSs ($N = 5$) by adopting the EDCA protocol. Furthermore, similar to the explanation as described in Fig. 3.5, the two BE traffic by adopting proposed E-ARCR scheme (i.e., with $N = 5$ and 30) intersect with each other, which denotes higher throughput for the case of $N = 5$ compared to that for $N = 30$ under higher BER values. The reason is attributed

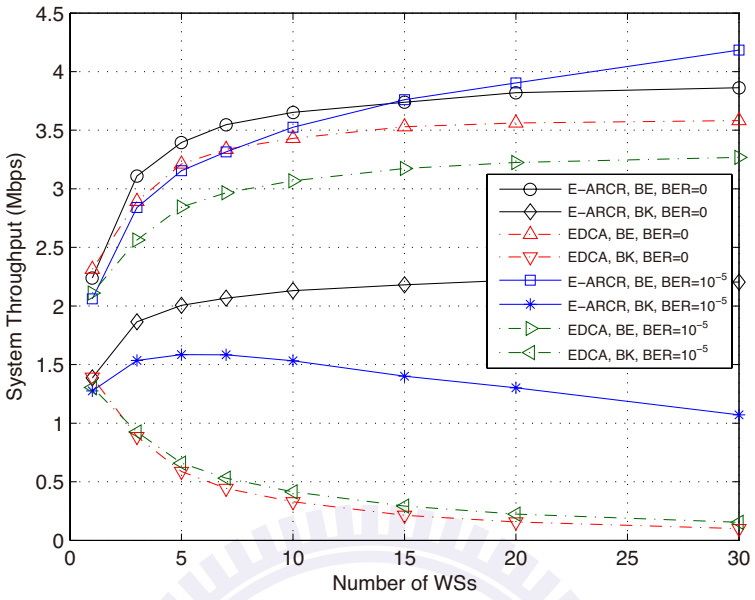

Figure 3.10: Performance comparison for E-ARCR protocol: system throughput versus number of WSs for the BE and BK traffic.

to the situation that most of the ACs are removed from the reservation tables by adopting the E-ARCR protocol, which results in higher packet collisions in the network.

Fig. 3.10 illustrates the system throughput of both BE and BK traffic versus the number of WSs under BER $= 0$ and 10^{-5}; while Fig. 3.11 depicts that versus BER under $N = 5$ and 30. The prioritized blocking situation as described in Fig. 3.6 is also observed in Fig. 3.10 by adopting the proposed E-ARCR scheme with BE traffic, where higher throughput is obtained under BER $= 10^{-5}$ compared to that at BER $= 0$ with larger number of WSs. This phenomenon also results in the increased system throughput at BER $= 10^{-5}$ by exploiting the E-ARCR protocol with BE at $N = 30$ as in Fig. 3.11. Furthermore, comparing the EDCA BE traffic in Fig. 3.10 with the EDCA VI traffic in Fig. 3.8, the throughput performance of the EDCA BE traffic will not decrease as the number of WSs is increased. The reason is that $W_{BE} = 32$ and $M_{BE} = 5$ are large enough for the EDCA BE traffic to handle additional backoff processes and consequently reduce the collision probability. On the other hand, the parameters $W_{VI} = 16$ and $M_{VI} = 1$ of EDCA VI traffic are comparably small that ACs with VI traffic will frequently collide with each other, which results in degraded system throughput as the number of WSs is augmented.

Finally, the proposed E-ARCR protocol is compared with the EDCA scheme by considering all different types of ACs, including VO, VI, BE, and BK traffic. Fig. 3.12 shows the

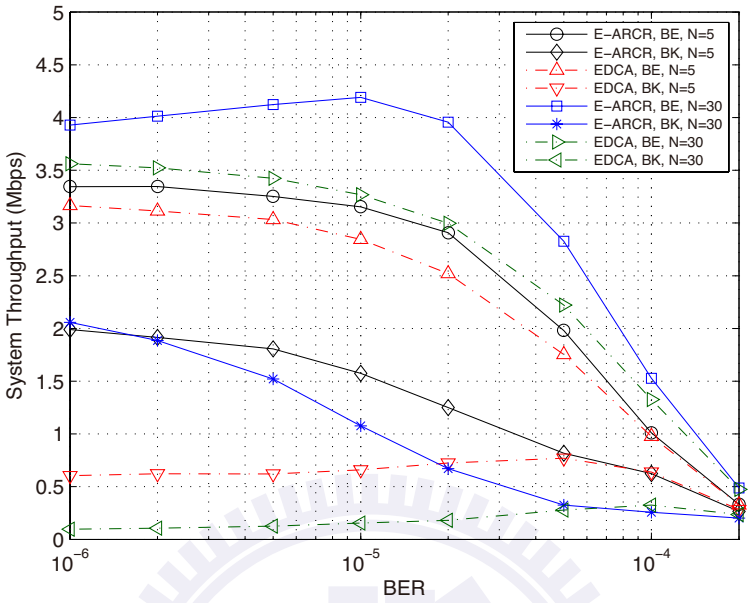

Figure 3.11: Performance comparison for E-ARCR protocol: system throughput versus BER for the BE and BK traffic.

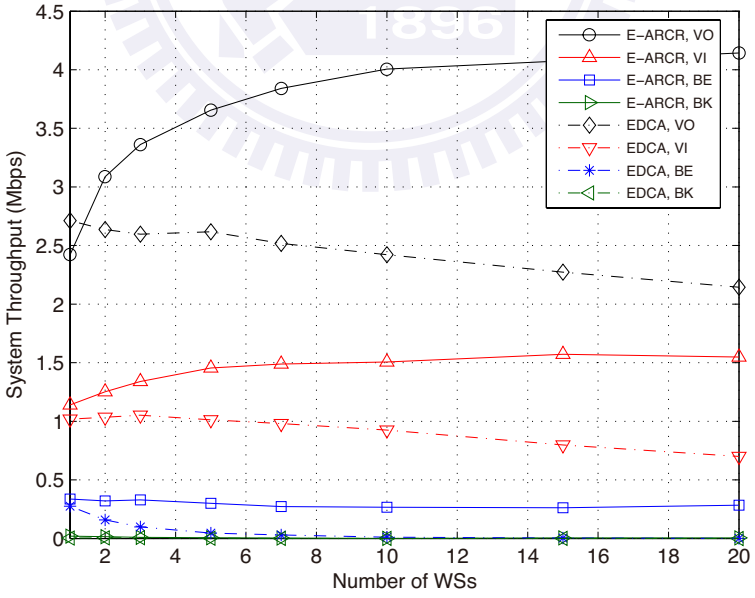

Figure 3.12: Performance comparison: system throughput versus the number of WSs for VO, VI, BE, and BK traffic (BER $= 0$).

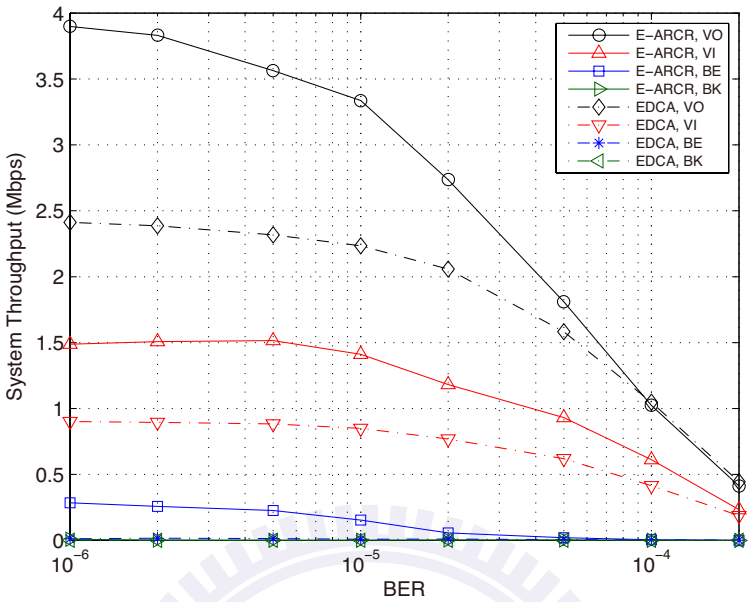

Figure 3.13: Performance comparison: system throughput versus BER for VO, VI, BE, and BK traffic ($N = 10$).

system throughput of each traffic type versus the number of WSs for BER $= 0$. It can be observed that the throughput of VO, VI and BE traffic from the proposed E-ARCR scheme increases with the number of WSs; while that for the EDCA protocol is decreased as the number of WSs is augmented. Noted that the throughput of BK traffic in both the E-ARCR and EDCA methods is nearly equal to zero due to its lowest channel access priority. The reason for the degraded throughput performance of the EDCA scheme can be attributed to the small sizes of contention windows and insufficient backoff stages that are designed to secure high priority traffic, e.g., $M_{VO} = 1$ and $W_{VO} = 8$. This can result in severe packet collision in the case that there exists excessive number of WSs in the network. On the other hand, there are almost only four ACs (i.e., the first entry from each of the four reservation tables) competing for the channel access by adopting the proposed E-ARCR scheme under BER $= 0$. Consequently, the collisions scarcely happen and the QoS requirement of the E-ARCR VI traffic can be achieved without sacrificing system throughput. Fig. 3.13 depicts the system throughput for each of the four traffic types versus BER given that $N = 10$. It can be observed that the proposed E-ARCR can outperform the conventional EDCA scheme under most of the BER values, e.g., with additional 1.1 Mbps of system throughput can be acquired by the E-ARCR VO traffic under BER $= 10^{-5}$. The merits of proposed E-ARCR protocol can consequently be observed which can fulfill the QoS requirements

with enhanced network throughput.

3.5 Concluding Remarks

Served as an enhanced version of adaptive reservation-assisted collision resolution (ARCR) mechanism, an enhanced-ARCR (E-ARCR) protocol is proposed in this chapter by applying multiple reservation tables at the access point for each prioritized traffic. It will not only increase the throughput of access categories (ACs) with higher priority but also prevent the ACs with lower priority from starvation of channel access. Moreover, the analytical model of system throughput for the proposed E-ARCR protocol is derived and validated via simulations. For IEEE 802.11e networks, numerical results show that the proposed E-ARCR protocol is superior to the conventional enhanced distributed channel access scheme with improved system throughput.

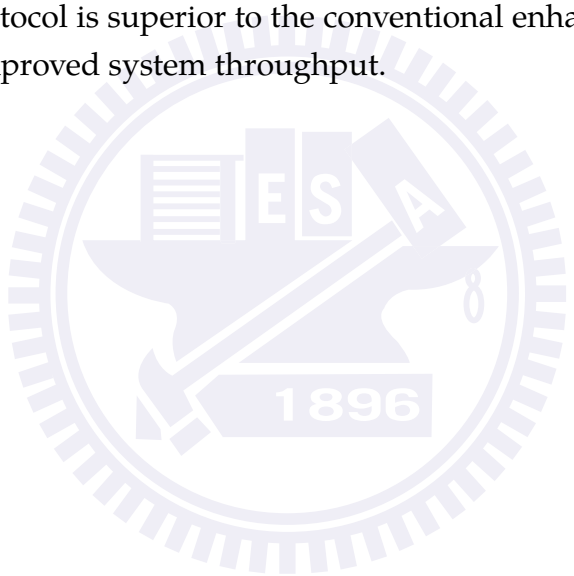

Chapter 4

Aggregated ARQ Protocols for IEEE 802.11n WLANs

*- In order to provide reliable data transmission and high throughput performance (**Problem 2**) for IEEE 802.11n Networks, two media access control (MAC)-defined automatic repeat reQuest (ARQ) protocols are proposed in this chapter to consider the effect from frame aggregation. By the adoptions of frame aggregation and block acknowledgement techniques, the efficiency of IEEE 802.11 MAC can be significantly improved compared to conventional stop-and-wait ARQ scheme.* [1]

4.1 Introduction

With increasing demands to support multimedia applications, the new amendment IEEE 802.11n [5, 6] has been proposed to achieve high throughput performance for wireless local area networks (WLANs). The IEEE 802.11 task group N (TGn) enhances the PHY layer data rate up to 600 Mbps by adopting advanced communication techniques, such as multi-input multi-output (MIMO) technology [9]. It is noted that the MIMO technique utilizes spatial diversity to improve both the range and spatial multiplexing for achieving higher data rate. However, it has been investigated in [10] that simply improves the physical (PHY) data rate will not be sufficient for enhancing the system throughput from

[1] The chapter is based on

- Jia-Shi Lin, Kai-Ten Feng, Yu-Zhi Huang, and Li-Chun Wang, "Novel Design and Analysis of Aggregated ARQ Protocols for IEEE 802.11n Networks," accepted and to appear in *IEEE Trans. Mobile Computing*.

the medium access control (MAC) perspective. Accordingly, the IEEE 802.11 TGn further exploits frame aggregation and block acknowledgement techniques [6, 11] to moderate the drawbacks that are originated from the MAC/PHY overheads.

The benefits of adopting frame aggregation techniques have been studied from different perspectives [11, 48–50]. Without the consideration of retransmission mechanisms, simplified performance analysis considering frame aggregation has been conducted in [48] based on channel utilization. The dynamic frame aggregation scheme [49] adaptively changes the number of aggregated frames based on the channel conditions. Moreover, the multi-user polling controlled channel access (MCCA) protocol [50] performs both frame aggregation and multi-user polling in order to further enhance network utilization. Although the frame aggregation techniques can reduce both the transmission time of frame headers and the contention time induced by the random backoff period, the enlarged aggregated frames will cause other wireless stations (WSs) to wait for an elongated time period before their next opportunity for channel access. Furthermore, under the error-prone channels, corrupting an aggregated frame can result in the wastage of a longer channel access period which consequently leads to inferior throughput performance. Therefore, a feasible design of retransmission mechanisms becomes an important topic with the adoption of frame aggregation scheme.

The automatic repeat reQuest (ARQ) [51–53] mechanisms have been extensively proposed in different wireless systems for reliable transmission. In order to reach more reliable transmissions within a shorter transmitting period, the hybrid ARQ (H-ARQ) schemes [54–58], which combine both the forward error correction (FEC) and retransmission mechanism, have been proposed for advanced multimedia applications. In general, the H-ARQ algorithms can be classified into three categories as follows. In the type-I H-ARQ scheme [56], as an error packet is detected via the cyclic redundancy check, the transmitter will retransmit the same packet either until the packet is successfully decoded at the receiver or a maximum retransmission limit is reached. Type-II of H-ARQ scheme is regarded as the full incremental redundancy (IR) technique [57], which decreases the coding rate in each retransmission by sending additional redundancy check digits. On the other hand, type-III of H-ARQ scheme [58], considered as a partial IR scheme, not only decrements the coding rate but also maintains the self-decoding capability in each retransmission. It is noted that the IR-based algorithms in general make use of either the rate compatible punctured convolutional (RCPC) codes [58, 59] or the rate compatible punctured turbo (RCPT) codes [60]. Furthermore, the transmission errors are corrected

in two phases based on the design concept of concatenate code [61]. The inner decoder, which is implemented in the PHY layer, adopts sophisticated algorithms for error correction; while the outer decoder is served as the second stage fine-tuning error corrector that is implemented in the MAC layer protocols. As a consequence, the FEC schemes in both type-II and III of H-ARQ algorithms are regarded as the inner decoders; while that of type-I scheme is considered as the outer decoders.

However, most of the existing ARQ algorithms did not explicitly consider the effects from frame aggregation. Even though ARQ scheme is utilized for multi-frame retransmission such as in [49], its design concept is primarily based on a pure stop-and-wait ARQ (SW-ARQ) mechanism. It is required to provide an efficient retransmission scheme in order to enhance the system throughput for the IEEE 802.11n networks. In this chapter, MAC-defined ARQ mechanisms are proposed to consider the effect from frame aggregation in order to improve the network throughput. An aggregated selective repeat ARQ (ASR-ARQ) algorithm is proposed which incorporates the conventional selective repeat ARQ scheme with the consideration of frame aggregation. On the other hand, an aggregated hybrid ARQ (AH-ARQ) mechanism is proposed to further enhance the throughput performance for the IEEE 802.11n networks under worse channel quality. The proposed AH-ARQ scheme can be categorized as type-I of H-ARQ algorithm, which is served as an outer code designed from the MAC layer perspective. The Reed-Solomon (RS) code [62, 63], which defines a finite codeword length, is adopted within the AH-ARQ scheme.

Furthermore, it will be beneficial to construct effective analytical models to evaluate the retransmission mechanisms for the IEEE 802.11n networks. There are existing studies that propose analytical models for performance evaluation of the MAC channel access [29, 64–66] and frame aggregation techniques [67–69] in the IEEE 802.11-based networks. However, none of these models explicitly considers efficient retransmission schemes that are especially feasible for high throughput requirements. The studies in [70, 71] investigate the impact of adopting block acknowledgement (BA) for high-speed WLANs and propose the analytical model for acquiring the system throughput. Nevertheless, these works did not construct the analytical models for aggregated packet delay distribution. Moreover, RS-based FEC mechanisms are adopted in [72–74] for the purpose of reducing the frame error probability. Three error-control schemes are considered in [72] to compare the performance and computation complexity; while the scheme in [73] combines the retransmission scheme with a newly defined PHY format for enhancing the network performance. However, these analytical models only consider a single WS in the network

that exclude the effect of channel contention between multiple WSs. Moreover, most of the existing studies did not include multiple opportunities for data transmission in one transmission opportunity (TXOP) that is allowed by the IEEE 802.11n standard.

As a consequence, with the consideration of multiple WSs, the service time distribution model with multiple transmission opportunities in one TXOP are constructed in order to observe the behaviors of both the ASR-ARQ and AH-ARQ algorithms. A novel approach based on the state diagram is utilized for the construction of analytical models for both schemes with the consideration of interfering WSs. Simulations are performed to both validate and compare the proposed ARQ schemes with conventional mechanism. It will be shown in the numerical results that the proposed AH-ARQ protocol can outperform the other mechanisms under worse channel condition; while the proposed ASR-ARQ scheme is superior to the other protocols under better channel condition.

The remainder of this chapter is organized as follows. Section 4.2 describes the frame aggregation mechanism of IEEE 802.11n standard and the proposed ARQ algorithms. The system modeling and performance analysis of proposed ARQ schemes are addressed in Section 4.3. Section 4.4 provides the performance evaluation; while the conclusions are drawn in Section 4.5.

4.2 Proposed MAC-Defined Aggregated ARQ Schemes

In this section, the frame aggregation structure defined in the IEEE 802.11n MAC protocol is reviewed in Subsection 4.2.1. The proposed ASR-ARQ and AH-ARQ protocols are explained in Subsections 4.2.2 and 4.2.3, respectively.

4.2.1 Frame Aggregation/De-aggregation of IEEE 802.11n MAC Protocol

The IEEE 802.11n standard mandates the implementation of frame aggregation scheme for the sake of promoting transmission efficiency. It is noted that the transmission efficiency is defined as the time for delivering the information payload over the time duration for transmitting the entire aggregated frame associated with the required control frames and contention periods. With the frame format as shown in Fig. 4.1(a), multiple MAC protocol data units (MPDUs) are combined into an aggregated MPDU (A-MPDU), which is consequently transported into a single PHY service data unit (PSDU). Intuitively, the transmission efficiency can be improved with the utilization of A-MPDU since more

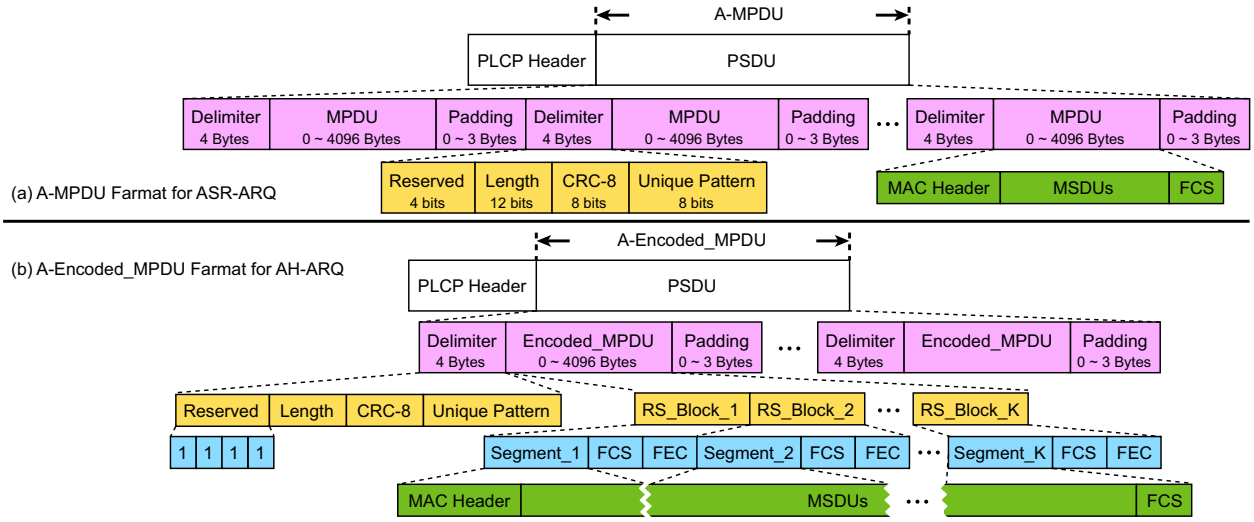

Figure 4.1: (a) A-MPDU Farmat for proposed ASR-ARQ scheme. (b) A-Encoded_MPDU Farmat for proposed AH-ARQ scheme.

MPDUs are transmitted with a communion of control overhead.

Each MPDU is padded with an MPDU delimiter for the purpose of extracting the corresponding MPDU from the aggregated frame. The extracting delimiter is composed of four bytes as shown in Fig. 4.1(a), including the reserved, MPDU length, cyclic redundancy check (CRC), and unique pattern (UP) fields. It is noted that the UP field, which is set to the ASCII value of character 'N', is employed to detect the location of an MPDU delimiter while scanning within the aggregated frame. Moreover, each MPDU is padded to become a multiple of four octets as shown in Fig. 4.1(a). The de-aggregation procedure at the receiver side described in the standard is shown in Fig. 4.2. The receiver verifies the validity of MPDU delimiter based on the 8-bits CRC and the observation of UP field, i.e., to exam the correctness of character 'N'. An MPDU can be successfully extracted from the A-MPDU if the corresponding MPDU delimiter is found to be valid. Otherwise, the de-aggregation process will continue to move forward with four bytes, i.e., via the offset parameter in Fig. 4.2, and to verify if the next multiple of four octets contains a valid delimiter.

4.2.2 Proposed Aggregated Selective Repeat (ASR) ARQ Scheme

The design of retransmission mechanisms is an open topic from the standpoint of IEEE 802.11n standard. In this chapter, the proposed ASR-ARQ scheme is enhanced from conventional selective repeat ARQ mechanism to consider frame aggregation within the de-

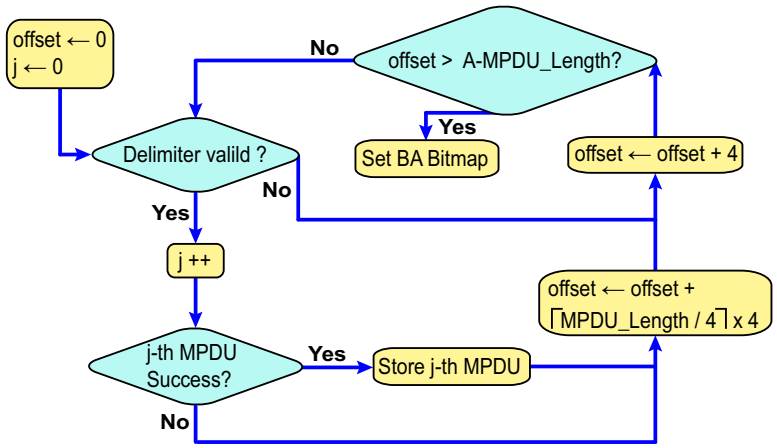

Figure 4.2: The flow diagram of MPDUs de-aggregation procedure for proposed ASR-ARQ scheme.

sign of retransmission algorithm. Contributing from the availability of BA scheme within the IEEE 802.11n standard, the ASR-ARQ algorithm can be effectively designed to provide transmission efficiency. Instead of sending individual acknowledgement (ACK) frame, the receiver replies with a BA frame for acknowledging the entire A-MPDU that is initiated from the transmitter. Since compressed BA is employed for this chapter, the BA frame will consist of 32 octets that contains an 8 octets bitmap field. Each bit within the bitmap field identifies whether the corresponding MPDU from the aggregated frame has been correctly received. As shown in Fig. 4.2, the receiver will set the bitmap of BA after completing all the MPDU de-aggregations and validations from an A-MPDU. Intuitively, a single BA frame can reduce the control overheads that are required by conventional design, which replies multiple ACK frames in response to an aggregated data frame.

In the proposed ASR-ARQ scheme, each MPDU within an A-MPDU is identified via a unique sequence number as the aggregated frame is transmitted. In the case that some of the MPDUs within an A-MPDU are missing during the transmission, the ASR-ARQ algorithm will continue to retransmit those unsuccessfully transmitted MPDUs until all the MPDUs have either been positively acknowledged by the BA frame or reached the retry limitation. For instance, there are 10 MPDUs contained within an A-MPDU that are identified by the sequence numbers from 1 to 10. If the MPDUs with sequence numbers 3 and 5 are corrupted and are identified via the CRC check, the receiver will reply with the BA frame which denotes two zero flags at the corresponding third and fifth bits within the bitmap field. A new A-MPDU, which includes only the third and fifth MPDUs, will be delivered by the transmitter at the next transmission opportunity. The retransmission

procedure terminates until either all the MPDUs with sequence numbers from 1 to 10 are correctly accepted by the receiver or the maximum number of retransmission trials (i.e., identified by the Retry_Limit parameter) has achieved.

4.2.3 Proposed Aggregated Hybrid (AH) ARQ Scheme

In order to further enhance the transmission efficiency, the AH-ARQ scheme is proposed in this chapter to integrate both the RS-based FEC construction and de-aggregated retransmission mechanism, which are described in the next two subsubsections.

4.2.3.1 RS-based FEC Construction

With the compliance to existing IEEE 802.11n MAC frame structure, the proposed FEC mechanism is constructed according to the RS code [62, 63] that is well-adopted in the design of outer decoders. The coefficients of generator polynomial $G(x)$ are elements in a finite field $GF(2^{n_b})$, where $n_b = 8$ is chosen according to the byte-oriented system. For a RS(n_c, n_i) code with $n_c = 2^{n_b} - 1 = 255$ as the codeword length, n_i as the size of original information symbols, and $\theta = (n_c - n_i)/2$ as the error correction capability, the set of roots $\boldsymbol{\alpha} = \{\alpha, \alpha^2, ..., \alpha^{2\theta}\}$ of $G(x)$ is selected from $GF(2^8)$ where α is a primitive element of the finite field. As a result, the generator polynomial $G(x)$ can be represented as $G(x) = \prod_{i=1}^{2\theta}(x+\alpha^i) = x^{2\theta} + \sum_{i=0}^{2\theta-1} g_i x^i$ with g_i representing the coefficients for all $i \in \{0, ..., 2\theta-1\}$. Based on the cyclic property of RS code, the set of codewords can be formed with the multiplication of both $G(x)$ and the information symbol polynomial $I(x)$. Moreover, the RS code will have the minimum codeword distance $d_{min} \geq 2\theta + 1$ in the case that all the coefficients g_i are not equal to zero. Therefore, the corresponding RS code possesses the correcting capability of θ error symbols associated with the codeword length of n_c octets and n_i information octets. There are total of $n_c - n_i = 2\theta$ parity check octets, which are served as the remainder $R(x)$ while dividing $x^{2\theta} I(x)$ by the generator polynomial $G(x)$.

4.2.3.2 De-aggregation and Retransmission Mechanism

A newly defined Aggregated-Encoded_MPDU (A-Encoded_MPDU) structure for the proposed AH-ARQ scheme is illustrated in Fig. 4.1(b). The original MPDU, including MAC header, MSDUs, and frame check sequence (FCS), is divided as several segments each with $(n_i - 4)$ bytes, and the CRC-32 value can be calculated as the FCS and is attached after each segment to verify its correction. Moreover, the FEC value is computed according to both the segment and FCS in order to implement forward error correction. Note that

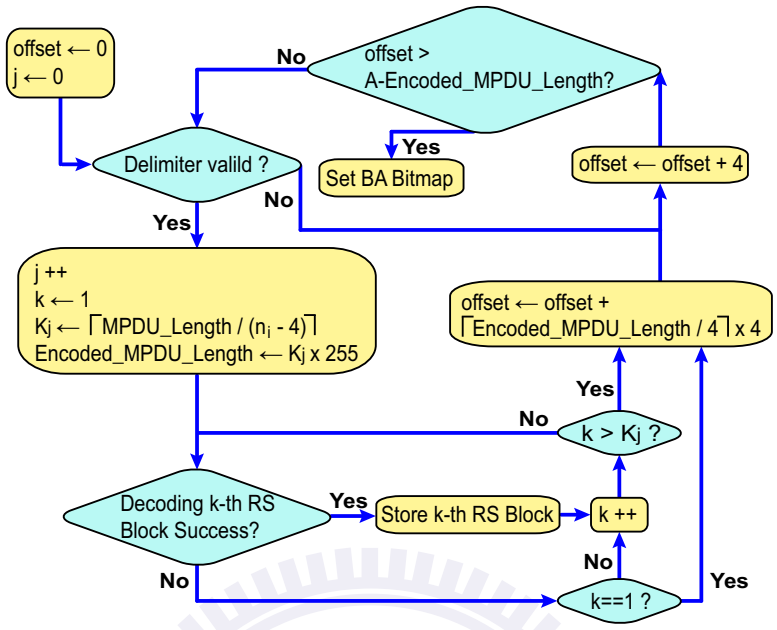

Figure 4.3: The flow diagram of Encoded_MPDUs de-aggregation procedure for proposed AH-ARQ scheme.

the total size for a RS block, including segment, FCS, and FEC, will be $(n_i-4)+4+2\theta = 255$ bytes. Furthermore, a series of zeros will be padded after the original MPDU such that its size will become the multiple of $(n_i - 4)$ bytes. The receiver can acquire the original size of the MPDU according to the Length field of the delimiter. In order to extract the A-Encoded_MPDUs that adopt the FEC mechanism, a modified de-aggregation procedure is performed as shown in Fig. 4.3. At the beginning, the scanning process will start to search for the UP field. After the UP has been identified, a predefined symbol will be traversed in order to verify the usage of FEC scheme. In other words, a valid delimiter will be identified if both the reserved field within the delimiter matches the '1111', i.e., '0xF', and the CRC-8 value is determined correct. The receiver can start to execute the de-aggregation procedure if all the verifications are valid. The number of RS blocks for the jth Encoded_MPDU can be calculated as

$$K_j = \left\lceil \frac{MPDU\_Length_j}{n_i - 4} \right\rceil, \tag{4.1}$$

where the $MPDU\_Length_j$ is obtained from the Length field of jth delimiter. Therefore, the receiver will be aware of the size of jth Encoded_MPDU, i.e., equal to $K_j \times 255$, and also the location of the next delimiter. The next step is to execute the CRC-32 validation

for each RS block in the Encoded_MPDU. If the result is valid, the receiver can store the RS block directly. Otherwise, the RS decoding procedure will be performed for this RS block. Note that the Berlekamp's iterative algorithm [75] is adopted to implement the decoding procedure. After completing the decoding process, the receiver will execute the CRC-32 check to verify if the decoded RS block can pass the verification. If not, this RS block will be dropped.

After all the Encoded_MPDUs have been extracted with all RS blocks been processed, the receiver starts to set the bits within the BA frame's bitmap field that map to the corresponding RS blocks. Considering a common scenario that the number of RS blocks in each Encoded_MPDU is a fixed value, i.e., $K_j = K$, the bitmap field within the BA for the proposed AH-ARQ protocol is extended to contain 256 bits in order to support J Encoded_MPDUs with K, $K \leq 256/J$, RS blocks in each Encoded_MPDU for a single data transmission. If the RS blocks are either correctly received or with correctable errors, the receiver will enable the corresponding bits in the bitmap field of BA frame. Otherwise, these bits will be disabled. The receiver will reply a BA frame to the transmitter after finishing setting up the bitmap of BA. The transmitter can initiate a retransmission of failed RS blocks according to the received BA. Note that all the RS blocks in the Encoded_MPDU can be considered independently, except for the first RS block. It is required for the entire Encoded_MPDU to be retransmitted if the first RS block fails in transmission since it contains the MAC header information of the Encoded_MPDU. The receiver cannot recognize the remaining RS blocks without the MAC header. Moreover, the first RS block is always needed in the Encoded_MPDU to provide important information, e.g., the receiver address, if there exists at least one other RS block in this Encoded_MPDU that should be retransmitted.

4.3 Performance Analysis of Proposed ARQ Schemes

In this section, novel analytical models based on the state diagram are exploited to analyze the performance of proposed ASR-ARQ and AH-ARQ mechanisms under saturated traffic. The service time distributions for both ARQ schemes are acquired with the consideration of interfering stations in the network. Distributed network topology is considered, where there are one access point (AP) and N WSs. The N WSs are contending for channel access in order to communicate with the AP for data transmission. Furthermore, the distributed coordination function (DCF) is employed as the medium access scheme for one access category between the transmitter and the receiver. The request-to-send/

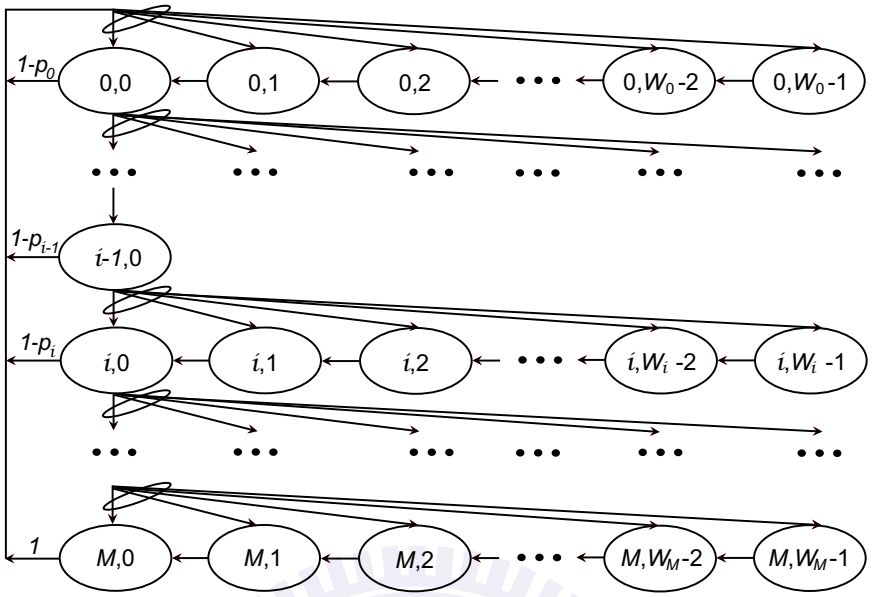

Figure 4.4: Two-dimensional Markov chain model for the backoff process of contention-based systems.

clear-to-send (RTS/CTS) mechanism is used for channel reservation in order to enhance the basic access mechanism. The proposed analytical models can be applied to all the N WSs contending the channel access. Moreover, the proposed models are also suitable for both the N WSs and the AP since all of them adopt the same contention-based protocol, e.g., the RTS/CTS handshaking and the backoff process. If the AP has data to be delivered to the WSs, the AP's behavior can be obtained by replacing the number N with $N+1$ in the analytical models since the number of total stations that contend the channel will include N WSs and one AP. Subsection 4.3.1 described the service model for contention-based systems. Subsection 4.3.2 explains the modeling of service time distribution for the proposed ASR-ARQ scheme; while that of the AH-ARQ algorithm is presented in Subsection 4.3.3.

4.3.1 Service Model for Contention-based Systems

There are existing research [29–34] establishing the analytical models for the backoff process of DCF scheme under different considerations, e.g., fading channel [30], backoff suspension [33], or retry limit [34]. The two-dimensional Markov chain model is adopted as the baseline model to analyze the channel contention behaviors for the proposed ARQ mechanisms. As shown in Fig. 4.4, $W_i = 2^i W$ is defined as the backoff window size at the stage i where W denotes the minimum backoff window size. According to the DCF-based

system, the steady state probability $b_{i,k}$ for the WS can be derived from the Markov chain model, where the subscript (i,k) indicates that the WS is at the ith backoff stage with its backoff counter equal to k. Therefore, the state probability $b_{i,k}$ can be inferred as

$$\begin{cases} P(b_{i,k}|b_{i,k+1}) = 1, & 0 \le k \le W_i - 2, 0 \le i \le M, \\ P(b_{0,k}|b_{i,0}) = \frac{1-p_i}{W_0}, & 0 \le k \le W_0 - 1, 0 \le i \le M-1, \\ P(b_{0,k}|b_{M,0}) = \frac{1}{W_0}, & 0 \le k \le W_0 - 1, \\ P(b_{i,k}|b_{i-1,0}) = \frac{p_{i-1}}{W_i}, & 0 \le k \le W_i - 1, 1 \le i \le M, \end{cases} \tag{4.2}$$

where M denotes the maximum number of backoff stage. Note that the retry limit is assumed equal to M in this chapter. Moreover, the parameter p_i represents the failed transmission probability at the ith stage. Each steady state probability can be expressed as a function of $b_{0,0}$ based on the equations in (4.2). Since the sum of all the states will be equal to 1, namely $\sum_{i=0}^{M}\sum_{k=0}^{W_i-1} b_{i,k} = 1$, $b_{0,0}$ can be obtained as

$$b_{0,0} = \left\{ \frac{W+1}{2}\left[1 - p_0 + \sum_{i=1}^{M-1}\left((1-p_i)\prod_{j=0}^{i-1} p_j\right) + \prod_{i=0}^{M-1} p_i\right] + \sum_{i=1}^{M}\left(\frac{2^i W + 1}{2}\prod_{j=0}^{i-1} p_j\right)\right\}^{-1}. \tag{4.3}$$

Let τ be defined as the probability that a WS transmits an RTS packet in a randomly selected time slot. Based on the model in Fig. 4.4, a WS can transmit its RTS packets only if the backoff counter k reaches zero. Therefore, the parameter τ can be acquired as

$$\tau = \sum_{i=0}^{M} b_{i,0} = \left[1 + \left(\sum_{i=1}^{M}\prod_{j=0}^{i-1} p_j\right)\right] b_{0,0}. \tag{4.4}$$

Let P_c represent the probability that the RTS packet issued by one WS collides with those from the other WSs, which can be calculated as

$$P_c = 1 - (1-\tau)^{N-1}. \tag{4.5}$$

Combining (4.3), (4.4), and (4.5), it is observed that P_c is a function of p_i for $0 \le i < M$. In order to solve these unknown parameters, it is required to provide another relationship between p_i and P_c. It is assumed that each WS possesses a saturated queue, and there exists J aggregated MPDUs in each transmission at the initial, i.e., the 0th, backoff stage. The WS will retransmit the failed MPDUs within the A-MPDU until either all the MPDUs are

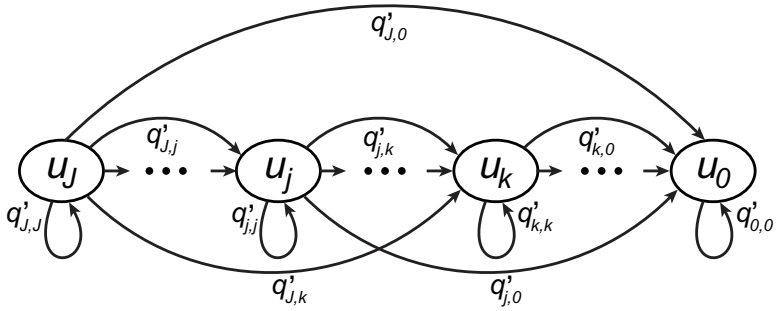

Figure 4.5: State diagram for the proposed ASR-ARQ and AH-ARQ schemes.

successfully received or the backoff stage has achieved the retry limit. Therefore, the state diagram for transmitting the failed MPDUs in one TXOP period can be modeled as shown in Fig. 4.5, where u_j indicates the state of j unsuccessful MPDUs and $q'_{j,k}$ represents the transition probability from state u_j to u_k. In other words, suppose that there are j failed MPDUs at the beginning of the TXOP, the probability that there still exists k failed MPDUs at the end of the TXOP is equal to $q'_{j,k}$. Considering that there are L opportunities for transmitting an A-MPDU in the TXOP, the transition probabilities $q'_{j,k}$ can be formulated as

$$\begin{pmatrix} q'_{j,0} \\ q'_{j,1} \\ \vdots \\ q'_{j,j} \end{pmatrix} = (1-P_c) \cdot \begin{pmatrix} q_{j,0}(1) \\ q_{j,1}(1) \\ \vdots \\ q_{j,j}(1) \end{pmatrix} + P_c \cdot \begin{pmatrix} 0 \\ \vdots \\ 0 \\ 1 \end{pmatrix}, \tag{4.6}$$

where

$$\begin{pmatrix} q_{j,0}(z) \\ q_{j,1}(z) \\ \vdots \\ q_{j,j}(z) \end{pmatrix} = \begin{pmatrix} 1 & C_0^1(1-P_e)\cdot z^{T_{D,M}} & \dots & C_0^j(1-P_e)^j \cdot z^{j\cdot T_{D,M}} \\ 0 & C_1^1 P_e \cdot z^{T_{D,M}} & \dots & C_1^j P_e(1-P_e)^{j-1} \cdot z^{j\cdot T_{D,M}} \\ \vdots & \vdots & \ddots & \vdots \\ 0 & 0 & \dots & C_j^j P_e^j \cdot z^{j\cdot T_{D,M}} \end{pmatrix}^L \cdot \begin{pmatrix} 0 \\ \vdots \\ 0 \\ 1 \end{pmatrix}. \tag{4.7}$$

Note that P_c is obtained from (4.5), and $T_{D,M}$ represents the required time for delivering both the delimiter and MPDU. The parameter P_e is equal to $P_{MPDU} + P_{DEL} - P_{MPDU} \cdot P_{DEL}$, where P_{MPDU} and P_{DEL} represent the probability of MPDU error and delimiter error, respectively. Note that $q_{j,k}(z)$ in (4.7) stands for the transition probability along with its required time in the power of z from state u_j to u_k without the consideration of RTS placket collisions. Moreover, it is noted that the WS is not able to transmit the MPDUs if its RTS packet collides with the other WSs in the network. At the ith backoff stage,

let $\alpha_{i,j}$ be denoted as the probability that there still exists j failed MPDUs after either the WS successfully sends its RTS packet and the corresponding A-MPDU or the RTS packet is failed in transmission. Therefore, $\alpha_{i,j}$ can be calculated based on the following $(J+1)\times(J+1)$ matrix operation as

$$\begin{pmatrix} \alpha_{i,0} \\ \alpha_{i,1} \\ \vdots \\ \alpha_{i,J} \end{pmatrix} = \begin{pmatrix} q'_{0,0} & q'_{1,0} & \cdots & q'_{J,0} \\ 0 & q'_{1,1} & \cdots & q'_{J,1} \\ \vdots & \vdots & \ddots & \vdots \\ 0 & 0 & \cdots & q'_{J,J} \end{pmatrix}^{i+1} \cdot \begin{pmatrix} 0 \\ \vdots \\ 0 \\ 1 \end{pmatrix}. \tag{4.8}$$

Finally, the probability of unsuccessful transmission at the ith backoff stage, i.e., p_i, can be formulated as

$$p_i = \begin{cases} 1-\alpha_{0,0}, & i=0, \\ \dfrac{1-\alpha_{i,0}}{1-\alpha_{i-1,0}}, & 0<i\leq M. \end{cases} \tag{4.9}$$

Combining (4.6), (4.8) and (4.9), the parameter p_i can be regarded as functions of P_c. Therefore, by iteratively solving the nonlinear functions (4.4) and (4.5), the two parameters τ and P_c can be obtained. Moreover, the parameters $q'_{j,k}$, $\alpha_{i,j}$, and p_i can also be calculated.

4.3.2 Modeling of Service Time Distribution for Proposed ASR-ARQ Scheme

In this subsection, the derivation of service time distribution for the WS will be described based on the proposed ASR-ARQ scheme under the existence of contending stations. Let $S_i(z)$ be defined as the probability generating function (PGF) of service time distribution on the condition that all the MPDUs are successfully received at the ith backoff stage. Furthermore, let $F_{i,j}(z)$ represent the PGF of total required time distribution on the condition that there are j ($j\neq 0$) failed MPDUs at the ith backoff stage. Note that both $S_i(z)$ and $F_{i,j}(z)$ do not include the backoff delay. Therefore, these two distributions can be formulated as

$$\begin{aligned} S_0(z) =& \frac{1-P_c}{\alpha_{0,0}} \cdot q_{J,0}(z) \cdot z^{T_A}, \\ S_i(z) =& \frac{1-P_c}{\alpha_{i,0}-\alpha_{i-1,0}} \left(\sum_{j=1}^{J} \alpha_{i-1,j} \cdot F_{i-1,j}(z) \cdot q_{j,0}(z) \right) \cdot z^{T_A}, \qquad 0<i\leq M, \end{aligned} \tag{4.10}$$

and

$$\begin{aligned} F_{0,J}(z) = & \frac{1}{\alpha_{0,J}}\left[(1-P_c)\cdot q_{J,J}(z)\cdot z^{T_A}+P_c\cdot z^{T_{out}}\right], \\ F_{0,j}(z) = & \frac{1-P_c}{\alpha_{0,j}}\cdot q_{J,j}\cdot z^{T_A}, && 0<j<J, \\ F_{i,j}(z) = & \frac{1-P_c}{\alpha_{i,j}}\left[\sum_{r=j}^{J}\alpha_{i-1,r}\cdot F_{i-1,r}(z)\cdot q_{r,j}(z)\cdot z^{T_A}\right], \\ & +\tfrac{P_c}{\alpha_{i,j}}\cdot\alpha_{i-1,j}\cdot F_{i-1,j}(z)\cdot z^{T_{out}}, && 0<i\le M,\ 0<j<J, \end{aligned} \tag{4.11}$$

where $T_A = T_{DIFS}+T_{RTS}+T_{CTS}+L\cdot T_{PHY\_Header}+L\cdot T_{BA}+(2L+1)\cdot T_{SIFS}+(2L+2)\cdot\delta$. The parameter $T_{out} = T_{DIFS}+T_{RTS}+T_{CTS}+T_{SIFS}+2\delta$ denotes the required timeout interval. Note that the parameters T_{DIFS}, T_{SIFS}, T_{RTS}, T_{CTS}, T_{PHY_Header}, T_{BA}, and δ are defined as the required time intervals for DIFS, SIFS, RTS packet transmission, CTS packet transmission, PHY header transmission, and propagation delay, respectively. Note also that (4.10) and (4.11) are approximated forms since a total of L opportunities are assumed for A-MPDU transmissions in a TXOP. In reality, the WS will not utilize the rest of transmission opportunities if all its MPDUs have been successfully transmitted. Furthermore, considering that there exists a specific WS in the backoff process, three exclusive events may occur in a slot time as follows: (a) there does not exist any other WS that sends the RTS packet; (b) there only exists one other WS sending its RTS packet; and (c) there exists at least two other WSs that send out their RTS packets. Let P_{idle}, P_{succ}, P_{col} be denoted as the probability for events (a), (b), and (c) to occur in a slot time, which can respectively be calculated as

$$\begin{cases} P_{idle} = (1-\tau)^{N-1}, \\ P_{succ} = (N-1)\tau(1-\tau)^{N-2}, \\ P_{col} = 1-(1-\tau)^{N-1}-(N-1)\tau(1-\tau)^{N-2}. \end{cases} \tag{4.12}$$

On the condition that a specific WS is in the backoff process, P_{col} denotes the probability that at least two of the other $(N-1)$ WSs contend the channel unsuccessfully due to the RTS packet collisions. Note that P_{col} is different from P_c in (4.5) which indicates the collision probability on the condition that the RTS packet is delivered by this specific WS. It is noticed that the reason for calculating (4.12) is to formulate the PGF of slot time delay distribution $H_d(z)$ from the backoff delay as illustrated in Fig. 4.6, where $D(z)$, $X(z)$, and $C(z)$ are denoted as the PGF of required time distribution given the event (a), (b), and (c), respectively. Therefore, $H_d(z)$ can be derived as

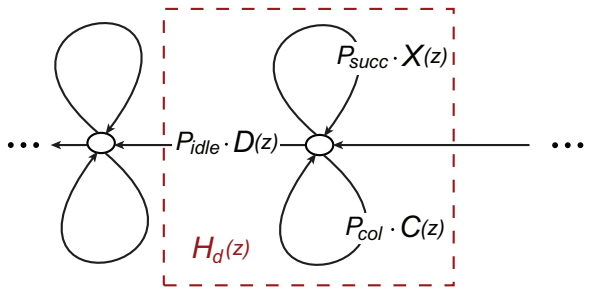

Figure 4.6: Schematic diagram for the PGF of slot time delay distribution $H_d(z)$.

$$\begin{aligned} H_d(z) &= P_{idle}D(z) + P_{succ}X(z)H_d(z) + P_{col}C(z)H_d(z) \\ \Rightarrow\ H_d(z) &= \frac{P_{idle} \cdot D(z)}{1 - P_{succ} \cdot X(z) - P_{col} \cdot C(z)}. \end{aligned} \tag{4.13}$$

It is also noted that Fig. 4.6 can be considered as an extension of the original Markov chain model in Fig. 4.4 to further account for the delay time distribution. In other words, Fig. 4.4 is utilized to analytically compute the system throughput which can be simplified from Fig. 4.6 by setting $P_{idle} = 1$ in a slot time, i.e., only event (a) will occur in a slot time such that the time delays costs from the PGFs $D(z)$, $X(z)$, and $C(z)$ are not considered. On the other hand, it is considered computationally complex to calculate (4.13) owing to the complexity in the denominator, i.e., $1 - P_{succ} \cdot X(z) - P_{col} \cdot C(z)$. In order to reduce the complicated computation, events (b) and (c) are assumed to occur at most once in a backoff time slot. Therefore, (4.13) can be approximated as

$$H_d(z) \approx P_{idle} \cdot D(z) + P_{succ} \cdot X(z)D(z) + P_{col} \cdot C(z)D(z). \tag{4.14}$$

Moreover, the expressions of $D(z)$, $X(z)$ and $C(z)$ can be obtained as

$$\begin{cases} D(z) = z^{\sigma}, \\ X(z) = \sum_{i=0}^{M} \frac{b_{i,0}}{\tau} \sum_{j=1}^{J} \left[P_{X,i,j} \cdot \left(\sum_{r=0}^{j} q_{j,r}(z) \cdot z^{T_A} \right) \right], \\ C(z) = z^{T_{out}}, \end{cases} \tag{4.15}$$

where

$$P_{X,i,j} = \begin{cases} 1, & i = 0,\ j = J, \\ 0, & i = 0,\ 0 < j < J, \\ \dfrac{\alpha_{i-1,j}}{1 - \alpha_{i-1,0}}, & 0 < i \leq M,\ 0 < j \leq J, \end{cases} \tag{4.16}$$

and the parameter σ represents a slot time. Consequently, the total backoff delay at the ith backoff stage, $H_i(z)$, can be derived as

$$H_i(z) = \frac{1}{2^i W} \sum_{r=0}^{2^i W - 1} \big(H_d(z)\big)^r, \ 0 \le i \le M. \tag{4.17}$$

Let $\phi_{succ,i}$ indicates the probability that all the MPDUs have been successfully received at the ith backoff stage, which can be calculated as

$$\phi_{succ,i} = \begin{cases} \alpha_{0,0}, & i = 0, \\ \alpha_{i,0} - \alpha_{i-1,0}, & 0 < i \le M. \end{cases} \tag{4.18}$$

As a result, the PGF of total service time distribution $T(z)$ can be obtained as

$$T(z) = \left(\sum_{i=0}^{M} \phi_{succ,i} \cdot S_i(z) \cdot \prod_{r=0}^{i} H_r(z) \right) + \left(\sum_{j=1}^{J} \alpha_{M,j} \cdot F_{M,j}(z) \right) \prod_{r=0}^{M} H_r(z), \tag{4.19}$$

where the parameter $\alpha_{M,j}$, which can be obtained in (4.8), denotes the probability of j failed MPDUs that are dropped after reaching the retry limit.

4.3.3 Modeling of Service Time Distribution for Proposed AH-ARQ Scheme

In this subsection, the performance analysis and modeling for the service time distribution of proposed AH-ARQ scheme is presented. Based on the RS code, the decoding errors occur while there are more than θ corrupted symbols within a predefined block. Therefore, a decoding error probability B_e of a block can be formulated as

$$B_e = \sum_{r=\theta+1}^{n_c} C_r^{n_c} s_e^r (1 - s_e)^{n_c - r}. \tag{4.20}$$

The parameter s_e represents the error rate of an RS symbol defined in $GF(2^{n_b})$ with n_b bits, i.e., $s_e = 1 - (1 - \text{BER})^{n_b}$ where BER denotes the bit error rate. It is noticed that B_e as defined in (4.20) is usually served as an upper bound of decoding errors for the RS code. Let H_e be denoted as the probability that either the delimiter or the first RS block in the

Encoded_MPDU fails in transmission, which can be calculated as

$$H_e = B_e + P_{DEL} - B_e \cdot P_{DEL}. \tag{4.21}$$

Note again that the entire Encoded_MPDU should be retransmitted if either the delimiter or the first RS block fails in transmission. Within an A-Encoded_MPDU, it is assumed that there are J Encoded_MPDUs and each has K RS blocks. In order to distinguish the first RS block and the remaining RS blocks, the parameter $K' = K - 1$ is utilized to indicate the number of remaining RS blocks in an Encoded_MPDU, and K' will start from two for identifying each RS block. Refer to Fig. 4.5, let $\widetilde{u}_k$ be defined as the state of k failed RS blocks in a specific Encoded_MPDU, and $\widetilde{q'}_{k,l}$ represents the transition probability from the state $\widetilde{u}_k$ to $\widetilde{u}_l$ in a single A-Encoded_MPDU transmission. The probability $\widetilde{q'}_{k,l}$ can be formulated as

$$\widetilde{q'}_{k,l} = \begin{cases} H_e + (1 - H_e)B_e^k, & k = l, \\ (1 - H_e) \cdot B_e^l (1 - B_e)^{k-l}, & k > l, \\ 0, & k < l, \end{cases} \tag{4.22}$$

for $0 \leq k, l \leq K'$. Note that $\widetilde{q'}_{k,l}$ is defined for a single A-Encoded_MPDU transmission transmission given the successful transmission of the RTS packet. Hence, $\widetilde{q}_{k,l}(z)$, the transition probability along with required time in the power of z from state $\widetilde{u}_k$ to $\widetilde{u}_l$ in the L opportunities for A-Encoded_MPDU transmissions, can be derived as

$$\begin{pmatrix} \widetilde{q}_{k,0}(z) \\ \widetilde{q}_{k,1}(z) \\ \vdots \\ \widetilde{q}_{k,k}(z) \end{pmatrix} = \begin{pmatrix} 1 & \widetilde{q'}_{1,0} \cdot z^{T_{RS}} & \cdots & \widetilde{q'}_{k,0} \cdot z^{k \cdot T_{RS}} \\ 0 & \widetilde{q'}_{1,1} \cdot z^{T_{RS}} & \cdots & \widetilde{q'}_{k,1} \cdot z^{k \cdot T_{RS}} \\ \vdots & \vdots & \ddots & \vdots \\ 0 & 0 & \cdots & \widetilde{q'}_{k,k} \cdot z^{k \cdot T_{RS}} \end{pmatrix}^L \cdot \begin{pmatrix} 0 \\ \vdots \\ 0 \\ 1 \end{pmatrix}, \tag{4.23}$$

where the parameters T_{RS} represents the transmission time of one RS block. Moreover, let x_j for $0 \leq x_j \leq K'$ be denoted as the number of failed RS blocks except for the first one in the jth Encoded_MPDU, which are integrated into the vector $\mathbf{x} = [x_1\ x_2\ \ldots\ x_j\ \ldots\ x_J]$ for $1 \leq j \leq J$. Furthermore, at the ith backoff stage, let $\widetilde{\alpha}_{i,\mathbf{x}}$ be denoted as the probability that there are still x_j failed RS blocks in the jth Encoded_MPDU for $1 \leq j \leq J$ after either the WS successfully sends its RTS packet and the corresponding A-MPDU or the RTS packet

is failed in transmission, which can be derived as

$$\begin{aligned}
\widetilde{\alpha}_{0,\mathbf{x}} &= P_c + (1-P_c)\cdot\left(\widetilde{q}_{K',K'}(1)\right)^J, && i=0, \mathbf{x}=K'\cdot\mathbf{1},\\
\widetilde{\alpha}_{0,\mathbf{x}} &= (1-P_c)\cdot\left[\prod_{j=1}^{J}\widetilde{q}_{K',x_j}(1)\right], && i=0, \mathbf{x}\neq K'\cdot\mathbf{1},\\
\widetilde{\alpha}_{i,\mathbf{x}} &= P_c\cdot\widetilde{\alpha}_{i-1,\mathbf{x}} + (1-P_c)\sum_{\mathbf{r}\in\mathbf{U}_\mathbf{x}}\left[\widetilde{\alpha}_{i-1,\mathbf{r}}\cdot\prod_{j=1}^{J}\widetilde{q}_{r_j,x_j}(1)\right], && 0<i\leq M,
\end{aligned} \tag{4.24}$$

where $K'\cdot\mathbf{1}$ denotes a $1\times J$ vector with all elements equal to K', $\mathbf{r}=[r_1\ r_2\ \ldots\ r_J]$, and the set $\mathbf{U}_\mathbf{x}=\{\mathbf{r}|K'\geq r_1\geq x_1, K'\geq r_2\geq x_2,\ldots,K'\geq r_J\geq x_J\}$. Let $\widetilde{p}_i$ represents the failed transmission probability at the ith stage, which can be calculated as

$$\widetilde{p}_i=\begin{cases}1-\widetilde{\alpha}_{0,\mathbf{0}}, & i=0,\\ \dfrac{1-\widetilde{\alpha}_{i,\mathbf{0}}}{1-\widetilde{\alpha}_{i-1,\mathbf{0}}}, & 0<i\leq M,\end{cases} \tag{4.25}$$

where $\mathbf{0}$ represents a $1\times J$ vector with all elements equal to 0. By replacing p_i in (4.3) with $\widetilde{p}_i$ in (4.25), the parameters P_c and τ can be iteratively solved based on (4.3), (4.4), and (4.5). Moreover, $\widetilde{q}_{k,l}(z)$, $\widetilde{\alpha}_{i,\mathbf{x}}$, and $\widetilde{p}_i$ can also be obtained after acquiring the parameter P_c.

Furthermore, let $\widetilde{S}_i(z)$ be defined as the PGF of A-Encoded_MPDU′ service time distribution on the condition that all the Encoded_MPDUs are successfully received at the ith backoff stage, and let $\widetilde{F}_{i,\mathbf{x}}(z)$ represent the PGF of total required time distribution on the condition that there are x_j failed RS blocks except for the first one in the jth Encoded_MPDU for $1\leq j\leq J$ at the ith backoff stage. Without the consideration of backoff delay, these two distributions can be respectively formulated as

$$\begin{aligned}
\widetilde{S}_0(z) &= \frac{1-P_c}{\widetilde{\alpha}_{0,\mathbf{0}}}\left(\widetilde{q}_{K',0}(z)\cdot z^{L\cdot T_H}\right)^J\cdot z^{T_A},\\
\widetilde{S}_i(z) &= \frac{1-P_c}{\widetilde{\alpha}_{i,\mathbf{0}}-\widetilde{\alpha}_{i-1,\mathbf{0}}}\left[\sum_{\substack{\mathbf{x}\in\mathbf{U}_\mathbf{0}\\(\mathbf{x}\neq\mathbf{0})}}\widetilde{\alpha}_{i-1,\mathbf{x}}\cdot\widetilde{F}_{i-1,\mathbf{x}}(z)\cdot\left(\prod_{j=1}^{J}\widetilde{q}_{x_j,0}(z)\cdot z^{L\cdot T_H}\right)\right]\cdot z^{T_A},\quad 0<i\leq M,
\end{aligned} \tag{4.26}$$

and

$$\begin{aligned}
\widetilde{F}_{0,\mathbf{x}}(z) = &\ \frac{1-P_c}{\widetilde{\alpha}_{0,\mathbf{x}}}\left(\widetilde{q}_{K',K'}(z)\cdot z^{L\cdot T_H}\right)^J \cdot z^{T_A} + \frac{P_c}{\widetilde{\alpha}_{0,\mathbf{x}}}\cdot z^{T_{out}}, && i=0,\ \mathbf{x}=K'\cdot\mathbf{1},\\
\widetilde{F}_{0,\mathbf{x}}(z) = &\ \frac{1-P_c}{\widetilde{\alpha}_{0,\mathbf{x}}}\prod_{j=1}^{J}\left(\widetilde{q}_{K',x_j}(z)\cdot z^{L\cdot T_H}\right)\cdot z^{T_A}, && i=0,\ \mathbf{x}\neq K'\cdot\mathbf{1},\\
\widetilde{F}_{i,\mathbf{x}}(z) = &\ \frac{1-P_c}{\widetilde{\alpha}_{i,\mathbf{x}}}\left[\sum_{\mathbf{r}\in\mathbf{U}_\mathbf{x}}\widetilde{\alpha}_{i-1,\mathbf{r}}\cdot\widetilde{F}_{i-1,\mathbf{r}}(z)\cdot\prod_{j=1}^{J}\left(\widetilde{q}_{r_j,x_j}(z)\cdot z^{L\cdot T_H}\right)\right]\cdot z^{T_A}+ &&\\
&\ \frac{P_c}{\widetilde{\alpha}_{i,\mathbf{x}}}\cdot\widetilde{\alpha}_{i-1,\mathbf{x}}\cdot\widetilde{F}_{i-1,\mathbf{x}}(z)\cdot z^{T_{out}}, && i\neq 0,
\end{aligned} \tag{4.27}$$

where T_H indicates the required time for sending one delimiter and the first RS block in an Encoded_MPDU. Note that the approximated formulations in (4.26) and (4.27) is obtained based on the condition that all the delimiters and the first RS blocks in the Encoded_MPDUs will be transmitted until the entire service finishes.

Furthermore, the three exclusive events that occur in a slot time with the existence of a specific WS in the backoff process will be the same as presented in (4.12). The corresponding time costs will also be identical to those in (4.15) except for the PGF $X(z)$ that represents event (b). Let $\widetilde{X}(z)$ be defined as the PGF of required time distribution given the occurrence of event (b) for the proposed AH-ARQ algorithm, which can be acquired as

$$\widetilde{X}(z)=\sum_{i=0}^{M}\left\{\frac{b_{i,0}}{\tau}\left[\sum_{\substack{\mathbf{x}\in\mathbf{U_0}\\(\mathbf{x}\neq\mathbf{0})}}\left(\widetilde{P}_{X,i,\mathbf{x}}\cdot\prod_{j=1}^{J}\sum_{r=0}^{x_j}\widetilde{q}_{x_j,r}(z)\cdot z^{L\cdot T_H}\right)\cdot z^{T_A}\right]\right\}, \tag{4.28}$$

where

$$\widetilde{P}_{X,i,\mathbf{x}}=\begin{cases}1, & i=0,\ \mathbf{x}=K'\cdot\mathbf{1},\\ 0, & i=0,\ \mathbf{x}\neq K'\cdot\mathbf{1},\\ \dfrac{\widetilde{\alpha}_{i-1,\mathbf{x}}}{1-\widetilde{\alpha}_{i-1,\mathbf{0}}}, & 0<i\leq M.\end{cases} \tag{4.29}$$

Moreover, the approximated PGF of slot time delay distribution $\widetilde{H}_d(z)$ for the AH-ARQ scheme can also be obtained by replacing $X(z)$ in (4.14) with $\widetilde{X}(z)$. The total backoff delay $\widetilde{H}_i(z)$ at the ith backoff stage for the AH-ARQ scheme will be of the same form as in (4.17). Let $\widetilde{\phi}_{succ,i}$ indicates the probability that all the Encoded_MPDUs have been successfully

received at the ith backoff stage, which can be computed as

$$\widetilde{\phi}_{succ,i} = \begin{cases} \widetilde{\alpha}_{0,\mathbf{0}}, & i = 0, \\ \widetilde{\alpha}_{i,\mathbf{0}} - \alpha_{i-1,\mathbf{0}}, & 0 < i \leq M. \end{cases} \tag{4.30}$$

Finally, the PGF of total service time distribution, i.e., $\widetilde{T}(z)$, for the proposed AH-ARQ algorithm can be obtained as

$$\widetilde{T}(z) = \left(\sum_{i=0}^{M} \widetilde{\phi}_{succ,i} \cdot \widetilde{S}_i(z) \cdot \prod_{r=0}^{i} H_r(z) \right) + \left(\sum_{\substack{\mathbf{x} \in \mathbf{U_0} \\ (\mathbf{x} \neq \mathbf{0})}} \widetilde{\alpha}_{M,\mathbf{x}} \cdot \widetilde{F}_{M,\mathbf{x}}(z) \right) \cdot \prod_{r=0}^{M} H_r(z). \tag{4.31}$$

4.4 Performance Evaluation

In this section, the performance of proposed ASR-ARQ and AH-ARQ schemes will be validated and compared via simulations. Additive white Gaussian noise (AWGN) is assumed for performance comparison under error-prone channels. Modulation and coding schemes (MCSs) are employed for the purpose of adapting channel quality which is evaluated by the received signal-to-noise ratio (SNR). Moreover, the effective BERs for MCSs can be pre-computed by MATLAB tools in order to accelerate the simulation runs. Note that the notation "MCS(mod, R)" represents the modulation type mod and convolutional code with coding rate R that are applied for MCS. Note also that the reference data rate with MCS(16QAM, 1/2) is set to 60 Mbps, and the data rates with other MCSs can therefore be computed. A system C/C++ network simulation model is constructed by considering the AP based single-hop communications. As shown in Table 4.1, the MAC-defined parameters that are described in the IEEE 802.11n standard is adopted in both the analytical models and the simulations. Performance validation of the proposed ASR-ARQ and AH-ARQ schemes is conducted in Subsection 4.4.1, and performance comparison with other schemes will be shown in Subsection 4.4.2.

4.4.1 Performance Validation

As illustrated from Figs. 4.7 to 4.12, the proposed analytical models for both the ASR-ARQ and AH-ARQ schemes are validated with simulation results. Note that three WSs, i.e., $N = 3$, are concurrently accessing the channel to communicate with the AP within the network. Fig. 4.7 shows the model validation for ASR-ARQ scheme via the cumulative

Parameter	Value	
	ASR-ARQ	AH-ARQ
Minimum window size (W)	32	
Maximum backoff stage (M)	5	
Retry limit	5	
Basic rate	15 Mbps	
Slot time (σ)	20 μs	
T_{SIFS}	10 μs	
T_{DIFS}	50 μs	
PHY header	24 Bytes	
Propagation delay (δ)	1 μs	
MPDU payload size	848 Bytes	
Delimiter	4 Bytes	
MAC header	28 Bytes	
RTS	20 Bytes	
CTS	14 Bytes	
BA	32 Bytes	56 Bytes

Table 4.1: System parameters and MAC configurations for proposed Aggregated ARQ mechanisms

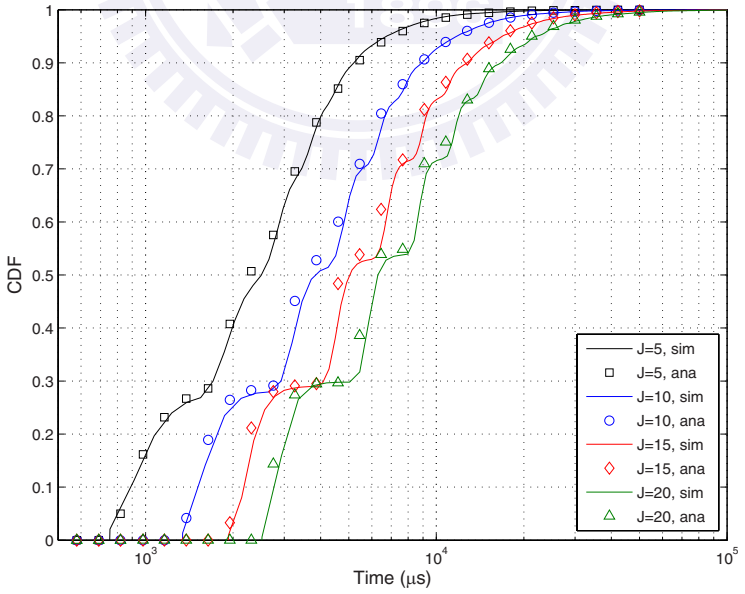

Figure 4.7: Performance validation for ASR-ARQ scheme: CDF of service time distribution, i.e., inverse z-transform of $T(z)$, under SNR $= 10$ dB, MCS(16QAM, 1/2), and $L = 2$.

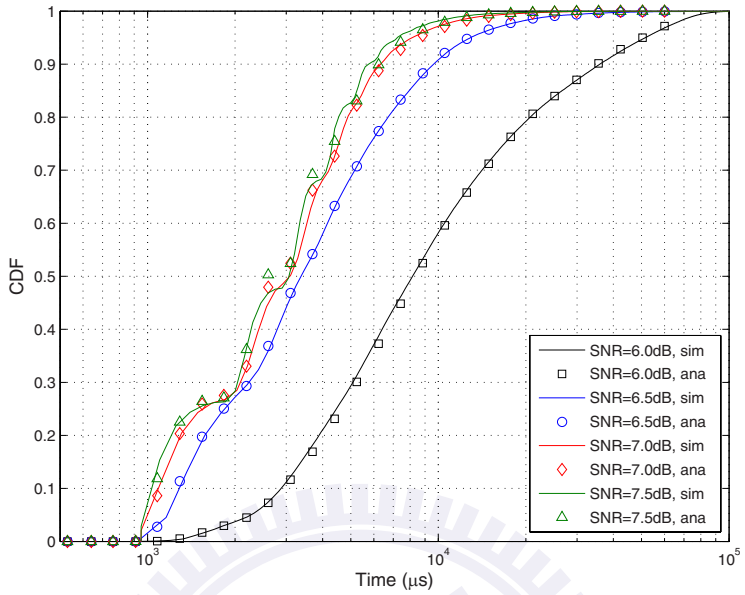

Figure 4.8: Performance validation for ASR-ARQ scheme: CDF of service time distribution, i.e., inverse z-transform of $T(z)$, under $J = 5$, MCS(QPSK, 3/4), and $L = 2$.

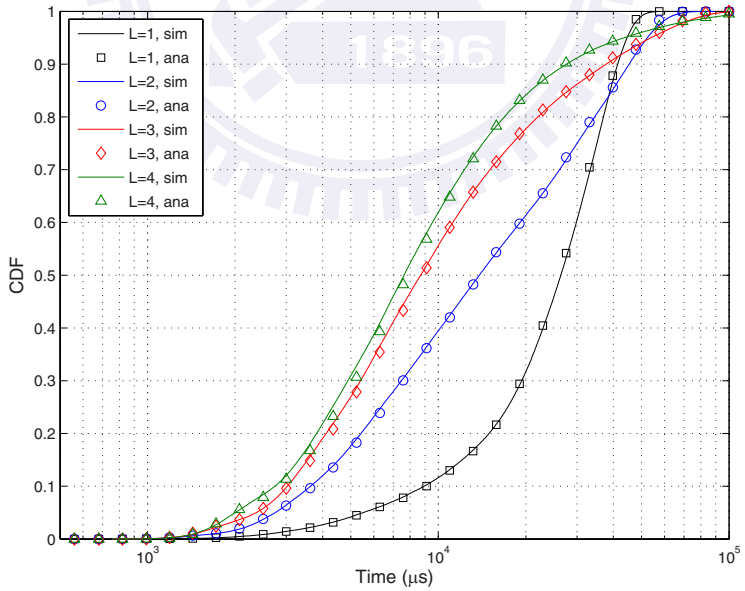

Figure 4.9: Performance validation for ASR-ARQ scheme: CDF of service time distribution, i.e., inverse z-transform of $T(z)$, under $J = 5$, SNR $= 8.8$ dB, and MCS(16QAM, 1/2).

distribution function (CDF) of service time by performing inverse z-transform of $T(z)$ in (4.19) under SNR $=$ 10 dB, MCS(16QAM, 1/2), and the number of opportunities for A-MPDU transmissions $L = 2$. Each MPDU consists of 848-bytes information payload. Four different numbers of aggregated MPDUs within an A-MPDU are considered for model validation, i.e., $J = 5$, 10, 15, and 20. The results obtained from the analytical model are denoted as "ana"; while that from the simulations are represented as "sim". Intuitively, it is shown in the figure that the service time is increased as the number of aggregated MPDUs J is augmented. Fig. 4.8 illustrates the performance validation for the ASR-ARQ scheme for the number of aggregated MPDU $J = 5$, MCS(QPSK, 3/4), and $L = 2$ under different SNR values. It can be observed that the CDF of service time is decreased as the SNR value is increased. Fig. 4.9 displays the performance validation condition on the number of aggregated MPDU $J = 5$, SNR $=$ 8.8 dB and MCS(16QAM, 1/2) under different numbers of opportunities for A-MPDU transmissions L. It can be observed that there exists crossing effect between the curves, which denotes that larger value of L does not necessarily result in shorter service time. The reason is that both WS in concern and the other WSs possess the same opportunities to transmit their MPDUs, which may not result in shorter packet service time with larger value of L. For those WSs with shorter service time can benefit from larger L, which becomes a drawback for those WSs with longer service time. Moreover, as shown in all three figures, the results from the simulations and the analytical model are consistent with each other under different conditions.

On the other hand, considering that two Encoded_MPDUs are aggregated in an A-Encoded_MPDU, Fig 4.10 illustrates the CDF of service time by conducting the inverse z-transform of $\widetilde{T}(z)$ in (4.31) for the proposed AH-ARQ algorithm with SNR $=$ 4.5 dB, MCS(QPSK, uncoded), and $L = 2$ under different values of K; while Fig. 4.11 displays the performance validation for the scenario of $K = 4$, MCS(16QAM, 1/2), and $L = 2$ under different SNR values. Moreover, the performance validation under different L values are considered in Fig. 4.12 with $K = 4$, SNR $=$ 4.4 dB, and MCS(QPSK, uncoded). Note that $K = 4$ corresponds to $K' = 3$. The RS$(255, 223)$ code over $GF(2^8)$ is constructed for the proposed AH-ARQ scheme via the primitive polynomial $1 + x^2 + x^3 + x^4 + x^8$. Each 848-bytes information payload contained in an original MPDU is partitioned into four RS blocks. The first RS block contains 191-bytes information octets and 28-bytes MAC header, and each of the remaining three RS block consists of 219-bytes information octets. Note that the remaining 4 bytes are occupied by the FCS for validation purpose. Similar to Figs. 4.7 and 4.8, longer service time will be incurred with either larger K or lower SNR value in

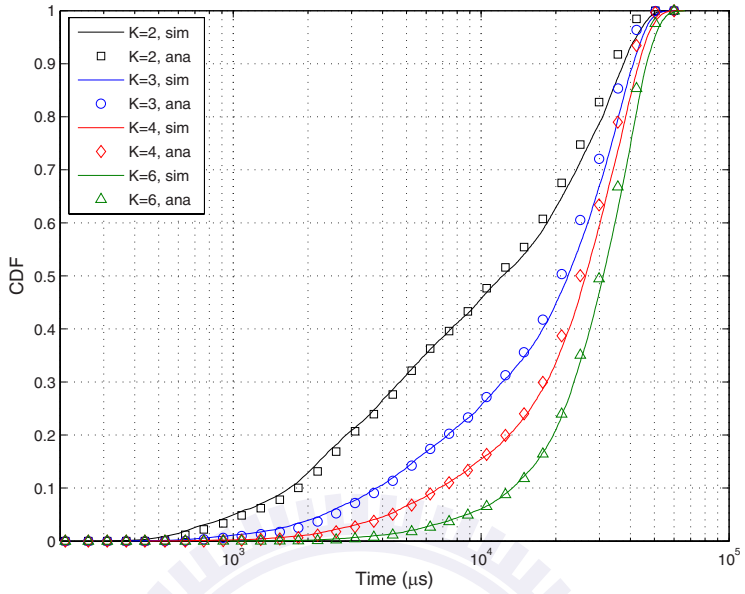

Figure 4.10: Performance validation for AH-ARQ scheme: CDF of service time distribution, i.e., inverse z-transform of $\widetilde{T}(z)$, under SNR $= 4.5$ dB, MCS(QPSK, uncoded), and $L = 2$.

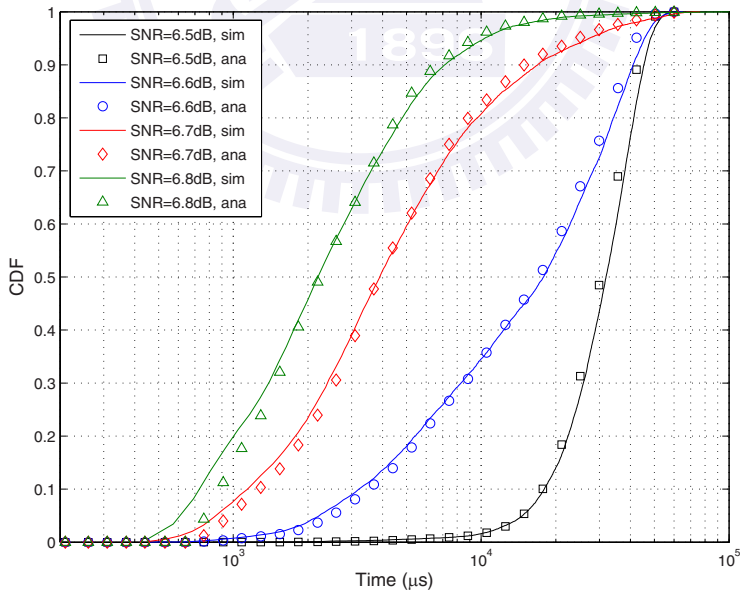

Figure 4.11: Performance validation for AH-ARQ scheme: CDF of service time distribution, i.e., inverse z-transform of $\widetilde{T}(z)$, under the number of RS blocks $K = 4$, MCS(16QAM, 1/2) and $L = 2$.

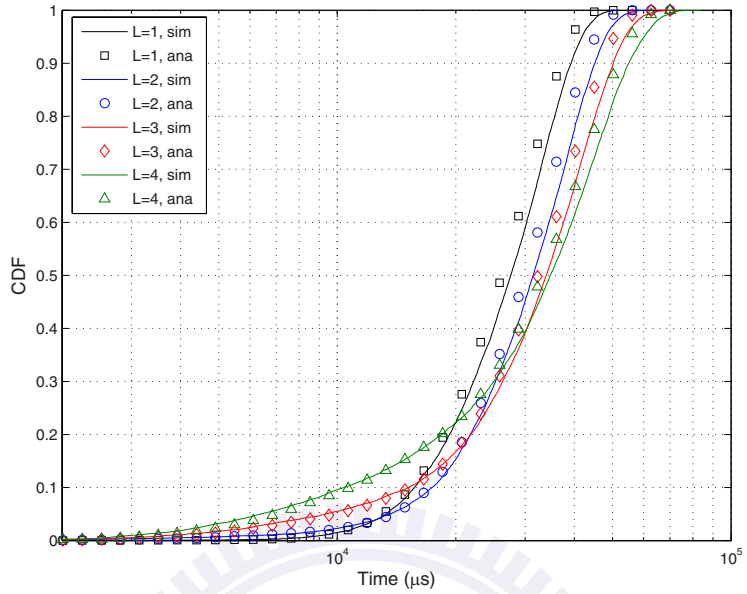

Figure 4.12: Performance validation for AH-ARQ scheme: CDF of service time distribution, i.e., inverse z-transform of $\widetilde{T}(z)$, under the number of RS block $K = 4$, SNR $= 4.4$ dB, and MCS(QPSK, uncoded).

Figs. 4.10 and 4.11, respectively. In Fig. 4.12, the crossing effect between different L curves is observed, which can also be explained similar to Fig. 4.9 for the ASR-ARQ scheme. It can be seen from all three figures that in most cases the proposed analytical model can match with the simulation results under different K, SNR, and L values.

4.4.2 Performance Comparison

Figs. 4.13 to 4.18 illustrate performance comparisons for proposed schemes under different parameter settings. If not further specified, the following parameters are set as the default values for performance comparison: number of WSs $N = 10$, number of transmission opportunities for A-MPDU/ A-Encoded_MPDU $L = 2$, MCS(16QAM,1/2), aggregated MPDUs $J = 10$, number of RS blocks $K = 4$, and RS$(255, 223)$ code. Fig. 4.13 shows the performance comparison for both the system throughput and mean service time under different SNR values with the number of aggregated MPDUs $J = 10$ and 20. The SW-ARQ scheme is also implemented in the simulations for comparison purpose. The SW-ARQ approach denotes that only a single MPDU is delivered for data transmission, which can be regarded as a special case of the ASR-SRQ scheme by setting $J = 1$. It can be observed that

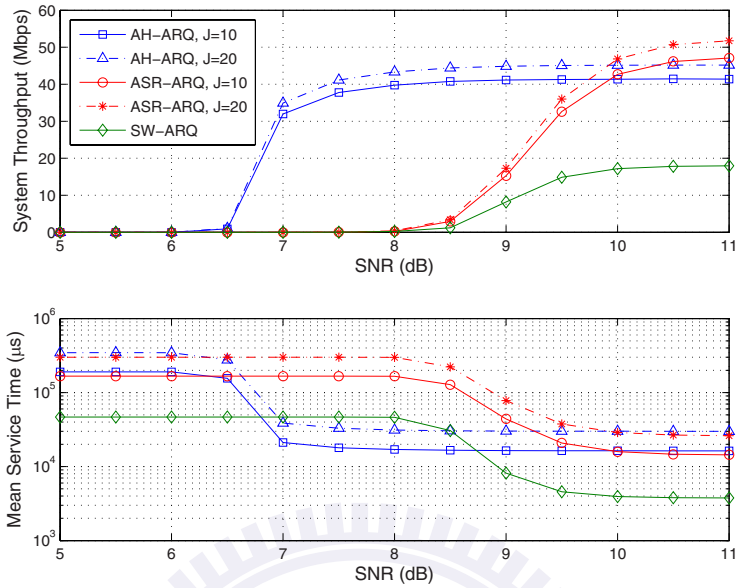

Figure 4.13: Performance comparison: system throughput and mean service time versus SNR values under different numbers of MPDUs (J).

the proposed AH-ARQ algorithm outperforms the other two schemes under lower SNR values, i.e., for SNR < 10 dB. The reason is that there is higher probability for the AH-ARQ scheme to correct packet errors compared to the other mechanisms without RS codes since packet transmission tends to fail under lower SNR environments. Moreover, the system throughput of the AH-ARQ approach can maintain at the same level under different SNR values; while the performances of the other two schemes significantly drop with decreased SNR values. On the other hand, the proposed AH-ARQ algorithm is inferior to the ASR-ARQ scheme under higher SNR values, i.e., SNR > 10 dB. The redundant FEC field in the proposed AH-ARQ scheme will become communication overheads under better channel conditions. It can also be observed that both the proposed aggregation-based algorithms, i.e., the AH-ARQ and ASR-ARQ schemes, can provide better performance compared to the SW-ARQ scheme since MPDU aggregation can effectively improve channel utilization. Moreover, under the same scheme, system throughput can be enhanced with larger number of aggregated MPDUs J due to the increased channel utilization. However, elongated mean service time is required under larger J since each WS will spend more time both on its own data transmission and waiting for other WS's data delivery.

Figs. 4.14 display the performance comparison for both the system throughput and

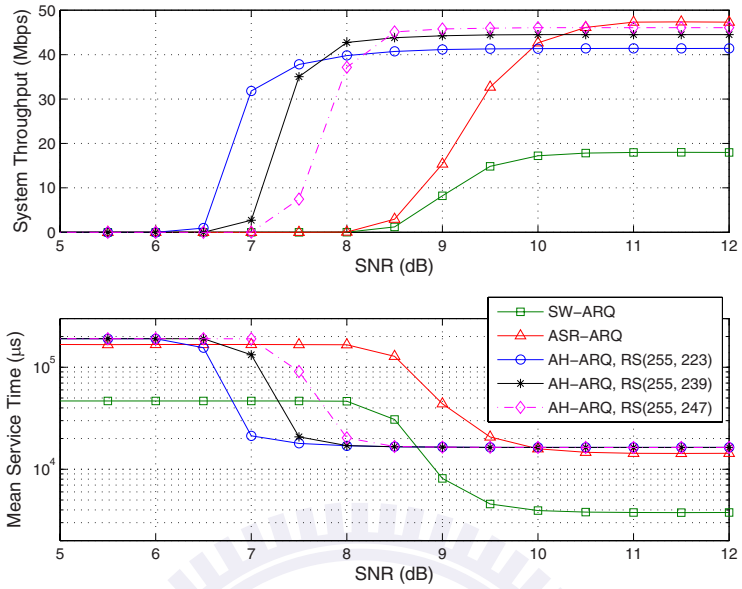

Figure 4.14: Performance comparison: system throughput and mean service time versus SNR values under different RS code rates.

mean service time with different RS coding rates. For fair comparison, the sizes of both MPDU and Encoded_MPDU are fixed as 1020 bytes. Therefore, the payloads for ASR-ARQ/SW-ARQ mechanisms are $1020 - 28 = 992$ bytes; while the payloads for AH-ARQ scheme with RS$(255, 223)$, RS$(255, 239)$, and RS$(255, 247)$ will be 848, 912, 944 bytes, respectively. Note that the 848-bytes MPDU is computed from 219 (payload per RS block) $\times(K = 4) - 28$ (MAC header) $= 848$, where the number of RS blocks is chosen as $K = 4$. It can be seen from both figures that the AH-ARQ scheme with lower RS coding rate outperforms the other algorithms under lower SNR channel since the scheme with lower RS coding rate can protect more information bytes. For instance, the throughput of AH-ARQ scheme with RS$(255, 223)$ can still be maintained at around 32 Mbps even if the SNR value approaches 7 dB; while that from the other schemes drops quickly under low SNR values. On the other hand, the ASR-ARQ scheme will provide higher system throughput under high SNR values due to the required FEC overhead from the AH-ARQ approach. Moreover, under higher SNR channel, the AH-ARQ scheme with higher RS coding rate will provide larger system throughput than that with lower RS coding rate since low RS coding rate will incur reduced number of successfully received information bytes.

As shown in Figs. 4.13 and 4.14, the performance of SW-ARQ scheme is inferior to the

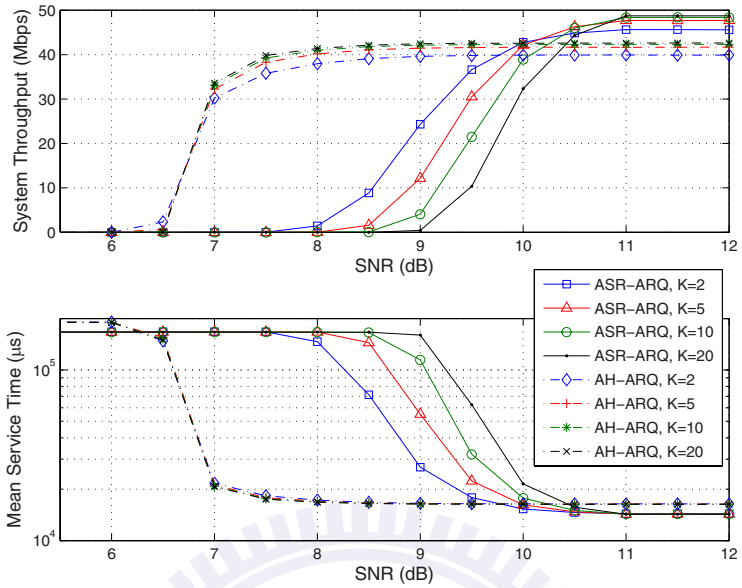

Figure 4.15: Performance comparison: system throughput and mean service time versus SNR values under different MPDU/Encoded_MPDU sizes with a roughly fixed A-MPDU/A-Encoded_MPDU length.

proposed ASR-ARQ and AH-ARQ schemes under most cases. Therefore, the SW-ARQ scheme will be omitted in the following plots to provide better performance comparisons between the ASR-ARQ and AH-ARQ algorithms. Fig. 4.15 displays the performance comparison for both the system throughput and mean service time under different MPDU/Encoded_MPDU sizes with a roughly fixed A-MPDU/A-Encoded_MPDU length. For fair comparison, both the MPDU and Encoded_MPDU payload sizes for curve K are computed as $219 \times K - 28$ that follows the computation for the RS block, even though it is not adopted in MDPU for the ASR-ARQ scheme. In order to approximately fix the the length of A-MPDU/A-Encoded_MPDU, the number of aggregated MPDUs/Encoded_MPDUs J in an A-MPDU/A-Encoded_MPDU is calculated by $40/K$. It can be observed that larger MPDU size can lead to higher system throughput for the ASR-ARQ scheme under higher SNR values, which is mainly caused by higher channel utilization. However, larger payload size results in worse performance under lower SNR values due to higher failure rate for transmitting larger MPDUs. On the other hand, the AH-ARQ scheme with larger Encoded_MPDU size outperforms that with smaller payload size under different SNR values due to the reason that each Encoded_MPDU is divided into several self-correcting RS blocks. On the other hand, the number of aggregated MPDUs/Encoded_MPDUs J can

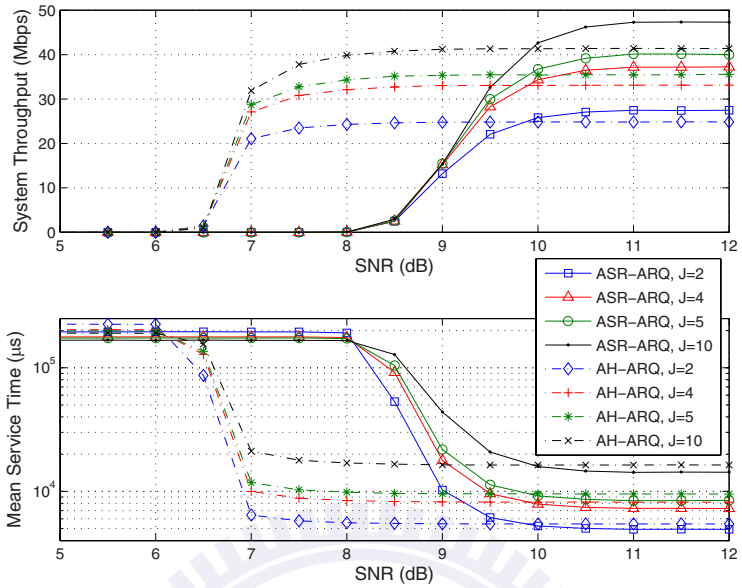

Figure 4.16: Performance comparison: system throughput and mean service time versus SNR values under different numbers of MPDUs (J) with a roughly fixed TXOP duration.

provide complementary effect as the MPDU/Encoded_MPDU size to the system performance. For the AH-ARQ scheme, adding J value will cause augmentation of the MAC header overhead which slightly decreases the throughput performance for the case $K = 2$ compared to the curve $K = 20$. Moreover, for ASR-ARQ scheme, larger J value (e.g., $K = 2$ case) can conquer the worse channel condition with its MAC header protection, which lead to higher system throughput. In addition, it can still be observed from both system throughput and mean service time that the proposed AH-ARQ algorithm can outperform the ASR-ARQ scheme under worse channel condition; while the ASR-ARQ protocol is slightly superior to the AH-ARQ scheme under better channel condition.

Fig. 4.16 shows the performance comparison for both the system throughput and mean service time considering the tradeoff between the number of MPDUs in an A-MPDU (i.e., J) and the number of A-MPDUs (L) in a fixed TXOP duration. The maximum transmission opportunities L for A-MPDU/A-Encoded_MPDU transmissions can be computed as $20/J$ such that the TXOP duration can be approximately fixed. In other words, smaller transmission opportunities L will be acquired if the number of MPDU/Encoded_MPDU J is enlarged. It can be seen from the figure that larger J value leads to higher system throughput for both the ASR-ARQ and AH-ARQ schemes since large J value can effectively en-

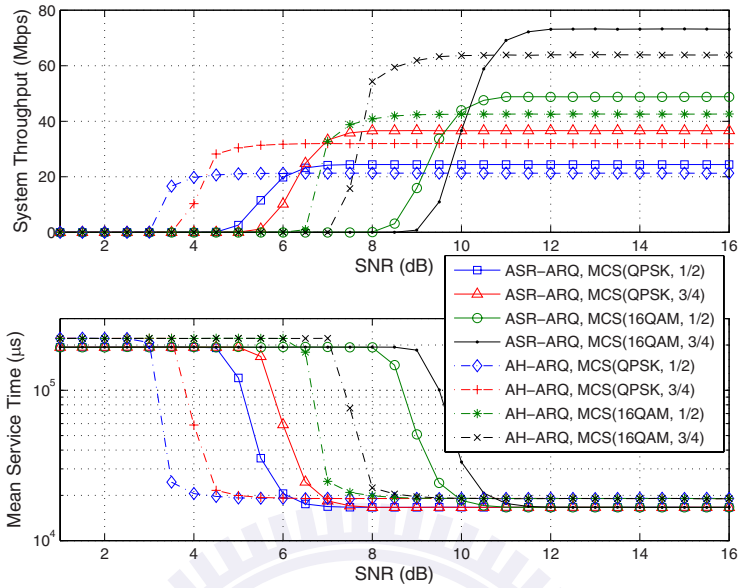

Figure 4.17: Performance comparison: system throughput and mean service time versus SNR values under different MCSs.

hance channel utilization. Therefore, the throughput performance is almost dominated by the J value rather than L due to the reason that adding L may furthermore cause extra communication overheads, e.g., ACK frame and SIFS interval. Moreover, it is not required for the WS to completely utilize all L opportunities if its packets have all been successfully transmitted. Hence, it can be seen that the throughput performance can be effectively enhanced by increasing J compared to the augmentation of L.

Fig. 4.17 shows the performance comparison for both the system throughput and mean service time for different MCSs. Note that the data rates of MCS(QPSK, 1/2), MCS(QPSK, 3/4), MCS(16QAM, 1/2), and MCS(16QAM, 3/4) are respectively 30 Mbps, 45 Mbps, 60 Mbps, and 90 Mbps. For fair comparison, the corresponding number of aggregated MPDUs J are respectively chosen as 6, 9, 12, and 18 in order to result in an identical TXOP period. It can be observed from the perspectives of both system throughput and mean service time that MCS with lower data rate can provide better performance than that with higher data rate under lower SNR values. The reason is that adopting MCS with lower data rate can decrease BER compared to that with higher data rate under the same SNR value. On the other hand, adopting MCS with higher date rate can lead to better performance compared to that with lower data rate under higher SNR values since more MPDUs

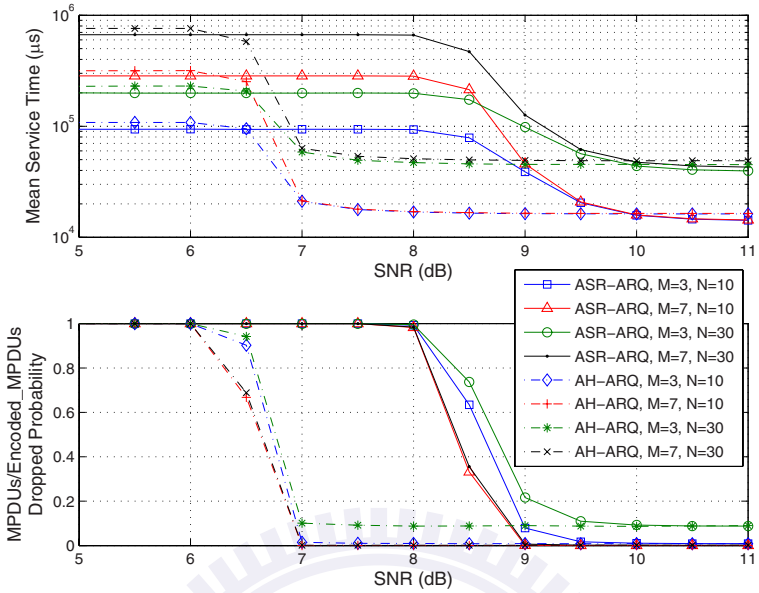

Figure 4.18: Performance comparison: mean service time and MPDUs/ Encoded_MPDUs dropped probability versus SNR values under different retry limits (M) and number of WSs (N).

can be accommodated within a single TXOP duration. From Fig. 4.17, it can be seen that the proposed AH-ARQ scheme provides better performance compared to the ASR-ARQ method under worse channel conditions.

Finally, Fig. 4.18 shows the performance comparison for both mean service time and MPDUs/Encoded_MPDUs dropped probability under different retry limits M and numbers of WSs N. Note that system throughput is not considered in this figure since mean service time and MPDUs/Encoded_MPDUs dropped probability are observed to be more sensitive to the variations of parameters M and N. It can be seen from the upper plot that longer service time will be acquired in both algorithms under larger M and N values, i.e., the case with $M = 7$ and $N = 30$. On the other hand, it is intuitive that lower MPDUs/ Encoded_MPDUs dropped probability can be achieved with larger value of retry limit M, i.e., the cases with $M = 7$ in the lower plot. Furthermore, it can still be observed that the proposed AH-ARQ scheme is superior to the ASR-ARQ protocol under different SNR, M, and N values.

4.5 Concluding Remarks

In this chapter, two automatic repeat request (ARQ) mechanisms are proposed with the consideration of frame aggregation under the IEEE 802.11n networks. The aggregated selective repeat ARQ (ASR-ARQ) protocol is proposed by incorporating the conventional stop-and-wait ARQ scheme; while the aggregated hybrid ARQ (AH-ARQ) algorithm further enhances throughput performance by adopting the Reed-Solomon block code for error correction under worse channel quality. Analytical models are constructed to evaluate the performance of proposed ASR-ARQ and AH-ARQ algorithms with the consideration of interfering stations. Simulations are also conducted to validate and compare the effectiveness of proposed ARQ mechanisms via both the mean service time and throughput performance. Numerical results show that the proposed AH-ARQ protocol can outperform the other schemes under worse channel condition; while the proposed ASR-ARQ protocol is superior to the other mechanisms under better channel condition.

Chapter 5

Femtocell Access Strategies in Heterogeneous Networks

*- In order to address **Problem 3**, game theory-based cell selection schemes are constructed in this chapter for the description of users' selfish behaviors. By the observation at Nash Equilibria, it is suggested that hybrid access mode can achieve higher flexibility for the performance enhancement of all subscribers, entire system system and operator compared to both open and closed access modes* [1]

5.1 Introduction

Long-term evolution-advanced (LTE-A) techniques are proposed by the 3rd generation partnership project (3GPP) to provide higher spectrum efficiency and data rate. According to the technical report from 3GPP [76], the downlink and uplink peak data rates are respectively required to achieve 1 Gbps and 500 Mbps in order to fulfill the quality-of-service (QoS) requirement for the user equipment (UE). For achieving these objectives, imposing additional low-power base stations (BSs) into the original networks naturally becomes a feasible solution for increasing the spectrum efficiency and data rate. On the other hand, according to the statistical data in [7], it is expected that there will be nearly 90% of data services and 60% of phone calls taken place in indoor environments. Hence,

[1] The chapter is based on

- Jia-Shi Lin and Kai-Ten Feng, "Femtocell Access Strategies in Heterogeneous Networks using a Game Theoretical Framework," major revision in *IEEE Trans. Mobile Computing*.

femtocell BSs (fBSs) with the properties of short-range, low-power, low-cost, and plug-and-play are designed to connect into the end user's broadband line in order to provide high throughput and QoS for the UEs. Moreover, installation of fBSs can share the traffic load of its coexisting macrocell BSs (mBSs) [8].

For the macrocell/femtocell heterogeneous networks (HetNets), it has been studied in [77] that co-channel deployment of frequency spectrum can achieve higher system throughput than independent channel deployment because of spectrum reuse. However, critical challenge associated with femtocell technology is the co-channel interference if the fBSs utilize the same frequency spectrum as the overlay mBSs, especially in the case that fBSs are operated in the closed access mode. Note that the closed and open access modes are two different access methods for the femtocell. The closed access mode only allows specific UEs that possess proper authorization, i.e., *subscribers*, to access the corresponding fBS. In general, *subscribers* are the UEs who purchase closed access fBS in order to improve their own throughput; while the *nonsubscribers* are prohibited to access the closed accessed fBS. On the other hand, the open access mode provides all the UEs with the permission to connect and access the fBS. One severe problem for this type of HetNets is that the fBS will produce strong interference to those UEs that are situated close by this fBS but not connect to it. Apparently, this problem tends to occur in closed access mode since those *nonsubscribers* close to the fBS are not allowed to access it. Note that for the closed access mode, *nonsubscribers* are defined as the UEs who are not permitted to access the fBS; while *subscribers* represent those UEs that are authorized and allowed to connect with the fBS.

Different existing research works have been proposed to alleviate the interference problem for HetNets. Distributed utility functions are designed in [78, 79] to achieve minimum signal-to-interference-plus-noise-ratio (SINR) for the femtocells, and the authors prove the existence of Nash equilibrium (NE) based on those utility functions. Novel preamble structure and self-organized power control scheme are proposed in [80] such that *non-subscribers* can detect the signals from the mBS even if they are located close to fBS. By estimating the path loss between the fBS and mBS, a power control scheme for femtocell has been designed in [81] to reduce the interference with mBS. Considering the tradeoffs between the co-channel and independent channel deployments, a hybrid spectrum usage scheme has been proposed in [82] to take advantage of their corresponding merits for interference mitigation. Based on the LTE-A system, a simple and fast distributed resource allocation scheme is proposed in [83] associated with cell splitting, range expansion, and semi-static resource negotiation. By adopting the cognitive radio (CR) approach to sense

the resource usage of mBS, a CR resource management scheme is proposed in [84] to deal with the interference problem between the fBS and mBS.

Furthermore, the impacts from different access policies for femtocell networks have been studied in many existing works. Assuming that the distributions of UEs' locations follow homogeneous spatial poisson point process, the uplink capacity analysis and interference avoidance strategy were proposed in [85] for the HetNets. It has been described in [85, 86] and 3GPP [13] that open access mode can alleviate the interference and improve throughput for the entire network under feasible numbers of fBSs and UEs. Moreover, the gaming model for different access strategies from economic aspects are established in [87]. The authors conclude that it is beneficial to both operators and users if open access mode is adopted. Although the open access mode was suggested to increase the entire network throughput, this mode is an obvious obstruction to promote the popularization of femtocells since users will not be interested in installing fBSs but accessed by other users. Customer surveys [12] have shown that open access mode is a main drawback to persuade users to purchase the fBSs and also pay for the expense of backhaul network. The tradeoffs between closed and open access modes for both the *subscribers* and entire network system were investigated in [88], and the uplink performances were also evaluated. The authors in [89] suggested the necessity to adopt hybrid access mode since both the closed and open access modes suffer from various disadvantages. The hybrid access mode has been proposed in [90, 91] to allow limited numbers of *nonsubscribers* to connect to fBS in order to reduce co-channel interference. The authors in [91] proposed a solution to increase overall performance with the guarantee of required network throughput for *subscribers*. However, these hybrid access schemes consider the tradeoff between the *subscribers* throughput and total network throughput, which consequently sacrifice the maximum achievable performance of *subscribers*.

A crucial issue in HetNet will be investigated in this chapter: which femtocell access strategy is recommended considering performance from the perspectives of *subscribers*, entire HetNet, and operator? To address the answer, *subscribers'* throughput, HetNet system throughput, and operator's revenue will be compared under closed, open, and hybrid access modes. In order to describe selfish behavior of individual UE, the cell selection schemes for *nonsubscribers* to access the fBS are formulated based on a theoretical gaming model. Both channel capacity and payment to the operator are considered for the design of utility function. Two different network scenarios are considered in our problem including co-channel spectrum deployment and independent channel deployment. Based on

the defined cell selection games, the existence of a pure strategy NEs will be illustrated and proven.

Moreover, the concept of primary users and secondary users in CR approach, e.g., [92, 93], is applied to resolve the prioritized access issue for co-channel HetNet. In co-channel scenario, fBS utilizes the same spectrum as mBS, which may produce strong interference to mBS's UEs. In order to reduce this potential interference, the UEs that connect to the mBS are defined as the primary UEs (PUEs); while connected to fBS are defined as the secondary UEs (SUEs). Since PUEs have higher priorities to access spectrum than SUEs, SUEs can be served by fBS only if PUEs are not significantly interfered by fBS. While prioritized access issue is solved, interference to mBS's UEs can therefore be mitigated. Based on proposed two cell selection games, three main conclusions from numerical results of this chapter are summarized as follows:

- Hybrid access mode is superior to closed access mode no matter which perspective, *subscribers*, entire HetNet, or operator revenue, is considered.
- Open access mode can result in higher capacity for the entire HetNet and greater revenue for operator compared to both the hybrid and closed access modes.
- *Subscribers* can obtain higher capacity in the hybrid access mode compared to both the open and closed access modes.

Therefore, it is concluded in this chapter that hybrid access mode can achieve better trade-off among the performance of *subscribers*, the performance of entire HetNet system, and the operator's revenue compared to both open and closed access modes. Note that some existing works, e.g., [90, 91], have also suggested hybrid access mode rather than closed access mode. However, none of these work considers the capacity of *subscribers*, the capacity of HetNets, and operator's revenue at the same time. Moreover, for cell selection in the HetNets, game theoretical models have never been utilized in existing research works to describe selfish behaviors of UEs. Most of existing works only focus on maximization of system capacity.

The rest of this chapter is organized as follows. Cell selection game *I* which considers frequency reuse and large-scale fading are established in Section 5.2. On the other hand, independent channel with both large-scale and small-scale fading are adopted for cell selection game *II* in Section 5.3. Section 5.4 illustrates performance evaluation for open, closed, and hybrid access modes. Conclusions are drawn in Section 5.5.

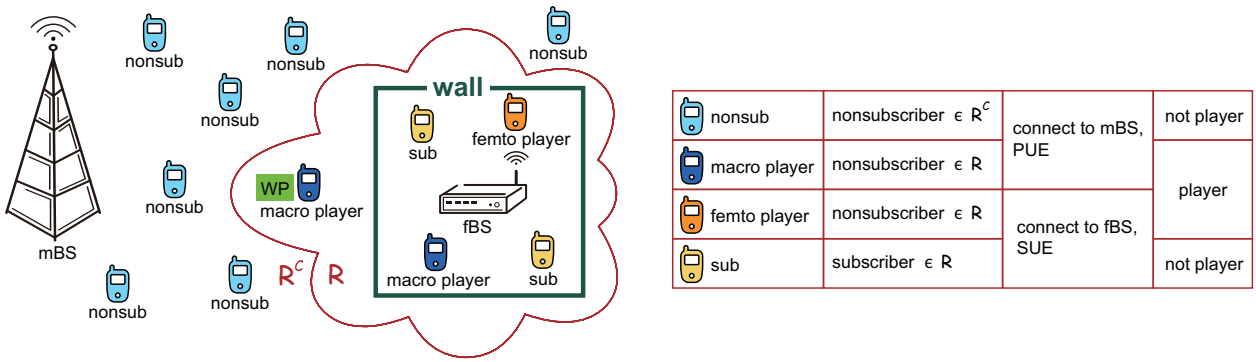

Figure 5.1: HetNet scenario and the definitions of different types of UEs

5.2 Construction of Cell Selection Game *I*

In this section, cell selection game *I* will be established for the HetNets. Every player in the game will select either the femtocell or macrocell as its targeting access network according to its utilities. Existence of pure strategy NE is proven for arbitrarily utility function. In this case, the following network scenarios are considered: (a) large-scale fading including both path loss and shadowing, and (b) co-channel deployment between macrocell and femtocell.

5.2.1 Network Scenarios

The concept of CR is utilized to model the behaviors of spectrum-sharing and interference control between the femtocell and macrocell. As mentioned above, the UEs that connect to the mBS are defined as PUEs; while those connecting to fBS are defined as SUEs. This definition is feasible since the main purpose of licensed spectrum is to allow the UEs to access the macrocell; while the fBSs are considered auxiliary equipments to increase the probability of spectrum reuse. If a channel is utilized by a PUE, the SUE can only transmit data in the channel with interference constraint in order to guarantee the QoS requirements of PUE.

Fig. 5.1 illustrates the HetNet scenarios and the definitions of different types of UEs. Let R and R^C respectively be defined as a set of UEs whose reference signal receiving powers (RSRPs) from fBS are larger and smaller than that from mBS. By definition, all *subscribers* are considered in R in order to access their subscribing femtocell. The *nonsubscribers* can be classified according to whether they are in R or in R^C. Naturally, those *nonsubscribers* in R^C tend to select the macrocell as their target network, which are consid-

ered independent to our gaming problem. On the other hand, those *nonsubscribers* in R will have the choice to connect either to mBS or to fBS in order to pursue their maximum utilities. The set of *nonsubscribers* $\in R$ are denoted as the *players* in the game. To simplify the analysis, it is assumed that *subscribers* can only connect to the fBS. However, even *subscribers* are not players in this game, they are provided with the rights to affect the game, which will be explained in the next subsection. Furthermore, let macro player and femto player be respectively defined as the player that connects to mBS and fBS. Based on CR concept, both *nonsubscribers* $\in R^C$ and macro players are considered as PUEs; while the *subscribers* and femto players are denoted as SUEs.

5.2.2 Existence of Pure Strategy NE

One of the major objectives in this chapter is to observe the NE of a game, where the existence of NE should first be proven. There are two main types of NE defined in non-cooperative game [94], i.e., the pure strategy NE and mixed strategy NE. Since the mixed strategies are considered impractical to describe the cell selection problem, the major concern in HetNet is to obtain the existence of pure strategy NE. To consider performance of all players in a more conservative manner, the utility designs of all players are assumed to be based on the player whose channel quality is the worst of all players, e.g., worst player (WP) in Fig. 5.1. Moreover, it is considered that the femto players have the same scheduling priority and preferences, and so do the macro players. The scheduling policies and preferences, i.e., capacity, power, cost, or security, cannot be determined since the total number of players connecting to the femtocell has yet to be decided in this game. Hence, the scheduling policies and preferences of the players are assumed to be identical within either the femtocell or macrocell. Note that it is implied that all players will possess the same utility function, and the utility function only depends on the number of players connecting to the femtocell. Based on [94], the following game can be defined to formulate cell selection problem.

Definition 5.1 (General Form of Cell Selection Game). *Consider the HetNet, a cell selection game is defined as a triplet*

$$\langle I, (S_i)_{i\in I}, (u_i)_{i\in I}\rangle, \tag{5.1}$$

where $I = \{1, ..., N\}$ is a finite set of players, i.e., the set of nonsubscribers $\in R$, and N denotes the number of players. $(S_i)_{i\in I}$ represents the set of pure strategies, where S_i is the non-empty set of actions for player i. Let "0" and "1" be defined as the pure strategy of connecting to the mBS

and fBS respectively for each player, i.e., $S_i = \{0,\ 1\}$. *By defining* $S = \prod_i S_i$ *as the set of action profiles,* $(u_i)_{i\in I}$ *indicates the set of utility functions where* $u_i : S \to \mathbb{R}$ *is a function from the set of all action profiles* S *to real numbers.*

Note that utility functions u_i of all players are identical as was explained in previous paragraph. Moreover, a tuple action profile is defined as (s_i, s_{-i}) where s_i and s_{-i} corresponds to the element in S_i and S_{-i} respectively. The set $S_{-i} = \prod_{j\neq i} S_j$ is denoted as the action profiles for all players except i. Note that the expression of action profile can be verbose owing to the element s_{-i}, e.g., $(s_i, s_{-i}) = (1, (1, 0, ...))$. Fortunately, every player will have the same utility function which only depends on its own strategy and the number of players except itself that connects to the fBS. Since the total number of players in cell selection game will be the major concern, the sum of all elements of s_{-i}, denoted as $\|s_{-i}\|_0$, will be considered instead of the individual element in s_{-i}. Note that $\|\mathbf{x}\|_0$ represents zero norm of vector $\mathbf{x}$, which is defined as the number of non-zero elements of $\mathbf{x}$. Therefore, the utility function for each player i can be stated as

$$u_i(s_i, s_{-i}) = \begin{cases} \tilde{u}_0(0, \|s_{-i}\|_0), & s_i = 0, \\ \tilde{u}_1(1, \|s_{-i}\|_0), & s_i = 1. \end{cases} \tag{5.2}$$

Note that $\tilde{u}_c$ represents the utility function of each player connecting to BS c, where $c = 0$ indicates mBS and $c = 1$ represents fBS. Both utility functions $\tilde{u}_0$ and $\tilde{u}_1$ only depend on the number of players connecting to the fBS. Note that $(s_i, \|s_{-i}\|_0)$ can contain different action profiles. For example, let $N = 5$ and $\|s_{-i}\|_0 = 2$, $(s_i, \|s_{-i}\|_0) = (1, 2)$ inherently represents various action profiles as $(1, (1, 1, 0, 0))$, $(1, (1, 0, 1, 0))$, $(1, (0, 1, 1, 0)), \ldots$, i.e., $u_i(1, (1, 1, 0, 0)) = u_i(1, (1, 0, 1, 0)) = u_i(1, (0, 1, 1, 0)) = \ldots = u_i(1, 2)$. Let $\|s\|_0 = s_i + \|s_{-i}\|_0 = \sum_i s_i$ be defined as the number of players that connect to the femtocell, (5.2) can further be simplified as

$$u_i(s) = \begin{cases} \tilde{u}_0(\|s\|_0), & s_i = 0, \\ \tilde{u}_1(\|s\|_0), & s_i = 1. \end{cases} \tag{5.3}$$

In order to prove the existence of a pure strategy NE of cell selection game, the potential game and its associated pure strategy NE as defined in [95] are stated as follows.

Definition 5.2 (Potential Game). *A function* $\Phi : S \to \mathbb{R}$ *is called a potential function for the game* Γ *if* $\forall i, \forall s_{-i} \in S_{-i}$,

$$u_i(x, s_{-i}) - u_i(y, s_{-i}) = \Phi(x, s_{-i}) - \Phi(y, s_{-i}), \forall\ x, y \in S_i. \tag{5.4}$$

If a potential function Φ exists, the game Γ is called a potential game.

Property 5.1. *The set $s^* \in S$ is a pure strategy Nash equilibrium (NE) of a potential game if and only if*

$$\Phi(s_i^*, s_{-i}^*) \geq \Phi(s_i, s_{-i}^*) \ \ \forall i, \forall s_i \in S_i. \tag{5.5}$$

Note that potential function Φ is a global function which can be employed to express the incentive of all players to change their strategies. With this function, descriptions of players' interaction can be simplified. Based on the definition of potential game, the following theorem will illustrate the existence of a pure strategy NE for cell selection game *I*.

Theorem 5.1. *Cell selection game I $\langle I, (S_i)_{i\in I}, (u_i)_{i\in I}\rangle$ is a potential game and has a pure strategy Nash equilibrium (NE).*

Proof. Based on Definition 5.1 for cell selection game I $\langle I, (S_i)_{i\in I}, (u_i)_{i\in I}\rangle$, the potential function of this game can be selected as the combination of its utility functions defined in (5.3), i.e.,

$$\Phi(s) = \tilde{\Phi}(\|s\|_0) = \sum_{n=1}^{\|s\|_0} \tilde{u}_1(n) + \sum_{n=\|s\|_0}^{N-1} \tilde{u}_0(n). \tag{5.6}$$

It is observed from (5.3) that there are only two choices for each player, i.e., $u_i(s) = \tilde{u}_0(\|s\|_0)$ for $s_i = 0$ and $u_i(s) = \tilde{u}_1(\|s\|_0)$ for $s_i = 1$. Furthermore, since we are only interested in the total number of players, the relationship for potential game in (5.4) can be rewritten by substituting (5.6) as

$$\begin{aligned}
&\Phi(1, s_{-i}) - \Phi(0, s_{-i}) = \tilde{\Phi}(1 + \|s_{-i}\|_0) - \tilde{\Phi}(0 + \|s_{-i}\|_0) \\
&= \sum_{n=1}^{1+\|s_{-i}\|_0} \tilde{u}_1(n) + \sum_{n=1+\|s_{-i}\|_0}^{N-1} \tilde{u}_0(n) - \left[\sum_{n=1}^{\|s_{-i}\|_0} \tilde{u}_1(n) + \sum_{n=\|s_{-i}\|_0}^{N-1} \tilde{u}_0(n) \right] \\
&= \tilde{u}_1(1 + \|s_{-i}\|_0) - \tilde{u}_0(0 + \|s_{-i}\|_0) = u_i(1, s_{-i}) - u_i(0, s_{-i}).
\end{aligned} \tag{5.7}$$

It is observed from (5.7) that the defined cell selection game *I* belongs to the class of potential games, which indicates the existence of a pure strategy NE according to Property 5.1. This completes the proof. □

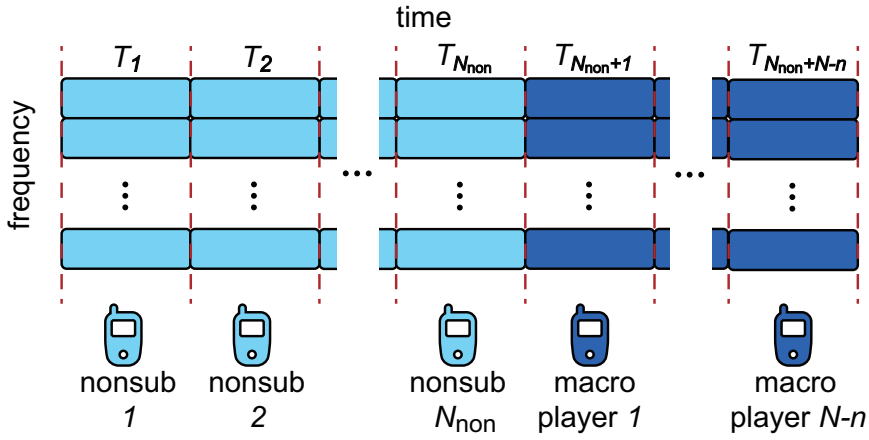

Figure 5.2: Round robin scheduling in macrocell for cell selection game *I*.

5.2.3 Design of Utility Functions for Cell Selection Game *I*

Previous subsection proves the existence of pure strategy NE for general utility functions $\tilde{u}_0$ and $\tilde{u}_1$ under the specified assumptions. In this subsection, practical utility functions that focus on channel capacity and charging policy will be demonstrated. Considering round robin scheduling for downlink scenario, the time dimension is divided into equal-length slots for the usages of PUEs. Fig. 5.2 shows a specific time period of round robin scheduling in macrocell with N_{non} *nonsubscribers* $\in R^C$ and n players connecting to fBS, i.e., with $N-n$ players connecting to mBS. Therefore, there are total $N_{\text{non}}+N-n$ PUEs connecting to mBS. For each UE, RSRP from serving cell and neighboring cell will be measured by this UE and will be reported back to its serving cell. Therefore, mBS will be aware of all the channel qualities of PUEs. Let $Rsrp_{k,c}^{\text{PUE}}$ be denoted as the value of RSRP of kth PUE received from BS c (BS $c=0$ indicates mBS; while BS $c=1$ represents fBS), which can be written as

$$Rsrp_{k,c}^{\text{PUE}} = P_{\text{MAX},c} \cdot L_{k,c}^{\text{PUE}}. \tag{5.8}$$

The parameter $P_{\text{MAX},c}$ represents the maximum transmission power of BS c, and $L_{k,c}^{\text{PUE}}$ indicates the large-scale channel gain (including path loss, shadowing, penetration loss) between BS c and kth PUE. It is noted that the first N_{non} PUEs are *nonsubscribers* $\in R^C$; while the remaining PUEs are macro players. Let T_k be defined as the time slot utilized by mBS to serve kth PUE as shown in Fig. 5.2. It is considered that fBS can schedule SUEs during the time slot T_k if the interference from fBS to kth PUE is not significant. Note that this concept is similar as almost blank subframe (ABS) defined in the LTE-A systems [96]. In the ABSs, fBS is not allowed to transmit any message except for important ones, e.g.,

reference signals. Hence, macro players can be scheduled in the ABSs in order to obtain better link qualities. Let p_k be denoted as allowable power of fBS for data transmission during the time slot T_k. In order to reduce communication overhead between mBS and fBS, it is considered that fBS only has two power levels as follows:

$$p_k = \begin{cases} P_{\text{MAX},1}, & Rsrp_{k,0}^{\text{PUE}}[\text{dBm}] \geqslant Rsrp_{k,1}^{\text{PUE}}[\text{dBm}] + \beta, \\ 0, & Rsrp_{k,0}^{\text{PUE}}[\text{dBm}] < Rsrp_{k,1}^{\text{PUE}}[\text{dBm}] + \beta, \end{cases} \tag{5.9}$$

where the parameter β is a threshold to determine the interference level. Obviously, larger β can significantly reduce interference to PUEs. However, it will also reduce the available resource of fBS. Note that BS always transmits reference signals such that UE can measure RSRP and evaluate channel qualities. As mentioned in previous subsection, the performance of WP is utilized to design utility function for all players. Considering that fBS allocates all its resource for WP, the cell capacity of fBS $C_{\text{fBS}}^{\text{WP}}$ given that n players connecting to fBS can be formulated as

$$C_{\text{fBS}}^{\text{WP}}(n) = \frac{W}{N_{\text{non}} + N - n} \sum_{k=1}^{N_{\text{non}}+N-n} \cdot \log_2 \left(1 + \frac{p_k \cdot L_{\text{WP},1}}{\sigma_{\text{N}}^2 + P_{\text{MAX},0} \cdot L_{\text{WP},0}}\right). \tag{5.10}$$

The parameters W, $L_{\text{WP},c}$, and σ_{N}^2 respectively represent system bandwidth, large-scale channel gain between BS c and WP, and additive white Gaussian noise (AWGN) power over the system bandwidth. Moreover, in most situations, the fBS is not allowed to transmit any power during the slots from $T_{N_{\text{non}}+1}$ to $T_{N_{\text{non}}+N-n}$ since these slots are utilized by macro players. The fBS will produce strong interference to macro players if fBS transmits during those time slots owing to the reason that $Rsrp_{k,0}^{\text{PUE}} < Rsrp_{k,1}^{\text{PUE}} + \beta$ usually holds for $N_{\text{non}} + 1 \leqslant k \leqslant N_{\text{non}} + N - n$. Let $U = \sum_{k=1}^{N_{\text{non}}} \mathbf{1}(Rsrp_{k,0}^{\text{PUE}} < Rsrp_{k,1}^{\text{PUE}} + \beta)$, where $\mathbf{1}(\cdot)$ stands for indicator function, i.e., $\mathbf{1}(\text{True}) = 1$ and $\mathbf{1}(\text{False}) = 0$. Therefore, (5.10) can be rewritten as

$$C_{\text{fBS}}^{\text{WP}}(n) = \frac{(N_{\text{non}} - U) \cdot W}{N_{\text{non}} + N - n} \cdot \log_2 \left(1 + \frac{P_{\text{MAX},1} \cdot L_{\text{WP},1}}{\sigma_{\text{N}}^2 + P_{\text{MAX},0} \cdot L_{\text{WP},0}}\right). \tag{5.11}$$

Since *subscribers* should possess higher priority to access the fBS, it is not fair for those players connecting to the femtocell to be designed with the same scheduling priority as *subscribers*. Therefore, a system admission control parameter, called closed rate α, is defined in this chapter. It indicates that all *subscribers* can firstly be allocated with the ratio α of total resource for the femtocell, and all the SUEs will share the remaining $(1 - \alpha)$ of resource. Hence, given that n players connecting to the fBS, each *subscribers* can share

$\left(\frac{\alpha}{N_{\text{sub}}} + \frac{1-\alpha}{N_{\text{sub}}+n}\right)$ of resource. If $\alpha = 1$, $\left(\frac{1}{N_{\text{sub}}}\right)$ of resource represents that the femtocell is completely closed since total resource are allocated to the *subscribers*. On the other hand, if $\alpha = 0$, $\left(\frac{1}{N_{\text{sub}}+n}\right)$ of resource indicates that the femtocell is completely open. Moreover, each femto player can be allocated with $\left(\frac{1-\alpha}{N_{\text{sub}}+n}\right)$ of resource. Finally, let θ be defined as the price that operator can charge on each player who connects to fBS. The utility function $u_i(s)$ for each player i can be formulated as

$$u_i(s) = \begin{cases} \tilde{u}_0(\|s\|_0) = \dfrac{W}{N_{\text{non}} + N - \|s\|_0} \cdot \log_2\left(1 + \dfrac{P_{\text{MAX},0} \cdot L_{\text{WP},0}}{\sigma_{\text{N}}^2}\right), & s_i = 0, \\ \tilde{u}_1(\|s\|_0) = \dfrac{1-\alpha}{N_{\text{sub}} + \|s\|_0} \cdot C_{\text{fBS}}^{\text{WP}}(\|s\|_0) - \kappa \cdot \theta, & s_i = 1, \end{cases} \tag{5.12}$$

where $\kappa = 1$ Mbps is a constant such that $\frac{1-\alpha}{N_{\text{sub}}+\|s\|_0} \cdot C_{\text{fBS}}^{\text{WP}}(\|s\|_0)$ and $\kappa \cdot \theta$ possess the same unit. Furthermore, the operator can receive the amount of $\theta \cdot \|s\|_0$ as its revenue. By broadcasting all necessary parameters from fBS, e.g., α and $\|s\|_0$, the utility function can therefore be calculated by each player. Moreover, best response, $B_i(s_{-i}) = \arg\max_{s_i} u_i(s_i, s_{-i})$, can be executed by each player i to serve as a decentralized algorithm for achieving NE based on the property of potential game.

5.3 Construction of Cell Selection Game *II*

In previous section, it is considered that each player will possess the same utility function such that the existence of pure strategy NE can be proven for arbitrary utility function. In this section, cell selection game *II* will be established by considering that each player will have distinct utility function. Therefore, the design of utility functions will be highlighted and firstly described in this section.

5.3.1 Network Scenarios and Design of Utility Functions for Cell Selection Game *II*

In cell selection game *II*, independent channel deployment between macrocell and femtocell is considered. This corresponds to the network scenario that the fBS is located close to the mBS such that fBS cannot reuse the frequency spectrum with the overlay macrocell. This scenario is considered common in practice since the fBSs can be arbitrarily installed by the users in the network. The operator cannot guarantee that the locations of fBSs are located far away from the mBS. Moreover, for utility design, different from Subsection

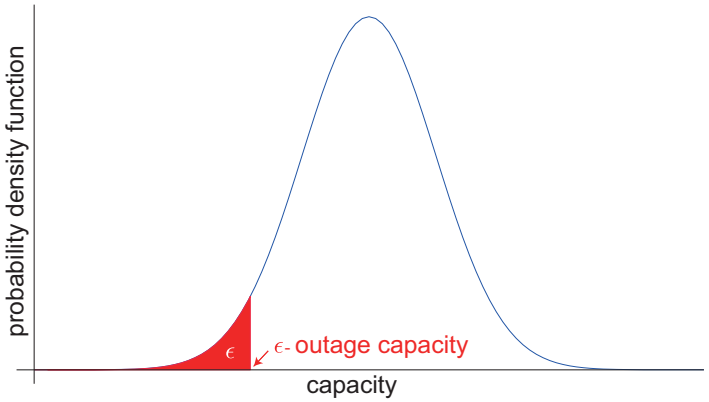

Figure 5.3: ϵ-outage capacity

5.2.3 that only considers large-scale fading, the channel model adopted in this section includes large-scale fading and small-scale fading where both slow fading and frequency selective fading are considered. It is assumed that a player will connect to a targeting network during a period of time which is much larger than the coherent time. Furthermore, the values of path loss and shadowing fading are considered fixed; while those of slow fading and frequency selective fading are random variables in cell selection game *II*. Note that slow fading means that the channels are almost time-invariant during the time period of packet transmission. However, it is still time-variant during the connection period to either the mBS or fBS since the coherent time is much shorter compared to connection time. In addition, the distribution of channel gain in each subchannel during every coherent time is assumed to be independent and identically distributed (i.i.d.) for a specific player. Considering slow fading effect, UEs can hardly transmit data if deep fade happens, i.e., very small channel gain, which will result in temporary failure of communication. Hence, for the utility design, the ϵ-outage capacity is employed for cell selection game *II*, which is defined as the largest capacity such that the outage probability is less than ϵ as shown in Fig. 5.3. For more details about ϵ-outage capacity, please refer to chapter 5 of [97]. In order to derive the ϵ-outage capacity, it is necessary to formulate the distributions of capacity first. However, it is difficult to obtain accurate distributions of capacity for UEs since the number of samples of the distribution is not sufficient. Fortunately, the distribution of capacity in each coherent time can be approximated as Gaussian distribution if the number of subchannels is large enough.

Considering the scenario that the total available spectrum bandwidth W is divided into J subchannels with equal size. Since each player can measure RSRP for each subchannel,

the capacity of ith player provided by BS c in subchannel j for all coherent times can be formulated as

$$\mathbf{C}_{i,c}^{j} = \frac{W}{J} \cdot \log_2 \left(1 + \frac{P_{\text{MAX},c} \cdot L_{i,c} \cdot |\mathbf{H}_{i,c}^{j}|^2}{\sigma_{\text{N}}^2} \right). \tag{5.13}$$

The parameters $L_{i,c}$ and $|\mathbf{H}_{i,c}^{j}|^2$ respectively represent the large-scale channel gain and small-scale channel gain in subchannel j for the link between the ith player and BS c. Note that $|\mathbf{H}_{i,c}^{j}|^2$ is considered i.i.d. for all j given specific i and c such that $\mathbf{C}_{i,c}^{j}$ can be simplified as $\mathbf{C}_{i,c}$. Since each player i can measure RSRP from BS c for subchannel j, J samples ($C_{i,c}^{j}, 1 \leqslant j \leqslant J$) can be obtained to estimate the values of mean $\hat{m}_{i,c}$ and variance $\hat{\sigma}_{i,c}^2$ for $\mathbf{C}_{i,c}$ by $\hat{m}_{i,c} = \frac{1}{J}\sum_{j=1}^{J} C_{i,c}^{j}$ and $\hat{\sigma}_{i,c}^2 = \frac{1}{J-1}\sum_{j=1}^{J}(C_{i,c}^{j} - \hat{m}_{i,c})^2$. It is noted that $\hat{m}_{i,c}$ and $\hat{\sigma}_{i,c}^2$ are calculated during certain period of coherent time, but they can also be utilized to respectively represent estimated mean and variance for the future coherent time. Given that n players connect to the fBS, the number of UEs that connects to the fBS is $N_{\text{sub}} + n$; while the number of UEs that connect to the mBS is $N_{\text{non}} + N - n$. For fairness concern, the number of subchannels assigned to fBS is considered as $\frac{(N_{\text{sub}}+n)\cdot J}{N_{\text{non}}+N_{\text{sub}}+N}$. It is intuitively that $\frac{(N_{\text{sub}}+n)\cdot J}{N_{\text{non}}+N_{\text{sub}}+N}$ will not be an integer under most situations. Let ω_n and ρ_n be respectively denoted as integer and decimal parts of $\frac{(N_{\text{sub}}+n)\cdot J}{N_{\text{non}}+N_{\text{sub}}+N}$ as follows

$$\omega_n = \left\lfloor \frac{(N_{\text{sub}} + n) \cdot J}{N_{\text{non}} + N_{\text{sub}} + N} \right\rfloor, \tag{5.14}$$

$$\rho_n = \frac{(N_{\text{sub}} + n) \cdot J}{N_{\text{non}} + N_{\text{sub}} + N} - \left\lfloor \frac{(N_{\text{sub}} + n) \cdot J}{N_{\text{non}} + N_{\text{sub}} + N} \right\rfloor. \tag{5.15}$$

Therefore, as shown in Fig. 5.4, ω_n subchannels and ρ_n of time in a subchannel will be assigned to the fBS; while the remaining resource will be occupied by the mBS. In addition, round robin scheduling is also employed for mBS for fairness concern. Available time in each subchannel is divided as $N_{\text{non}}+N-n$ parts with equal length, each *nonsubscriber* $\in R^C$ or macro player will occupy one part, i.e., $\frac{1}{N_{\text{non}}+N-n}$ of available time. Given that n players connect to the fBS, let $\tilde{\mathbf{C}}_{i,c}(n)$ be denoted as a random variable of ith player's capacity during a period of coherent time if the ith player decides to connect to BS c, $\tilde{\mathbf{C}}_{i,0}(n)$ can first be written as

$$\tilde{\mathbf{C}}_{i,0}(n) = \frac{1}{N_{\text{non}} + N - n} \cdot \left[(1 - \rho_n) \cdot \mathbf{C}_{i,0}^{\omega_n+1} + \left(\sum_{j=\omega_n+2}^{J} \mathbf{C}_{i,0}^{j} \right) \right]. \tag{5.16}$$

Since $\mathbf{C}_{i,0}^{j}$ for $\forall j$ are i.i.d., $\sum_{j=\omega_n+2}^{J} \mathbf{C}_{i,0}^{j}$ can approach Gaussian distribution if $J - \omega_n - 1$

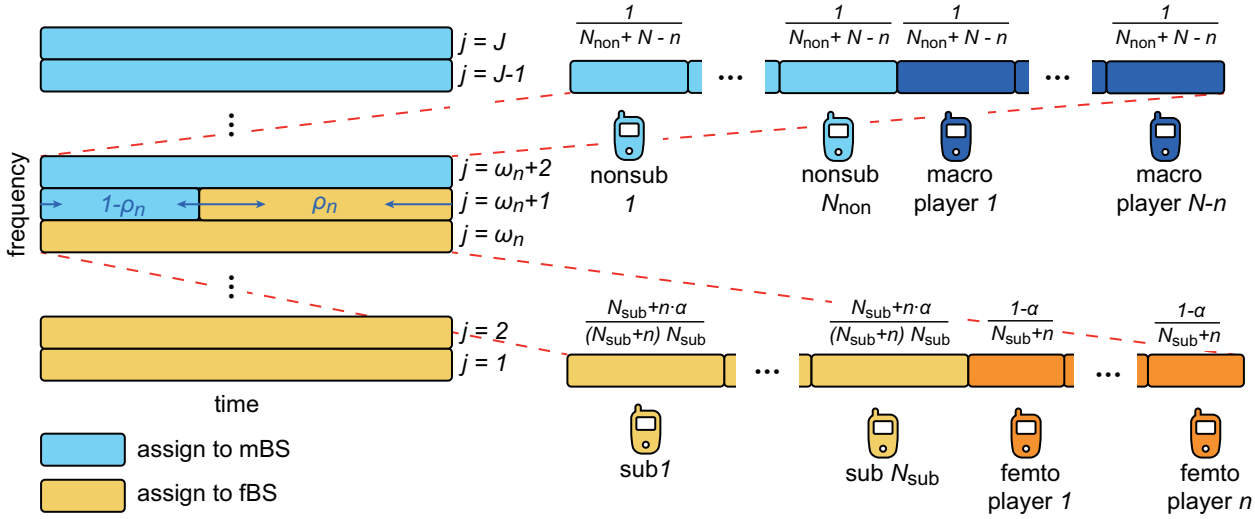

Figure 5.4: Subchannel assignment and scheduling scheme for cell selection game *II*.

is large enough. Moreover, $\sum_{j=\omega_n+2}^{J} \mathbf{C}_{i,0}^{j}$ is much larger compared to $(1-\rho_n)\cdot \mathbf{C}_{i,0}^{\omega_n+1}$. Therefore, $\tilde{\mathbf{C}}_{i,0}(n)$ can be approximated to follow Gaussian distribution. Besides, as mentioned previously, $\hat{m}_{i,c}$ and $\hat{\sigma}_{i,c}^2$ are respectively employed for estimated values of mean and variance of $\mathbf{C}_{i,c}^{j}$. The estimated values of mean and variance of $\tilde{\mathbf{C}}_{i,0}(n)$ will be

$$\begin{aligned}
\mathrm{E}[\tilde{\mathbf{C}}_{i,0}(n)] &= \frac{1}{N_{\text{non}}+N-n}\cdot\left[(1-\rho_n)\cdot\hat{m}_{i,0}+(J-\omega_n-1)\cdot\hat{m}_{i,0}\right] = \frac{\hat{m}_{i,0}\cdot J}{N_{\text{non}}+N_{\text{sub}}+N},\\
\mathrm{Var}[\tilde{\mathbf{C}}_{i,0}(n)] &= \frac{1}{(N_{\text{non}}+N-n)^2}\cdot\left[(1-\rho_n)^2\cdot\hat{\sigma}_{i,0}^2+(J-\omega_n-1)\cdot\hat{\sigma}_{i,0}^2\right]\\
&\simeq \frac{\hat{\sigma}_{i,0}^2\cdot J}{(N_{\text{non}}+N-n)\cdot(N_{\text{non}}+N_{\text{sub}}+N)}.
\end{aligned} \tag{5.17}$$

Note that the approximation in $\mathrm{Var}[\tilde{\mathbf{C}}_{i,0}(n)]$ is to provide clear formulation. As mentioned above, the utility design is based on the ϵ-outage capacity, which denotes the largest capacity such that the outage probability is less than ϵ. Let $\tilde{C}_{i,0}^{\epsilon}(n)$ be denoted as ϵ-outage capacity of the ith player if it connects to the mBS. Based on $\tilde{\mathbf{C}}_{i,0}(n) \sim \mathcal{N}(\mathrm{E}[\tilde{\mathbf{C}}_{i,0}(n)], \mathrm{Var}[\tilde{\mathbf{C}}_{i,0}(n)])$, the following equation will hold.

$$Q\left(\frac{\tilde{C}_{i,0}^{\epsilon}(n)-\mathrm{E}[\tilde{\mathbf{C}}_{i,0}(n)]}{\sqrt{\mathrm{Var}[\tilde{\mathbf{C}}_{i,0}(n)]}}\right) = 1-\epsilon, \tag{5.18}$$

where $Q(x)$ represents the Q-function defined as $Q(x)=\int_x^{\infty}\frac{1}{\sqrt{2\pi}}e^{-\frac{r^2}{2}}dr$. Therefore, $\tilde{C}_{i,0}^{\epsilon}(n)$

can be obtained as

$$\tilde{C}^{\epsilon}_{i,0}(n) = Q^{-1}(1-\epsilon)\cdot\sqrt{\mathrm{Var}[\tilde{\mathbf{C}}_{i,0}(n)]} + \mathrm{E}[\tilde{\mathbf{C}}_{i,0}(n)]. \tag{5.19}$$

Next, similar to cell selection game *I*, all *subscribers* can firstly be allocated with the ratio α of total resource for the femtocell. All the UEs that connect to the femtocell will share the remaining $(1-\alpha)$ ratio of system resource. As shown in Fig. 5.4, given that n players connect to fBS, each *subscriber* can occupy $\frac{\alpha}{N_{\text{sub}}} + \frac{1-\alpha}{N_{\text{sub}}+n} = \frac{N_{\text{sub}}+n\cdot\alpha}{(N_{\text{sub}}+n)\cdot N_{\text{sub}}}$ of time in each subchannel; while each femto player can share $\frac{1-\alpha}{N_{\text{sub}}+n}$ of time in each subchannel. Therefore, $\tilde{\mathbf{C}}_{i,1}(n)$ can be formulated as

$$\tilde{\mathbf{C}}_{i,1}(n) = \frac{1-\alpha}{N_{\text{sub}}+n}\cdot\left[\rho_n\cdot\mathbf{C}_{i,1}^{\omega_n+1} + \left(\sum_{j=1}^{\omega_n}\mathbf{C}_{i,1}^{j}\right)\right]. \tag{5.20}$$

Moreover, $\mathrm{E}[\tilde{\mathbf{C}}_{i,1}(n)]$ and $\mathrm{Var}[\tilde{\mathbf{C}}_{i,1}(n)]$ can respectively be obtained similar to the derivations of (5.17) as

$$\begin{aligned}\mathrm{E}[\tilde{\mathbf{C}}_{i,1}(n)] &= (1-\alpha)\cdot\frac{\hat{m}_{i,1}\cdot J}{N_{\text{non}}+N_{\text{sub}}+N},\\ \mathrm{Var}[\tilde{\mathbf{C}}_{i,1}(n)] &\simeq \frac{(1-\alpha)^2\cdot\hat{\sigma}^2_{i,1}\cdot J}{(N_{\text{sub}}+n)\cdot(N_{\text{non}}+N_{\text{sub}}+N)}.\end{aligned} \tag{5.21}$$

Hence, ϵ-outage capacity of the ith player connecting to the fBS $\tilde{C}^{\epsilon}_{i,1}(n)$ can be derived as

$$\tilde{C}^{\epsilon}_{i,1}(n) = Q^{-1}(1-\epsilon)\cdot\sqrt{\mathrm{Var}[\tilde{\mathbf{C}}_{i,1}(n)]} + \mathrm{E}[\tilde{\mathbf{C}}_{i,1}(n)]. \tag{5.22}$$

Finally, by incorporating (5.19) and (5.22), the utility function of the ith player can be written as

$$u_i(s) = \begin{cases}\tilde{C}^{\epsilon}_{i,0}(\|s\|_0), & s_i = 0,\\ \tilde{C}^{\epsilon}_{i,1}(\|s\|_0) - \kappa\cdot\theta, & s_i = 1.\end{cases} \tag{5.23}$$

Note that θ is the price that operator can take charge from each player who connects to the fBS, and $\kappa = 1$ Mbps is a constant such that $\tilde{C}^{\epsilon}_{i,1}(\|s\|_0))$ and $\kappa\cdot\theta$ have the same unit.

5.3.2 Existence of Pure Strategy NE

The general form of cell selection game as stated in Definition 5.1 will still be feasible for cell selection game *II*. However, since the characteristics of utility functions in cell selection

game *II* are different from that in game *I*, the existences of pure strategy NEs should be re-proven. In order to prove the existence of pure strategy NE for cell selection game *II*, another important type of games called supermodular game [98, 99] is defined as follows.

Definition 5.3 (Supermodular Game). *According to Definition 5.1, the strategic form of cell selection game* $\langle I, (S_i)_{i\in I}, (u_i)_{i\in I}\rangle$ *is a supermodular game if the following conditions are satisfied for all* i*:*

1. *The set* S *of feasible joint strategies is a sublattice of* $\mathbb{R}^{\Sigma_{i=1}^{N} m_i}$*, where* m_i *is the dimension of* s_i*;*
2. u_i *is supermodular in* s_i *on* $S_i, \forall i, \forall s_{-i} \in S_{-i}$*;*
3. u_i *has increasing differences in* (s_i, s_{-i})*.*

Note that a function $f(x)$ is supermodular on a sublattice X if

$$f(x) + f(x') \leq f(x \vee x') + f(x \wedge x'), \forall x, x' \in X, \tag{5.24}$$

where the notations "$\vee$" and "$\wedge$" are respectively defined as "join" (least upper bound) and "meet" (greatest lower bound), e.g., $(1 \vee 0) = (0 \vee 1) = 1$ and $(1 \wedge 0) = (0 \vee 1) = 0$. Note again that the sets S_i and $S_{-i} = \prod_{j\neq i} S_j$ are respectively denoted as the action profiles of ith player and the action profiles of all players except the ith player. Moreover, the function u_i has increasing differences[1] in (s_i, s_{-i}) can be denoted as

$$\begin{aligned} &u_i(s_i, s_{-i}) - u_i(s_i', s_{-i}) \geq u_i(s_i, s_{-i}') - u_i(s_i', s_{-i}') \\ &\text{if } s_i \geq s_i', s_{-i} \geq s_{-i}', \forall i, \forall s_i, s_i' \in S_i, \forall s_{-i}, s_{-i}' \in S_{-i}. \end{aligned} \tag{5.25}$$

Property 5.2. *If* $\langle I, (S_i)_{i\in I}, (u_i)_{i\in I}\rangle$ *is a supermodular game, the set of strategies that survive iterated strict dominance, i.e., iterated elimination of strictly dominated strategies (IESDS), has the greatest NE* $\overline{s}$ *and the least NE* $\underline{s}$*.*

In Property 5.2, strictly dominated strategies represent the strategies that are never selected by a player regardless of the other players decisions, and IESDS is a process in which strictly dominated strategies from a game can be iteratively deleted. Based on the description above for supermodular game, the existences of pure strategy NEs for cell selection game *II* can be proven as follows.

[1]For some $x, y \in S_{-i}$, "$x \geq y$" if and only if $x_j \geq y_j, \forall j, x = \{x_1, \ldots, x_j, \ldots, x_{N-1}\}, y = \{y_1, \ldots, x_j, \ldots, y_{N-1}\}$.

Theorem 5.2. *The cell selection game II* $\langle I, (S_i)_{i\in I}, (u_i)_{i\in I}\rangle$ *is a supermodular game and has the greatest and the least pure strategy NEs* $\overline{s}$ *and* $\underline{s}$ *respectively if* $\epsilon \leq 0.5$ *for* $u_i(s)$.

Proof. The existence of pure strategy NE for cell selection game *II* can be proved based on the required three conditions of supermodular game as stated in Definition 5.3 as follows.

1. The feasible set of S_i is independent from S_{-i}, $\forall i$. Hence, the first condition of Definition 5.3 can be simplified as to check if the individual S_i is a sublattice of $\mathbb{R}$. Since $S_i = \{0, 1\}$, it is intuitive that $a \vee b \in S_i$ and $a \wedge b \in S_i$ $\forall a, b \in S_i$. Therefore, S_i is a sublattice of $\mathbb{R}$.

2. Intuitively, the following relationship can be be acquired:

$$u_i(s_i \vee s_i', s_{-i}) + u_i(s_i \wedge s_i', s_{-i}) = u_i(s_i, s_{-i}) + u_i(s_i', s_{-i}), \forall i, \forall s_i, s_i' \in S_i, \forall s_{-i} \in S_{-i}. \tag{5.26}$$

   Therefore, u_i is supermodular in s_i on S_i.

3. For all i, it can be clearly observed from (5.19) and (5.22) that $\tilde{C}^{\epsilon}_{i,0}(\|s\|_0)$ and $\tilde{C}^{\epsilon}_{i,1}(\|s\|_0)$ are respectively non-increasing and non-decreasing with respect to $\|s\|_0$ when $\epsilon \leq 0.5$. If $s_{-i} \geq s'_{-i}, \forall s_{-i}, s'_{-i} \in S_{-i}$, it can be found that $1+\|s_{-i}\|_0 \geq 1+\|s'_{-i}\|_0$. Therefore, $\tilde{C}^{\epsilon}_{i,1}(1+\|s_{-i}\|_0)-\theta \geq \tilde{C}^{\epsilon}_{i,1}(1+\|s'_{-i}\|_0)-\theta$ such that $u_i(1, s_{-i}) \geq u_i(1, s'_{-i})$. Furthermore, since $\|s_{-i}\|_0 \geq \|s'_{-i}\|_0$, it can be acquired that $\tilde{C}^{\epsilon}_{i,0}(\|s_{-i}\|_0) \leq \tilde{C}^{\epsilon}_{i,0}(\|s'_{-i}\|_0)$ such that $u_i(0, s_{-i}) \leq u_i(0, s'_{-i})$. According to the above results, the following relationship can be obtained as

$$u_i(1, s_{-i}) - u_i(0, s_{-i}) \geq u_i(1, s'_{-i}) - u_i(0, s'_{-i}). \tag{5.27}$$

After all these three conditions are satisfied, The proof of cell selection game *II* to be a supermodular game can be completed. Note that ϵ is chosen as a small value for realistic cases. □

In addition, the NEs of cell selection game *II* can be obtained by iterating best response mapping [99], which indicates that the players in this iterated round choose their best strategies according to the results from previous iterated round. Moreover, similar as game *I*, by broadcasting all necessary parameters from fBS, e.g., α and $\|s\|_0$, the utility function can therefore be calculated by each player. the best response mapping can also be performed by each player i to serve as a decentralized algorithm for achieving NE.

Parameter	Value
Path loss (mBS $\rightarrow$ outdoor UE)	$15.3 + 37.6 \cdot \log_{10}(r)$
Path loss (mBS $\rightarrow$ indoor UE)	$15.3 + 37.6 \cdot \log_{10}(r)$
Path loss (fBS $\rightarrow$ outdoor UE)	$15.3 + 37.6 \cdot \log_{10}(r)$
Path loss (fBS $\rightarrow$ indoor UE)	$38.46 + 20.0 \cdot \log_{10}(r)$
Shadowing standard deviation (mBS $\rightarrow$ outdoor UE)	8 dB
Shadowing standard deviation (mBS $\rightarrow$ indoor UE)	8 dB
Shadowing standard deviation (fBS $\rightarrow$ outdoor UE)	8 dB
Shadowing standard deviation (fBS $\rightarrow$ indoor UE)	4 dB
Wall penetration loss	20 dB

Table 5.1: Large-scale channel model

Parameter	Value	
	Game *I*	Game *II*
Number of subchannels (J)	25	
System bandwidth (W)	5 MHz	
Number of indoor *subscribers* (N_{sub})	6	
Number of indoor *nonsubscribers*	8	
Number of outdoor *nonsubscribers*	10	
Max power of mBS ($P_{\text{MAX},0}$)	33 dBm	
Max power of fBS ($P_{\text{MAX},1}$)	10 dBm	
Noise figure	9 dB	
Channel noise density	-174 dBm/Hz	
Distance between mBS and fBS (D)	500 m	200 m
Interference threshold (β)	10 dB	Not applicable
Max outage probability (ϵ)	Not applicable	0.05

Table 5.2: System parameters for proposed cell selection games

5.4 Performance Evaluation

The effectiveness of proposed cell selection games *I* and *II* will be evaluated in this section based on the defined utility functions. Consider a HetNet as shown in Fig. 5.1, there exists one mBS with radius of transmission range equal to 866 m and one fBS that is located at the center of room of 30 m $\times$ 30 m. The large-scale channel model from [100] and default system parameters are respectively listed in Table 5.1 and 5.2 for both cell selection games *I* and *II*. The distance between the mBS and fBS is denoted as D. In addition, the locations of indoor and outdoor UEs are respectively uniformly distributed within the room and the maximum transmission range of mBS. Moreover, *nonsubscriber*

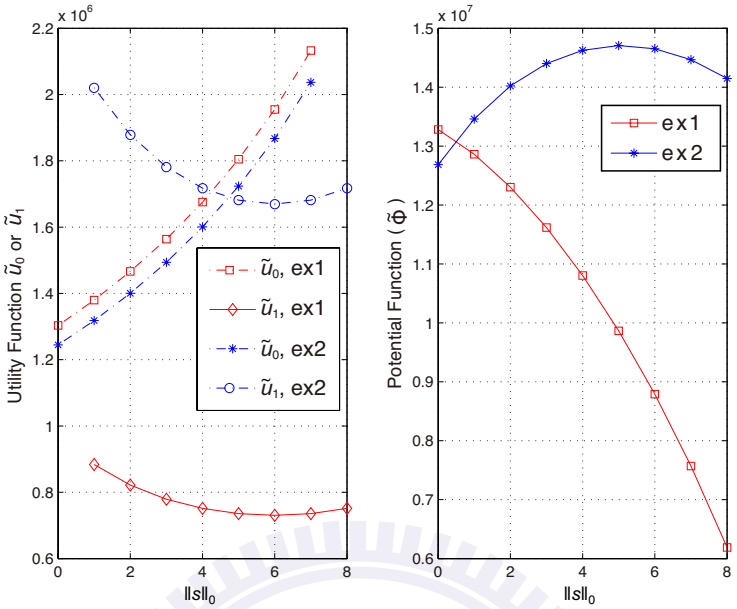

Figure 5.5: Utility functions $\tilde{u}_0$ and $\tilde{u}_1$ (left subplot) for each player and their corresponding potential functions (right subplot) versus number of players connecting to the fBS $\|s\|_0$ under $\alpha = 0.7$ for ex1 and $\alpha = 0.4$ for ex2.

will first measure the RSRPs respectively from the mBS and fBS to determine whether it is a player of cell selection game. If RSRP from fBS is larger than that from mBS, the *nonsubscriber* is a player. The *nonsubscriber* is not a player if RSRP from fBS is smaller than that from mBS. Note that $100,000$ simulation runs are conducted for the following Figs. 5.6 to 5.13. After computing 95% confidence intervals for $100,000$ simulation runs, the confidence interval is short enough to be regard as almost a point. Therefore, we will neglect identifying the confidence interval in our simulation results in order to provide clear numerical results.

5.4.1 Performance Evaluation for Cell Selection Game *I*

In this subsection, performance evaluation without the consideration of small-scale fading is conducted for cell selection game *I*. If not further specified, the distance between mBS and fBS (D), and the price value (θ) are respectively set as 500 m and 0. The left subplot of Fig. 5.5 shows the utility functions $\tilde{u}_0$ and $\tilde{u}_1$ for each player versus the number of players $\|s\|_0$ connecting to the fBS under $\alpha = 0.7$ for example 1 (denoted as ex1) and $\alpha = 0.4$ for example 2 (denoted as ex2). Note that each example respectively represents

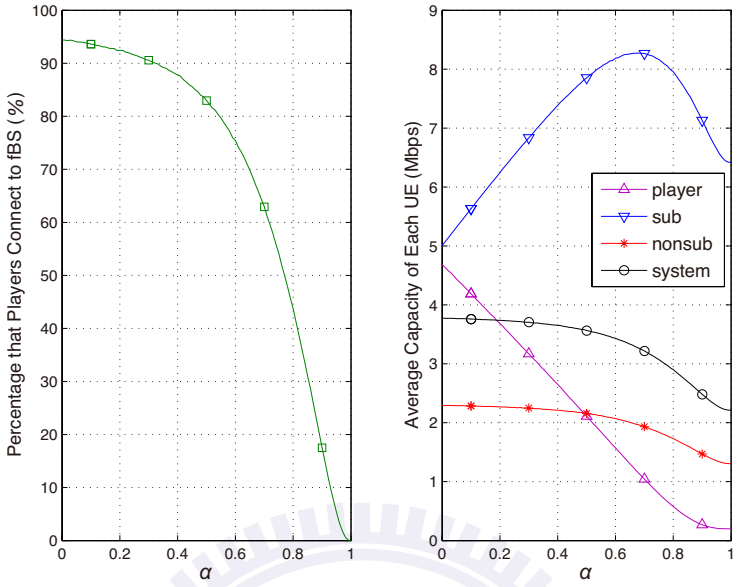

Figure 5.6: Average percentage that players connect to the fBS at NE versus α (left subplot), and average capacity of each UE at NE versus α for player, *subscriber*, *nonsubscriber* $\in R^C$, and each UE in the system (right subplot).

one simulation run of the game in order to clearly describe a player's utilities $\tilde{u}_0$ and $\tilde{u}_1$ and the corresponding NEs. It can be observed that $\tilde{u}_1$ in both cases decrease first, then increase with the augmentation of $\|s\|_0$. The reason is that two major factors that will affect the value of $\tilde{u}_1$, as $\|s\|_0$ increases, are enlarged total capacity of femtocell and less amount of resource shared for each femto player. The second factor dominates first factor under smaller $\|s\|_0$; while the opposite is true under the case of larger $\|s\|_0$. The right subplot of Fig. 5.5 illustrates the potential functions versus the number of players connecting to the fBS. The NEs of ex1 and ex2 are respectively located at $\|s\|_0 = 0$ and $\|s\|_0 = 5$ according to (5.5) in Property 5.1. It describes the characteristics of local maximum potential value that all players will not change their current strategies. Furthermore, compared to ex1 of $\alpha = 0.7$, the players in ex2 of $\alpha = 0.4$ will have more tendency connecting to the fBS. The reason is that its maximum potential value is located at a larger number of players $\|s\|_0 = 5$.

The left subplot of Fig. 5.6 demonstrates the average percentage that players connect to the fBS at NE decreases with the augmentation of α. The result is intuitive since lower α represents that there exists more femtocell resources for players to utilize, which will drive the players to connect to the fBS. On the other hand, players have the tendency to connect

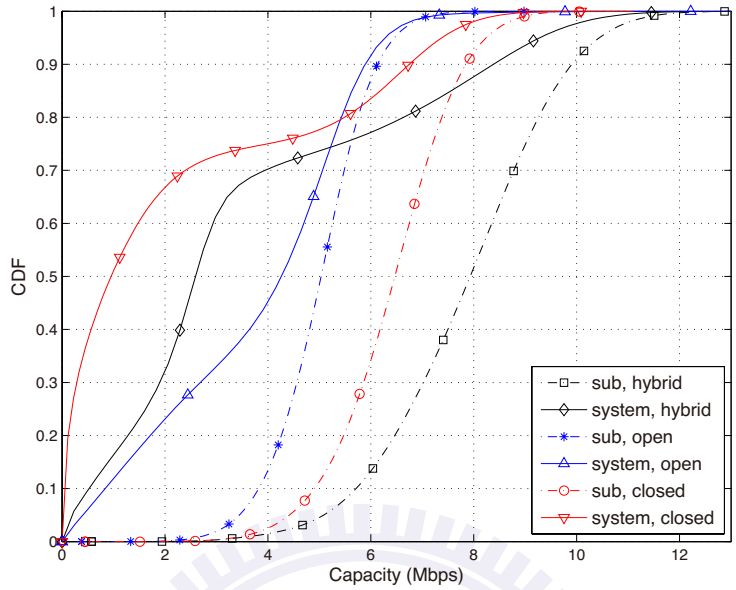

Figure 5.7: CDF of capacity at NE for the *subscriber* and system in hybrid (with $\alpha = 0.5$), open ($\alpha = 0.0$), and closed ($\alpha = 1.0$) access modes.

to the mBS under the condition of larger α which can be explained in similar manners. The right subplot of Fig. 5.6 shows the average capacity of each UE at NE versus the closed rate α for different types of UEs, where the legends "player", "sub", "nonsub", "system" are respectively denoted as each player, *subscriber*, *nonsubscribers* $\in R^C$, and each UE in the HetNet system. It can be seen that the average capacity for each UE in the system, i.e., the "system" curve, decreases with increased value of α. This result reveals that better average system capacity can be achieved if the access policy can be adopted in a more open manner. Furthermore, the average capacity of *subscribers* has a peak value at $\alpha \simeq 0.7$, which indicates that there exists certain value of α such that the performance of *subscribers* in hybrid access mode is superior to that in both closed access mode ($\alpha = 1$) and open access mode ($\alpha = 0$). The reason for hybrid access mode to outperform closed access mode is that *subscribers* can acquire additional resource from those players connecting to the fBS in hybrid access mode. On the other hand, *subscribers* will not increase their capacity gain in closed access mode while there does not exist any player connecting to the fBS. Besides, the average capacities of players and *nonsubscribers* $\in R^C$ also decrease with the augmentation of α.

Fig. 5.7 shows the cumulative distribution function (CDF) of capacity at NE for both

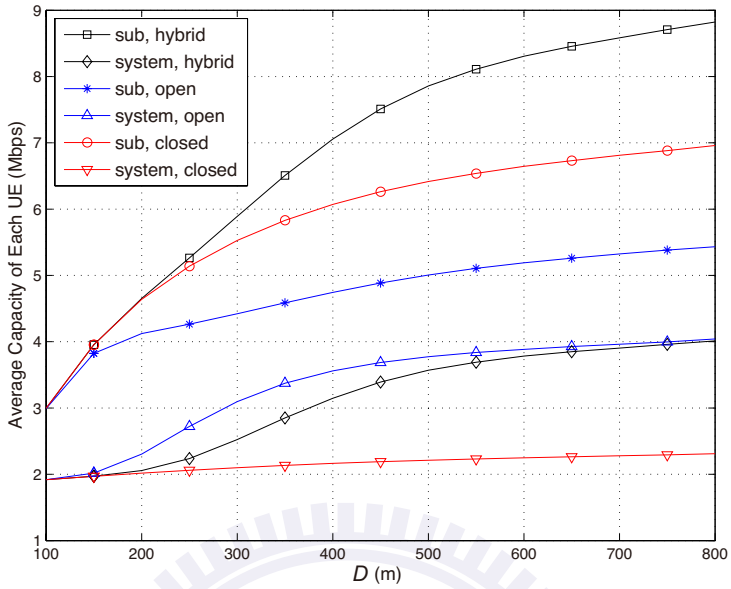

Figure 5.8: Average capacity of *subscriber* and system UE at NE versus the distance between mBS and fBS (D) in hybrid (with $\alpha = 0.5$), open ($\alpha = 0.0$), and closed ($\alpha = 1.0$) access modes.

the *subscriber* and system in hybrid (with $\alpha = 0.5$), open ($\alpha = 0.0$), and closed ($\alpha = 1.0$) access modes. Note that only the *subscriber*'s and system UE's performances are displayed since one of the important purposes of this chapter is to compare the performance tradeoff between the *subscriber* and system UE under different access policies. From the *subscriber*'s perspective, it can be seen that better performance can be obtained in hybrid access mode compared to the other two access strategies. Moreover, the entire system can lead to higher performance in open access mode relative to hybrid access mode for those UEs with relative worse performance; while the system performance in open access mode is inferior to that in hybrid access mode for those UEs with better performance. Therefore, by observing the gradually increasing trend of curve from open access mode as shown in Fig. 5.7, it can be intuitive concluded that higher fairness for resource sharing between the UEs can be achieved with the adoption of open access mode compared to hybrid access mode. Furthermore, considering the entire system, the performances for both the open and hybrid access modes are superior to that in closed access mode under most of cases.

Fig. 5.8 shows average capacity of *subscriber* and system UE at NE versus the distance D between mBS and fBS in hybrid (with $\alpha = 0.5$), open ($\alpha = 0.0$), and closed ($\alpha = 1.0$) access modes. It can be seen that average capacity of *subscriber* and system increase as D is

augmented for all the three access modes. The major reason is that the femocell network is less interfered by the mBS under larger distance D. Moreover, hybrid access mode can achieve better balance of performance between *subscribers* and system UEs compared to open and closed access modes. The left subplot of Fig. 5.9 displays average capacity of *subscriber* and system UE at NE versus the price θ; while the right subplot shows average revenue that operator can charge versus the price θ in hybrid (with $\alpha = 0.5$), open ($\alpha = 0.0$), and closed ($\alpha = 1.0$) access modes. Note that average revenue that operator can receive is equal to $\theta \cdot \|s\|_0$. It can be seen from left subplot that the average capacity of both *subscriber* and system UE in closed access mode remain constant due to the reason that the players can only connect to mBS. Moreover, the performance in hybrid and open access modes will become closer to that in closed access mode as θ is augmented since higher charge will drive players to connect to mBS. With enlarged θ, average capacity of *subscriber* in open access mode increases owing to the reason that less players share the femtocell resource. Furthermore, it can be observed from right subplot that average revenues in open access mode is larger than that in hybrid access mode since more players tend to connect to the fBS in open access mode. In addition, both hybrid and open access modes have peak values respectively at $\theta \simeq 1$ and $\theta \simeq 2$, which represents that there exist a optimal price that operator can charge from players in order to maximize its revenue.

5.4.2 Performance Evaluation for Cell Selection Game *II*

In this subsection, Rayleigh fading, i.e., $|\mathbf{H}_{i,c}^{j}|^2 \sim \text{Exp}(1)$, for each subchannel is additionally considered for small-scale fading. Besides, the NEs of cell selection game *II* can be obtained by iterating the best response mapping as in [99]. If not further specified, the distance between mBS and fBS (D) is chosen as 200m and the price value (θ) is set to be 0.

Fig. 5.10 displays the average percentage that players connect to the fBS at NE versus α, and average outage capacity of each UE at NE versus α for player, *subscriber*, *nonsubscriber* $\in R^C$, and each UE in the HetNet system. It can be observed that all the curves except for "non" have similar trend as their respective curves in Fig. 5.6. For instance, the performances of "player" and "system" decrease as parameter α is augmented; while a peak value occurs at $\alpha \simeq 0.7$ in the "sub" curve. On the other hand, enlarged α will drive the players to connect to the mBS, which result in *nonsubscribers* $\in R^C$ having more frequency diversity to achieve slightly higher outage capacity. In addition, it can be seen that the performances of *subscriber* at $\alpha = 0.0$ and $\alpha = 1.0$ are around the same. The reason is that none of the players are allowed to connect to the fBS in the closed access

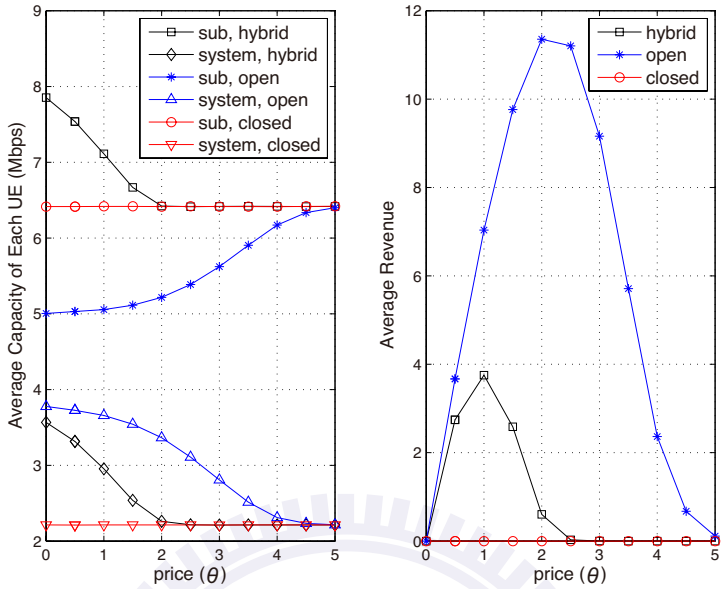

Figure 5.9: Average capacity of *subscriber* and system UE at NE versus the price (θ) (left subplot), and average revenue that operator can charge versus the price (θ) (right subplot) in hybrid (with $\alpha = 0.5$), open ($\alpha = 0.0$), and closed ($\alpha = 1.0$) access modes.

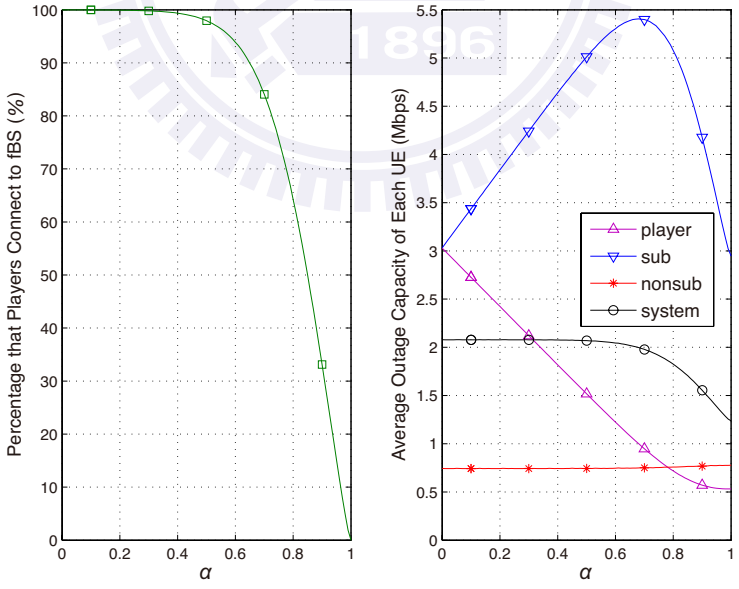

Figure 5.10: Average percentage that players connect to the fBS at NE versus α (left subplot), and average outage capacity of each UE at NE versus α for player, *subscriber*, *nonsubscriber* $\in R^C$, and each UE in the HetNet system (right subplot).

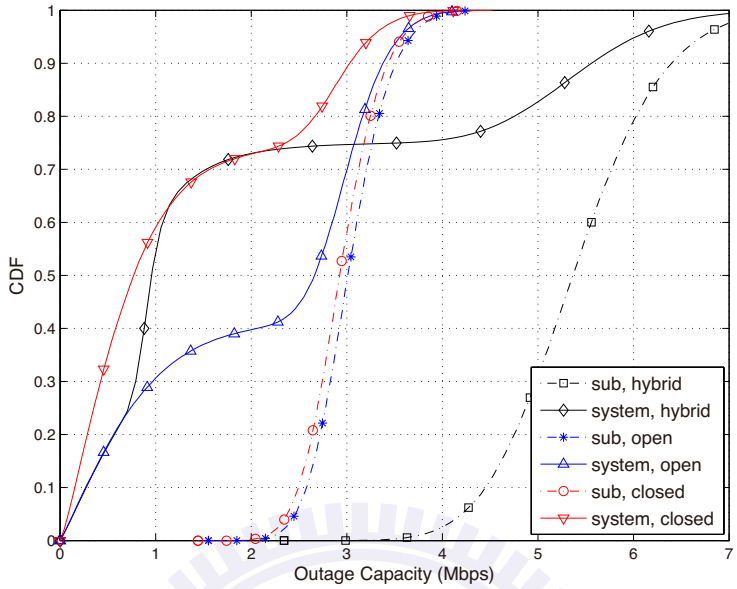

Figure 5.11: CDF of outage capacity at NE for *subscriber* and system UE in hybrid (with $\alpha = 0.7$), open ($\alpha = 0.0$), and closed ($\alpha = 1.0$) access modes.

mode, *subscribers* cannot acquire additional system resource to utilize. On the other hand, for open access mode, *subscribers* will not be the beneficiary since extra channel resources are allocated for all players connecting to the fBS. Therefore, no matter either the open or closed access mode is employed, *subscriber's* available resources are observed to be identical. Although *subscriber's* available resources in the open and closed access mode are the same, more frequency diversity can be provided in open access mode compared to that in closed mode, which lead to *subscriber's* performance in open access mode slightly outperforms that in closed access mode. Moreover, it can be observed from the system UE's performance curve that open access mode is still superior to that in both hybrid and closed access modes.

Fig. 5.11 shows the CDF of outage capacity at NE for *subscriber* and system UE in hybrid (with $\alpha = 0.7$), open ($\alpha = 0.0$), and closed ($\alpha = 1.0$) access modes. Similar to the explanation as Fig. 5.7, the average outage capacity of *subscriber* in hybrid access mode still outperforms those in both closed and open access modes. Note that similar performance of *subscriber* is obtained from both the closed and open access modes, which is resulted from the design of parameter α as explained in previous paragraph. Furthermore, for system UE, the gradually increasing performance curve by the adoption of open access

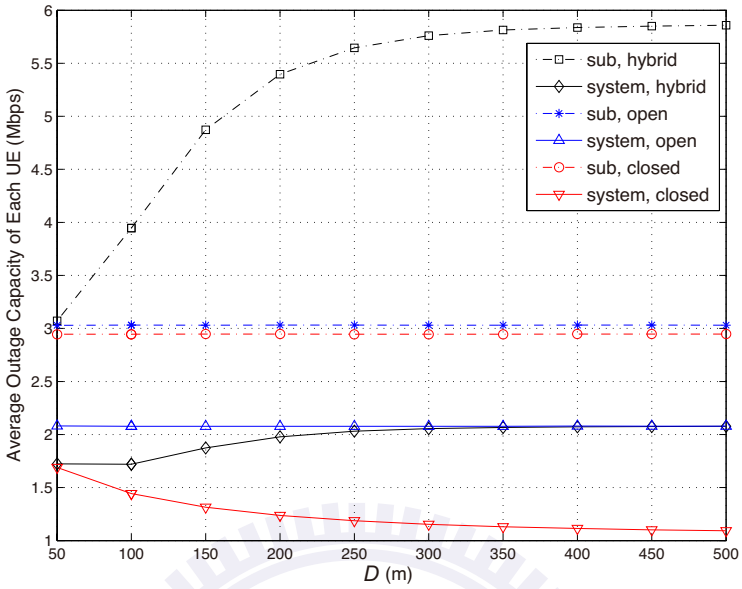

Figure 5.12: Average outage capacity of *subscriber* and system UE at NE versus the distance between mBS and fBS (D) in hybrid (with $\alpha = 0.7$), open ($\alpha = 0.0$), and closed ($\alpha = 1.0$) access modes.

mode can provide better fairness than that from the hybrid access mode. It is also observed that the performance of both hybrid and open access modes are superior to that in the closed access mode.

Fig. 5.12 illustrates the average outage capacity of *subscriber* and system UE at NE versus the distance between mBS and fBS (D) in hybrid (with $\alpha = 0.7$), open ($\alpha = 0.0$), and closed ($\alpha = 1.0$) access modes. It can be observed that the average outage capacity of system UE in both hybrid and open access modes almost keep constant values for larger value of distance D. The reason for these performance curves not to increase as D is augmented is that the HetNet with independent-channel deployment is considered for cell selection game *II*, which does not benefit from the spectrum reuse of femtocell as that in cell selection game *I*. The outage capacity of system UE for closed access mode is decreased with the augmentation of D. The main reason is that all players decide to connect to the mBS, where the pathloss will be increased with the increment of distance D. Moreover, it can be seen that average outage capacities of *subscribers* in both open and closed access modes are around the same and almost keep constant as distance D is increased, which is resulted from the same reason of independent channel access.

The left subplot of Fig. 5.13 displays average outage capacity of *subscribers* and system

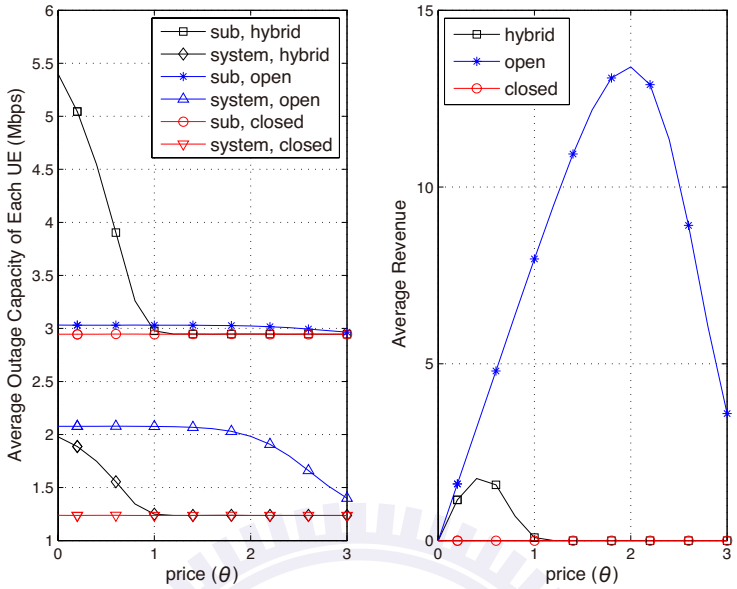

Figure 5.13: Average outage capacity of *subscribers* and system UE at NE versus the price (θ) (left subplot), and average revenue that operator can charge versus the price (θ) (right subplot) in hybrid (with $\alpha = 0.7$), open ($\alpha = 0.0$), and closed ($\alpha = 1.0$) access modes.

UE at NE versus the price θ; while the right subplot illustrates average revenue that operator can charge versus the price θ in hybrid (with $\alpha = 0.7$), open ($\alpha = 0.0$), and closed ($\alpha = 1.0$) access modes. It can be observed that most curves have similar trend as their respective curves in Fig. 5.9. For example, the performance of hybrid and open access modes will become closer to closed access mode as θ is augmented, average revenues in open access mode is larger than that in hybrid access, and both hybrid and open access modes have peak values respectively at $\theta \simeq 0.4$ and $\theta \simeq 2$. In addition, the outage capacity of *subscriber* slightly decreases as θ is increased since the players tend to connect to mBS, which corresponds to the case that *subscribers* possess less channel diversities.

5.4.3 Special Case: Non-Unique NE for Cell Selection Games *I* and *II*

In order to evaluate how often more than one NE occurs, one million simulation runs have been executed under $\alpha = 0.5$ and $\alpha = 0.7$ respectively for games I and II. Occurrence of more than one NE has not been observed for both games I and II. This shows that in general situations, there exists only one NE for the proposed games. Nevertheless, for certain specific cases, these games may possess more than one NE. Let's consider a

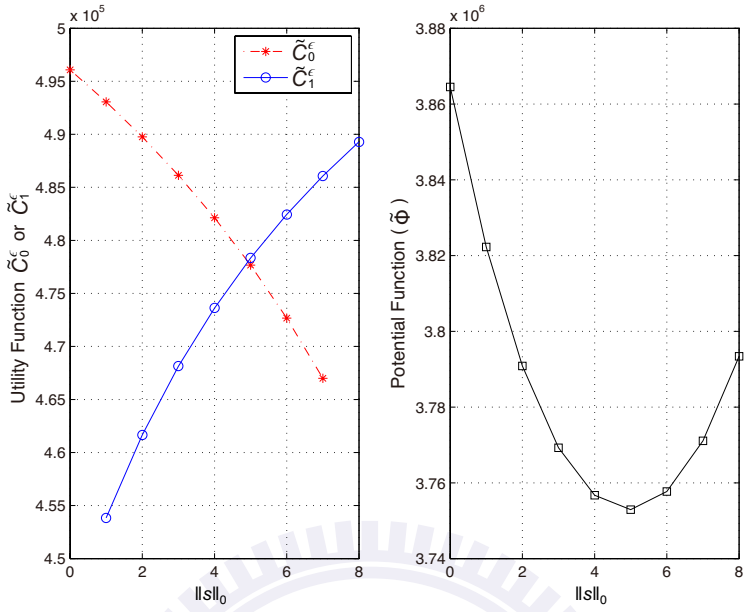

Figure 5.14: Utility functions ($\tilde{C}_0^\epsilon$ and $\tilde{C}_1^\epsilon$) (left subplot) for all players and corresponding potential function (right subplot) versus number of players connecting to the fBS $\|s\|_0$.

special cell selection game *II* that all players are located at the same place, received wideband signal-to-noise ratio from mBS ($P_{\text{MAX},0} \cdot L_{i,0}/\sigma_{\text{N}}^2$) and from fBS ($P_{\text{MAX},1} \cdot L_{i,1}/\sigma_{\text{N}}^2$) are respectively 10 dB and 16 dB for player i. Obviously, this game is not only cell selection game *II*, but also game *I* since all players have the same utility function. Under the case of $\alpha = 0.4$, Fig. 5.14 illustrates the utility function defined by the outage capacity and the corresponding potential function. Note that $\tilde{C}_{i,0}^\epsilon$ and $\tilde{C}_{i,1}^\epsilon$ can be respectively simplified as $\tilde{C}_0^\epsilon$ and $\tilde{C}_1^\epsilon$ for Fig. 5.14 since all players have the identical utility function. It can be observed from the right plot of Fig. 5.14 that there exists two local maximum values at $\|s\|_0 = 0$ and 8, which respectively represent two NEs for the game. Moreover, since the game is also a supermodular game, the greatest NE at $\overline{s} = [1, 1, 1, 1, 1, 1, 1, 1]$ ($\|s\|_0 = 8$) and the least NE at $\underline{s} = [0, 0, 0, 0, 0, 0, 0, 0]$ ($\|s\|_0 = 0$) can still be obtained by iterating the best response mapping. Note that initial state will determine the final NE to be either $\|s\|_0 = 0$ or 8 from the perspective of potential function. For example, it is clear to observe from the right plot of Fig. 5.14 that the NE will be at $\|s\|_0 = 0$ if initial state is located within $0 \leq \|s\|_0 \leq 4$; while the NE will become $\|s\|_0 = 8$ if initial state is located within $6 \leq \|s\|_0 \leq 8$. On the other hand, the final NE may occur at either $\|s\|_0 = 0$ or $\|s\|_0 = 8$ if initial state is at $\|s\|_0 = 5$ since it is a local minimum within the range $0 \leq \|s\|_0 \leq 8$. This example shows

that existence of unique NE cannot be guaranteed for both cell selection games *I* and *II*.

5.5 Concluding Remarks

In this chapter, two cell selection games are proposed for different network scenarios to describe the connection behaviors of *nonsubscribers* within the transmission range of femtocell base station. With the consideration of feasible utility functions for *nonsubscribers*, the existences of pure strategy Nash equilibria are respectively proven for the two cell selection games based on their distinct properties. Main numerical results can be summarized as follows:

- Hybrid access mode is superior to closed access mode no matter which perspective, *subscribers*, entire HetNet, or operator revenue, is considered.
- Open access mode can result in higher capacity for the entire HetNet and greater revenue for operator compared to both the hybrid and closed access modes.
- *Subscribers* can obtain higher capacity in the hybrid access mode compared to both the open and closed access modes.

Therefore, it is suggested to adopt hybrid access mode in order to provide higher flexibility for performance enhancement of all *subscribers*, entire system, and operator.

Chapter 6

Conclusions

In this dissertation, a series of short-range communication protocols is developed in order to enhance the wireless system performance. Two major techniques are considered for short-range wireless communications, including IEEE 802.11 and femtocell. Both IEEE 802.11 protocols and femtocell techniques can provide high data rate for users, nevertheless several crucial challenges described as follows restrain system performance from being further improved.

- **Problem 1**: How to reduce request-to-send (RTS) collision probability and backoff delay for IEEE 802.11 wireless local area networks (WLANs)?
- **Problem 2**: For IEEE 802.11n WLANs,, how to design efficient automatic repeat reQuest (ARQ) schemes to achieve both reliable data transmission and high system throughput?
- **Problem 3**: which femtocell access strategy is recommended considering performance from the perspectives of *subscribers*, entire heterogeneous network (HetNet), and operator?

In the conventional IEEE 802.11 WLANs, distributed coordination function (DCF) is applied to regulate the scheduling among wireless stations (WSs). However, the system throughput is significantly decreased due to RTS packet collision and backoff delay. Therefore, for **Problem 1**, an adaptive reservation-assisted collision resolution (ARCR) protocol is proposed in Chapter 2 to enhance the network throughput for WLANs. According to the ARCR scheme, adaptive reservation periods will be imposed within the

conventional contention-based system by adopting the proposed piggyback mechanisms. Based on the design of reservation table at the access point (AP), excessive packet collision can be effectively alleviated and the random access backoff delays can be reduced in the networks. Moreover, in order to support quality-of-service (QoS) requirements, an enhanced-ARCR (E-ARCR) protocol is proposed in Chapter 3 by applying multiple reservation tables at the AP for each prioritized traffic. It will not only increase the throughput of access categories (ACs) with higher priority but also prevent the ACs with lower priority from starvation of channel access. The analytical models of system throughput for both the proposed ARCR and E-ARCR protocols are derived and validated via simulations. Numerical results show that the proposed ARCR and E-ARCR protocols outperform the other existing schemes with enhanced network throughput and better channel utilization.

Furthermore, for **Problem 2**, two high-efficient ARQ mechanisms with the consideration of frame aggregation are developed in Chapter 4 for the IEEE 802.11n networks. The aggregated selective repeat ARQ (ASR-ARQ) protocol is proposed by incorporating the conventional stop-and-wait ARQ scheme; while the aggregated hybrid ARQ (AH-ARQ) algorithm further enhances throughput performance by adopting the Reed-Solomon block code for error correction under worse channel quality. Analytical models are constructed to evaluate the performance of proposed ASR-ARQ and AH-ARQ algorithms with the consideration of interfering stations. Simulations are also conducted to validate and compare the effectiveness of proposed ARQ mechanisms via both the mean service time and throughput performance. Numerical results show that the proposed AH-ARQ protocol can outperform the other schemes under worse channel condition; while the proposed ASR-ARQ protocol is superior to the other mechanisms under better channel condition.

Besides, to address **Problem 3**, two cell selection games are proposed in Chapter 5 for different network scenarios to describe the connection behaviors of *nonsubscribers* within the transmission range of femtocell base station. With the consideration of feasible utility functions for *nonsubscribers*, the existences of pure strategy Nash equilibria are respectively proven for the two cell selection games based on their distinct properties. Main numerical results can be summarized as follows:

- Hybrid access mode outperforms closed access mode no matter which perspective, *subscribers*, entire HetNet or operator revenue, is considered.

- Open access mode can lead to higher capacity for the entire HetNet and greater revenue for operator compared to both the hybrid and closed access modes.

- *Subscribers* can obtain higher capacity in the hybrid access mode compared to the both open and closed access modes.

Therefore, for **Problem 3**, it is suggested to adopt hybrid access mode in order to achieve better tradeoff for performance enhancement of all *subscribers*, entire system and operator.

A series of short-range communication protocols is proposed in this dissertation to resolve several crucial issues in the both IEEE 802.11 and femtocell networks. Moreover, analytical models are also developed for the validation of system performance. Both simulation and analytical results show that performance of IEEE 802.11 and femtocell networks can be further improved by adopting proposed algorithms in this dissertation.

References

[1] IEEE 802.11 WG, *IEEE Std 802.11a-1999(R2003): Part 11: Wireless LAN Medium Access Control (MAC) and Physical Layer (PHY) specifications: High-speed Physical Layer in the 5 GHz Band*, IEEE Standards Association Std., 2003.

[2] IEEE 802.11 WG, *IEEE Std 802.11b-1999(R2003): Part 11: Wireless LAN Medium Access Control (MAC) and Physical Layer (PHY) specifications: Higher-Speed Physical Layer Extension in the 2.4 GHz Band*, IEEE Standards Association Std., 2003.

[3] IEEE 802.11 WG, *IEEE Std 802.11g-2003: Part 11: Wireless LAN Medium Access Control (MAC) and Physical Layer (PHY) specifications: Amendment 4: Further Higher Data Rate Extension in the 2.4 GHz Band*, IEEE Standards Association Std., 2003.

[4] IEEE 802.11 WG, *IEEE Std 802.11e-2005: Part 11: Wireless LAN Medium Access Control (MAC) and Physical Layer (PHY) specifications: Amendment 8: Medium Access Control (MAC) Quality of Service Enhancements*, IEEE Standards Association Std., 2005.

[5] IEEE 802.11 WG, *IEEE P802.11n-2009: Part 11: Wireless LAN Medium Access Control (MAC) and Physical Layer (PHY) Specifications: Amendment 5: Enhancements for Higher Throughput*, IEEE Standards Association Std., Oct. 2009.

[6] S. Abraham, A. Meylan, and S. Nanda, "802.11n MAC Design and System Performance," in *"Proc. IEEE International Conference on Communications (ICC)"*, vol. 5, May 2005.

[7] G. Mansfield, "Femtocells in the US Market - Business Drivers and Consumer Propositions," in *Femtocells Europe 2008*, London, UK, June 2008.

[8] V. Chandrasekhar, J. G. Andrews, and A. Gatherer, "Femtocell Networks: A Survey," *IEEE Commun. Mag.*, vol. 46, no. 9, pp. 59–67, Sept. 2008.

[9] Y. Li, S. W. Kim, J. K. Chung, and H. G. Ryu, "SFBC-based MIMO OFDM and MIMO CI-OFDM Systems in the Nonlinear and NBI Channel," in *Proc. IEEE International Conference on Communications, Circuits, and Systems (ICCCAS)*, vol. 2, June 2006, pp. 898–901.

[10] Y. Li, X. Wang, and S. A. Mujtaba, "Impact of Physical Layer Parameters on the MAC Throughput of IEEE 802.11 Wireless LANs," in *Proc. IEEE Asilomar Conference on Signals, Systems, and Computers (ACSSC)*, vol. 2, Nov. 2004, pp. 1468–1472.

[11] D. Skordoulis, Q. Ni, H. H. Chen, A. P. Stephens, C. Liu, and A. Jamalipour, "IEEE 802.11n MAC Frame Aggregation Mechanisms for Next-generation High-throughput WLANs," *IEEE Wireless Commun. Mag.*, vol. 15, no. 1, pp. 40–47, Feb. 2008.

[12] M. Latham, "Consumer Attitudes to Femtocell Enabled in-home Services - Insights from a European Survey," in *Femtocells Europe 2008*, London, UK, June 2008.

[13] 3GPP TR25.820 v8.2.0, "3G Home NodeB Study Item Technical Report (Release 8)," Sept. 2008.

[14] Y. Kwon, Y. Fang, and H. Latchman, "A Novel MAC Protocol with Fast Collision Resolution for Wireless LANs," in *Proc. IEEE INFOCOM*, vol. 2, Mar. 2003, pp. 853–862.

[15] X. Peng, L. Jiang, and G. Xu, "Performance Analysis of Hybrid Backoff Algorithm of Wireless LAN," in *Proc. IEEE International Conference on Wireless Communications, Networking and Mobile Computing (WiCom)*, Sept. 2007, pp. 1853–1856.

[16] K. Sakakibara, Y. Kobayashi, and J. Taketsugu, "Saturation Throughput of IEEE 802.11 Using Carrier Sense Mechanism in Backoff Intervals," in *Proc. IEEE International Symposium on Communications, Control and Signal Processing (ISCCSP)*, Mar. 2008, pp. 899–904.

[17] J. Choi, J. Yoo, S. Choi, and C. Kim, "EBA: An Enhancement of the IEEE 802.11 DCF via Distributed Reservation," *IEEE Trans. Mobile Comput.*, vol. 4, no. 4, pp. 378–390, July 2005.

[18] Q. Li, "Reservation-based Distributed Collision Avoidance Channel Access Scheme for WLAN," in *Proc. IEEE Global Telecommunications Conference (GLOBECOM)*, Nov. 2008.

[19] L. Bo, T. Wenzhao, Z. Hu, and Z. Hui, "m-DIBCR : MAC Protocol with Multiple-Step Distributed In-Band Channel Reservation," *IEEE Commun. Lett.*, vol. 12, no. 1, pp. 23–25, Jan. 2008.

[20] C. Wang, B. Li, B. Li, and K. Sohraby, "An Effective Collision Resolution Mechanism for Wireless LAN," in *Proc. IEEE International Conference on Computer Networks and Mobile Computing (ICCNMC)*, Oct. 2003, pp. 18–25.

[21] C. Wang, B. Li, and L. Li, "A New Collision Resolution Mechanism to Enhance the Performance of IEEE 802.11 DCF," *IEEE Trans. Veh. Technol.*, vol. 53, no. 4, pp. 1235–1246, July 2004.

[22] Z. Chen and A.A. Khokhar, "A Channel Reservation Procedure for Fading Channels in Wireless Local Area Networks," *IEEE Trans. Wireless Commun.*, vol. 4, no. 2, pp. 689–699, Mar. 2005.

[23] A. Kanjanavapastit and B. Landfeldt, "An Analysis of a Modified Point Coordination Function in IEEE 802.11," in *Proc. IEEE International Symposium on Personal, Indoor and Mobile Radio Communications (PIMRC)*, vol. 2, Sept. 2003, pp. 1732–1736.

[24] I. Joe, "QoS-aware MAC with Reservation for Mobile Ad-Hoc Networks," in *Proc. IEEE Vehicular Technology Conference Fall (VTC-Fall)*, Sept. 2004.

[25] H.J. Lee, J.H. Kim, and S.H. Cho, "A Delay-based Piggyback Scheme in IEEE 802.11," in *Proc. IEEE Wireless Communications and Networking Conference (WCNC)*, Mar. 2007, pp. 447–451.

[26] ——, "A Novel Piggyback Selection Scheme in IEEE 802.11e HCCA," in *Proc. IEEE International Conference on Communications (ICC)*, June 2007, pp. 4529–4534.

[27] M. Ma and Y. Yang, "A Novel Contention-Based MAC Protocol with Channel Reservation for Wireless LANs," *IEEE Trans. Wireless Commun.*, vol. 7, no. 10, pp. 3748–3758, Oct. 2008.

[28] X. Yang, "IEEE 802.11 Performance Enhancement via Concatenation and Piggyback Mechanisms," *IEEE Trans. Wireless Commun.*, vol. 4, no. 5, pp. 2182–2192, Sept. 2005.

[29] G. Bianchi, "Performance Analysis of the IEEE 802.11 Distributed Coordination Function," *IEEE J. Sel. Areas Commun.*, vol. 18, no. 3, pp. 535–547, Mar. 2000.

[30] H.V. Zoran and S. Boris, "Saturation Throughput - Delay Analysis of IEEE 802.11 DCF in Fading Channel," in *Proc. IEEE International Conference on Communications (ICC)*, vol. 1, May 2003, pp. 121–126.

[31] Z. Eustathia and A. Theodore, "CSMA/CA Performance under High Traffic Conditions: Throughput and Delay Analysis," *Computer Communications*, vol. 25, no. 3, pp. 313–321, Feb. 2002.

[32] S. Ci, H. Sharif, and P. Mahasukhon, "Evaluating Saturation Throughput Performance of the IEEE 802.11 MAC under Fading Channels," in *Proc. IEEE International Conference on Broadband Networks (BROADNETS)*, vol. 1, Oct. 2005, pp. 676–681.

[33] J.S. Vardakas, M.K. Sidiropoulos, and M.D. Logothetis, "Performance Behaviour of IEEE 802.11 Distributed Coordination Function," *IET Circuits, Devices & Systems*, vol. 2, no. 1, pp. 50–59, 2008.

[34] H. Wu, Y. Peng, K. Long, S. Cheng, and J. Ma, "Performance of Reliable Transport Protocol over IEEE 802.11 Wireless LAN: Analysis and Enhancement," in *Proc. IEEE INFOCOM*, vol. 2, June 2002, pp. 599–607.

[35] The Network Simulator ns-2, http://www.isi.edu/nsnam/ns, 2011.

[36] R. Jain, A. Durresi, and G. Babic, "Throughput Fairness Index: An Explanation," *ATM Forum/99-0045*, Feb. 1999.

[37] T.H. Kim, L. Marwitz, and D.K. Kim, "Dynamic Offset Contention Window (DOCW) Algorithm for Wireless MAC in 802.11e Based Wireless Home Networks," *Lecture Notes in Computer Science*, vol. 2524, pp. 162–172, 2003.

[38] L. Romdhani, Q. Ni, and T. Turletti, "Adaptive EDCF: Enhanced Service Differentiation for IEEE 802.11 Wireless Ad-Hoc Networks," in *Proc. IEEE Wireless Communications and Networking Conference (WCNC)*, vol. 2, Mar. 2003, pp. 1373–1378.

[39] Y. Tanigawa, J.O. Kim, H. Tode, and K. Murakami, "Proportional Control and Deterministic Protection of QoS in IEEE 802.11e Wireless LAN," in *Proc. ACM International Wireless Communications and Mobile Computing Conference (IWCMC)*, 2006, pp. 1147–1152.

[40] S. Gaur, C. Tavares, and T. Cooklev, "Improved Performance of CSMA/CA WLAN using a Random Inter-Frame Spacing Algorithm," in *Proc. ACM International Wireless Communications and Mobile Computing Conference (IWCMC)*, 2006, pp. 407–412.

[41] T. Nilsson and J. Farooq, "A Novel MAC Scheme for Solving the QoS Parameter Adjustment Problem in IEEE 802.11e EDCA," in *Proc. IEEE International Symposium on a World of Wireless, Mobile and Multimedia Networks (WoWMoM)*, June 2008, pp. 1–9.

[42] X. Yang, "Performance Analysis of IEEE 802.11e EDCF under Saturation Condition," in *Proc. IEEE International Conference on Communications (ICC)*, vol. 1, June 2004, pp. 170–174.

[43] ——, "Performance Analysis of Priority Schemes for IEEE 802.11 and IEEE 802.11e Wireless LANs," *IEEE Trans. Wireless Commun.*, vol. 4, no. 4, pp. 1506–1515, July 2005.

[44] Z.N. Kong, H.K. Tsang, B. Bensaou, and D. Gao, "Performance Analysis of IEEE 802.11e Contention-Based Channel Access," *IEEE J. Sel. Areas Commun.*, vol. 22, no. 10, pp. 2095–2106, Dec. 2004.

[45] I. Inan, F. Keceli, and E. Ayanoglu, "Saturation Throughput Analysis of the 802.11e Enhanced Distributed Channel Access Function," in *Proc. IEEE International Conference on Communications (ICC)*, June 2007, pp. 409–414.

[46] J. Robinson and T. Randhawa, "Saturation Throughput Analysis of IEEE 802.11e Enhanced Distributed Coordination Function," *IEEE J. Sel. Areas Commun.*, vol. 22, no. 5, pp. 917–928, June 2004.

[47] H. Wu, X. Wang, Q. Zhang, and X. Shen, "IEEE 802.11e Enhanced Distributed Channel Access (EDCA) Throughput Analysis," in *Proc. IEEE International Conference on Communications (ICC)*, vol. 1, June 2006, pp. 223–228.

[48] B. Ginzburg and A. Kesselman, "Performance Analysis of A-MPDU and A-MSDU Aggregation in IEEE 802.11n," in *Proc. IEEE Sarnoff Symposium*, May 2007.

[49] S. Parthasarathy and Q. Zeng, "A Novel Adaptive Scheme to Improve the Performance of the IEEE 802.11n WLANs," in *Proc. IEEE dvanced Information Networking and Applications Workshops (AINAW)*, vol. 2, May 2007.

[50] S. Kim, S. Choi, Y. Kim, and K. Jang, "MCCA: a High-throughput MAC Strategy for Next-generation WLANs," *IEEE Wireless Commun. Mag.*, vol. 15, no. 1, pp. 32–39, Feb. 2008.

[51] D. Lu and J. Chang, "Analysis of ARQ Protocols via Signal Flow Graphs," *IEEE Trans. Commun.*, vol. 37, no. 3, pp. 245–251, Mar. 1989.

[52] Y. Hua and Z. Niu, "An Analytical Model for IEEE 802.11 WLANs with NAK-based ARQ Mechanism," in *Proc. Asia-Pacific Conference on Communications (APCC)*, Oct. 2007, pp. 277–280.

[53] J. B. Seo, N. H. Park, H. W. Lee, and C. H. Cho, "Impact of an ARQ Scheme in the MAC/LLC Layer on Upper-layer Packet Transmissions over a Markovian Channel," in *Proc. IEEE Vehicular Technology Conference Spring (VTC-Spring)*, vol. 4, May 2006.

[54] K. C. Beh, A. Doufexi, and S. Armour, "Performance Evaluation of Hybrid ARQ Schemes of 3GPP LTE OFDMA System," in *Proc. IEEE International Symposium on Personal, Indoor and Mobile Radio Communications (PIMRC)*, Sept. 2007, pp. 1–5.

[55] E. Malkamaki, D. Mathew, and S. Hamalainen, "Performance of Hybrid ARQ Techniques for WCDMA High Data Rates," in *Proc. IEEE Vehicular Technology Conference Spring (VTC-Spring)*, vol. 4, May 2001, pp. 2720–2724.

[56] T. F. Wong, L. Gao, and T. M. Lok, "A Type-I Hybrid ARQ Protocol over Optimal-sequence CDMA Link," in *Proc. IEEE Military Communications Conference (MILCOM)*, vol. 1, Oct. 2001, pp. 559–563.

[57] J. F. Cheng, Y. P. E. Wang, and S. Parkvall, "Adaptive Incremental Redundancy [WCDMA Systems]," in *Proc. IEEE Vehicular Technology Conference Fall (VTC-Fall)*, vol. 2, Oct. 2003.

[58] Q. Chen and P. Fan, "On The Performance of Type-III Hybrid ARQ with RCPC Codes," in *Proc. IEEE International Symposium on Personal, Indoor and Mobile Radio Communications (PIMRC)*, vol. 2, Sept. 2003, pp. 1297–1301.

[59] R. Guo and J. L. Liu, "BER Performance Analysis of RCPC Encoded MIMO-OFDM in Nakagami-m Channels," in *Proc. IEEE International Conference on Information Acquisition (ICIA)*, Aug. 2006, pp. 1416–1420.

[60] D. N. Rowitch and L. B. Milstein, "On the Performance of Hybrid FEC/ARQ Systems Using RCPT Codes," *IEEE Trans. Commun.*, vol. 48, no. 6, pp. 269–281, June 2000.

[61] J. Proakis, *Digital Communications 4th Edition*, McGRAW-HILL, 2001.

[62] U. Cheng, "On the Continued Fraction and Berlekamp's Algorithm," *IEEE Trans. Inform. Theory*, vol. 30, no. 3, pp. 541–544, May 1984.

[63] M. Khan, S. Afzal, and R. Manzoor, "Hardware Implementation of Shortened (48,38) Reed Solomon Forward Error Correcting Code," in *Proc. IEEE International Multitopic Conference (INMIC)*, Dec. 2003, pp. 90–95.

[64] O. Tickoo and B. Sikdar, "Queueing Analysis and Delay Mitigation in IEEE 802.11 Random Access MAC Based Wireless Networks," in *Proc. IEEE INFOCOM*, vol. 2, Mar. 2004, pp. 1404–1413.

[65] Y. Zheng, K. Lu, D. Wu, and Y. Fang, "Performance Analysis of IEEE 802.11 DCF in Binary Symmetric Channels," in *Proc. IEEE Global Telecommunications Conference (GLOBECOM)*, vol. 5, Nov. 2005, pp. 3144–3148.

[66] Q. Ni, T. Li, T. Turletti, and Y. Xiao, "Saturation Throughput Analysis of Error-Prone 802.11 Wireless Networks," *Journal of Wireless Communications and Mobile Computing, John Wiley & Sons Publisher*, vol. 5, no. 8, pp. 945–956, Dec. 2005.

[67] Y. Lin and V. W. S. Wong, "Frame Aggregation and Optimal Frame Size Adaptation for IEEE 802.11n WLANs," in *Proc. IEEE Global Telecommunications Conference (GLOBECOM)*, vol. 5, Nov. 2006, pp. 1–6.

[68] S. Kuppa and G. R. Dattatreya, "Modeling and Analysis of Frame Aggregation in Unsaturated WLANs with Finite Buffer Stations," in *Proc. IEEE International Conference on Communications (ICC)*, June 2006, pp. 967–972.

[69] C. W. Liu and A. P. Stephens, "An Analytic Model for Infrastructure WLAN Capacity with Bidirectional Frame Aggregation," in *Proc. IEEE Wireless Communications and Networking Conference (WCNC)*, vol. 1, Mar. 2005, pp. 113–119.

[70] T. Li, Q. Ni, and Y. Xiao, "Investigation of the Block ACK Scheme in Wireless Adhoc Networks," *Journal of Wireless Communications and Mobile Computing, John Wiley & Sons Publisher*, vol. 6, no. 6, pp. 877–888, Sept. 2006.

[71] T. Li, Q. Ni, D. Malone, D. Leith, Y. Xiao, and T. Turletti, "Aggregation with Fragmentation Retransmission for Very High-Speed Wireless LANs," *IEEE/ACM Trans. Netw.*, vol. 17, no. 2, pp. 591–604, Apr. 2009.

[72] S. Choi and K.G. Shin, "A Class of Adaptive Hybrid ARQ Scheme for Wireless Links," *IEEE Trans. Veh. Technol.*, vol. 50, no. 3, pp. 777–790, May 2001.

[73] S. Choi, Y. Choi, and I. Lee, "IEEE 802.11 MAC-Level FEC with Retransmission Combining," *IEEE Trans. Wireless Commun.*, vol. 5, no. 1, pp. 203–211, Jan. 2006.

[74] Y. Choi and S. Choi, "Above-MAC FEC Scheme in IEEE 802.11 WLAN," in *Proc. IEEE Asia Pacific Wireless Communication Symposium (APWCS)*, Aug. 2005.

[75] E. Berlekamp, *Algebraic Coding Theory*, McGraw-Hill, New York, 1968.

[76] 3GPP TR 36.913 v10.0.0, "Requirements for further advancements for Evolved Universal Terrestrial Radio Access (E-UTRA) (LTE-Advanced) (Release 10)," Mar. 2011.

[77] D. López-Pérez, A. Valcarce, G. de la Roche, and J. Zhang, "OFDMA Femtocells: A Roadmap on Interference Avoidance," *IEEE Commun. Mag.*, vol. 47, no. 9, pp. 41–48, Sept. 2009.

[78] V. Chandrasekhar, J.G. Andrews, T. Muharemovic, Z. Shen, and A. Gatherer, "Power Control in Two-Tier Femtocell Networks," *IEEE Trans. Wireless Commun.*, vol. 8, no. 8, pp. 4316–4328, Aug. 2009.

[79] V. Chandrasekhar, J.G. Andrews, Z. Shen, T. Muharemovic, and A. Gatherer, "Distributed Power Control in Femtocell-Underlay Cellular Networks," in *Proc. IEEE Global Telecommunications Conference (GLOBECOM)*, Dec. 2009, pp. 1–6.

[80] Y.J. Sang, H.G. Hwang, and K.S. Kim, "A Self-Organized Femtocell for IEEE 802.16e System," in *Proc. IEEE Global Telecommunications Conference (GLOBECOM)*, Dec. 2009, pp. 1–5.

[81] M. Morita, Y. Matsunaga, and K. Hamabe, "Adaptive Power Level Setting of Femtocell Base Stations for Mitigating Interference with Macrocells," in *Proc. IEEE Vehicular Technology Conference Fall (VTC-Fall)*, Sept. 2010, pp. 1–5.

[82] Y, Bai, J. Zhou, and L. Chen, "Hybrid Spectrum Usage for Overlaying LTE Macrocell and Femtocell," in *Proc. IEEE Global Telecommunications Conference (GLOBECOM)*, Dec. 2009, pp. 1–6.

[83] R. Madan, J. Borran, A. Sampath, N. Bhushan, A. Khandekar, and T. Ji, "Cell Association and Interference Coordination in Heterogeneous LTE-A Cellular Networks," *IEEE J. Sel. Areas Commun.*, vol. 28, no. 9, pp. 1479–1489, Dec. 2010.

[84] S.Y. Lien, C.C. Tseng, K.C. Chen, and C.W. Su, "Cognitive Radio Resource Management for QoS Guarantees in Autonomous Femtocell Networks," in *Proc. IEEE International Conference on Communications (ICC)*, May 2010, pp. 1–6.

[85] V. Chandrasekhar and J.G. Andrews, "Uplink Capacity and Interference Avoidance for Two-Tier Femtocell Networks," *IEEE Trans. Wireless Commun.*, vol. 8, no. 7, pp. 3498–3509, July 2009.

[86] H. Claussen, "Performance of Macro- and Co-channel Femtocells in a Hierarchical Cell Structure," in *Proc. IEEE International Symposium on Personal, Indoor and Mobile Radio Communications (PIMRC)*, Sept. 2007, pp. 1–5.

[87] S. Yun, Y. Yi, D.H. Cho, and J. Mo, "Open or Close: On the Sharing of Femtocells," in *Proc. IEEE INFOCOM*, Apr. 2011, pp. 116–120.

[88] P. Xia, V. Chandrasekhar, and J.G. Andrews, "Open vs. Closed Access Femtocells in the Uplink," *IEEE Trans. Wireless Commun.*, vol. 9, no. 12, pp. 3798–3809, Dec. 2010.

[89] G. de la Roche, A. Valcarce, D. López-Pérez, and J. Zhang, "Access Control Mechanisms for Femtocells," *IEEE Commun. Mag.*, vol. 48, no. 1, pp. 33–39, Jan. 2010.

[90] D. Choi, P. Monajemi, S. Kang, and J. Villasenor, "Dealing with Loud Neighbors : The Benefits and Tradeoffs of Adaptive Femtocell Access," in *Proc. IEEE Global Telecommunications Conference (GLOBECOM)*, Dec. 2008, pp. 1–5.

[91] A. Valcarce, D. López-Pérez, G. De La Roche, and J. Zhang, "Limited Access to OFDMA Femtocells," in *Proc. IEEE International Symposium on Personal, Indoor and Mobile Radio Communications (PIMRC)*, Sept. 2009, pp. 2251–2255.

[92] A.T. Hoang, Y.C. Liang, and M.H. Islam, "Maximizing Throughput of Cognitive Radio Networks with Limited Primary Users' Cooperation," in *Proc. IEEE International Conference on Communications (ICC)*, June 2007, pp. 5177–5182.

[93] L. Gao and S. Cui, "Multi-band Power and Rate Control for Cognitive Radios with Energy Constraints - A Dynamic Programming Approach," in *Proc. IEEE International Conference on Communications (ICC)*, May 2008, pp. 3563–3567.

[94] M.J. Osborne and A. Rubinstein, *A Course in Game Theory*. The MIT Press, 1994.

[95] D. Monderer and L.S. Shapley, "Potential Games," *Games and Econ. Behavior,*, vol. 14, pp. 124–143, 1996.

[96] 3GPP TS 36.423 v10.2.0, "X2 Application Protocol (X2AP) (Release 10)," June 2011.

[97] D. Tse and P. Viswanath, *Fundamentals of Wireless. Communication*. Cambridge Univ. Press, 2005.

[98] D.M. Topkis, *Supermodularity and Complementarity*. Princeton Univ. Press, 1998.

[99] I. Menache and A. Ozdaglar, *Network Games: Theory, Models, and Dynamics*. Jean Walrand, editor, Morgan and Claypool Publishers, 2010.

[100] 3GPP TR 36.814 v9.0.0, "Further Advancements for E-UTRA Physical Layer Aspects (Release 9)," Mar. 2010.

Publication List

Journal Papers

[J-1] Kai-Ten Feng, **Jia-Shi Lin**, and Wei-Neng Lei, "Design and Analysis of Adaptive Receiver Transmission Protocols for Receiver Blocking Problem in Wireless Ad-Hoc Networks," accepted and to appear in *IEEE Trans. Mobile Computing*.

[J-2] **Jia-Shi Lin**, Kai-Ten Feng, Yu-Zhi Huang, and Li-Chun Wang, "Novel Design and Analysis of Aggregated ARQ Protocols for IEEE 802.11n Networks," accepted and to appear in *IEEE Trans. Mobile Computing*.

[J-3] Chi-Mao Lee, **Jia-Shi Lin**, Kai-Ten Feng, and Chung-Ju Chang, "Design and Analysis of Transmission Strategies in Channel-Hopping Cognitive Radio Networks," accepted and to appear in *IEEE Trans. Mobile Computing*.

[J-4] **Jia-Shi Lin** and Kai-Ten Feng, "QoS-based Adaptive Contention/Reservation Medium Access Control Protocols for Wireless Local Area Networks," *IEEE Trans. Mobile Computing*, vol. 10, no. 12, pp. 1785-1803, Dec. 2011.

[J-5] **Jia-Shi Lin** and Kai-Ten Feng, "Design and Performance Analysis on Adaptive Reservation-Assisted Collision Resolution Protocol for WLANs," *ACM/Springer Journal on Wireless Networks (WINET)*, vol. 17, no. 4, pp. 973-986, May 2011.

[J-6] Kai-Ten Feng, Yu-Zhi Huang, and **Jia-Shi Lin**, "Design of MAC-Defined Aggregated ARQ Schemes for IEEE 802.11n Networks," *ACM/Springer Journal on Wireless Networks (WINET)*, vol. 17, no. 3, pp. 685-699, Apr. 2011.

Conference Papers

[C-1] Hsiu-Ming Tu, **Jia-Shi Lin**, Tain-Sao Chang, and Kai-Ten Fen, "Prediction-based Handover Schemes for Relay-enhanced LTE-A Systems," in *Proc. IEEE Wireless Communication and Networking Conference (WCNC 2012)*, Paris, France, Apr. 2012.

[C-2] Tain-Sao Chang, Kai-Ten Feng, **Jia-Shi Lin**, and Li-Chun Wang, "Green Resource Allocation for MIMO-OFDM Relay Networks," in *Proc. IEEE Wireless Communication and Networking Conference (WCNC 2012)*, Paris, France, Apr. 2012.

[C-3] Jui-Hung Chu, Kai-Ten Feng, **Jia-Shi Lin**, and Chung-Hsien Hsu, "Cognitive Radio-Enabled Optimal Channel-Hopping Sequence for Multi- Channel Vehicular Communications," in *Proc. IEEE Vehicular Technology Conference (VTC-Fall 2011)*, San Francisco, United States, Sept. 2011.

[C-4] **Jia-Shi Lin** and Kai-Ten Feng, "Game Theoretical Model and Existence of Win-Win Situation for Femtocell Networks," in *Proc. IEEE International Conference on Communications (ICC 2011)*, Kyoto, Japan, June 2011.

[C-5] Wan-Pan Chang, **Jia-Shi Lin**, and Kai-Ten Feng, "QoS-based Resource Allocation for Relay-Enhanced OFDMA Networks," in *Proc. IEEE Wireless Communication and Networking Conference (WCNC 2011)*, Cancun, Mexico, Apr. 2011.

[C-6] Shao-Kai Hsu, **Jia-Shi Lin**, and Kai-Ten Feng, "Stochastic Multiple Channel Sensing Protocol for Cognitive Radio Networks," in *Proc. IEEE Wireless Communication and Networking Conference (WCNC 2011)*, Cancun, Mexico, Apr. 2011

[C-7] Chi-Mao Lee, **Jia-Shi Lin**, Yu-Pin Hsu, and Kai-Ten Feng, "Design and Analysis of Optimal Channel-Hopping Sequence for Cognitive Radio Networks," in *Proc. IEEE Wireless Communication and Networking Conference (WCNC 2010)*, Sydney, Australia, Apr. 2010.

[C-8] Yu-Tzu Huang, **Jia-Shi Lin**, and Kai-Ten Feng, "Performance Analysis for Aggregated Selective Repeat ARQ Scheme in IEEE 802.11n Networks," in *Proc. IEEE International Symposium on Personal, Indoor and Mobile Radio Communications (PIMRC 2009)*, Tokyo, Japan, Sept. 2009.

[C-9] **Jia-Shi Lin**, Chien-Hua Chen, and Kai-Ten Feng, "Adaptive Reservation-Assisted Collision Resolution Protocol for Wireless Local Area Networks," in *Proc. IEEE Wireless Communication and Networking Conference (WCNC 2009)*, Budapest, Hungary, Apr. 2009.

Submitted Journal Papers

[S-1] **Jia-Shi Lin** and Kai-Ten Feng, "Femtocell Access Strategies in Heterogeneous Networks using a Game Theoretical Framework," major revision in *IEEE Trans. Mobile Computing*.

Submitted Patents

[P-1] Qos-based High Capacity Resource Allocation for Relay-Enhanced OFDMA Networks, submitted to *Chinese Patent* in Oct. 2010.

[P-2] Inter-Cell Interference Coordination without Backhaul Signaling between Macro and Femto eNBs, provisional patent, US Patent.

Technical Contributions

[T-1] 3GPP R1-105239, Specification impacts of eICIC in macro-femto deployment, MediaTek.

Vita

Jia-Shi Lin received the B.S. degree in the Department of Biomedical Engineering and Environmental Sciences from National Tsing Hua University, Hsinchu, Taiwan, in 2007, and the M.S. & Ph.D. degrees in the Institute of Communications Engineering from National Chiao Tung University, Hsinchu, Taiwan, in 2012. His current research interests include game theory, MAC protocol design, wireless local area networks, and cognitive radio networks.

Education

B.S. 2003-2007

Department of Biomedical Engineering and Environmental Sciences, National Tsing Hua University (NTHU), Hsinchu, Taiwan, R.O.C.

M.S. & Ph.D. 2007-2012

Institute of Communications Engineering, National Chiao Tung University (NCTU), Hsinchu, Taiwan, R.O.C.

Awards

- Ph.D. Semester Scholarship, *Feb., 2009*
- Ph.D. Semester Scholarship, *Sept., 2010*
- Ph.D. Semester Scholarship, *Feb., 2011*
- Ph.D. Semester Scholarship, *Sept., 2011*
- Ph.D. Semester Scholarship, *Feb., 2012*
- Ministry of Education for Fostering International Elites Scholarship, *Oct., 2010*
- Ministry of Education for Fostering International Elites Scholarship, *Oct., 2011*